

**Grantee Organization Name:** NJ Department of Environmental Protection

**Grant Number:** CD96284800

**Project Title:** New Jersey (USA) Wetlands Past, Present and Future: Using Sediment Archives to Inform and Guide Wetland Protection, Restoration and Resilience

**Project Period:** 2015-2017

**Contact Name and Telephone Number:** Mihaela Enache, 609-292-6134

**Reporting Period:** Final Report 2015-2017 (submitted January 2018)

## **Project contributors**

Dr. Nicholas Procopio, Manager; Division of Science, Research, and Environmental Health,  
New Jersey Department of Environmental Protection

Dorina Frizzera (retired); Division of Science, Research, and Environmental Health, New Jersey  
Department of Environmental Protection

Dr. Marina Potapova, Assistant Professor and Nina Desianti (PhD student); Academy of Natural  
Sciences of Drexel University

Dr. Daria Nikitina, Associate Professor, and students Beatrice O'Hara, (currently at Delaware  
Geological Survey), Alan Geyer, Daniel Jennings, Deven Scallo; West Chester University

Dr. Benjamin Horton, Professor, and postdoctoral fellows Jennifer Clear, Megan Christie, and  
PhD student Jennifer Walker; Rutgers University.

## **Table of Contents**

Introduction .....	4
Project Description .....	6
Project Methods .....	8
Study area and field sampling .....	10
Core subsampling .....	13
Core chronology: Carbon-14, Pb-210, and Cs-137 dating .....	13
Total Petroleum Hydrocarbons: PAHs, PCBs and OCPs .....	14
Trace metals.....	15
Sediment nitrogen .....	16
Diatom analysis .....	16
Pollen analyses .....	17
Land-use data .....	18
Data Analysis: Reconstruction of past environmental changes .....	19
Results and Discussion.....	19
Core chronology .....	19
Delaware Bay litho-stratigraphy of storm erosion events .....	20
Pollution histories .....	22
Diatom analysis .....	28
Land-use changes.....	34
Reference conditions.....	35
Anthropogenic impacts .....	36
Climate impacts - storm events.....	38
Refining the use of diatom species as coastal wetland ecological indicators .....	38
Informing future coastal wetland restoration targets.....	39
Conclusions .....	40
Acknowledgements.....	40
References .....	41
List of Tables .....	48
List of Figures .....	49

## **INTRODUCTION**

The New Jersey Department of Environmental Protection (NJDEP) recognizes the importance of tidal and freshwater wetlands. The New Jersey Legislature enacted the New Jersey Wetlands Act of 1970 and then the NJ Freshwater Wetlands Protection Act in 1987. These Acts provide additional protection beyond federal law and are considered some of the most stringent wetland laws in the US. The 1970 Legislature stated that “one of the most vital and productive areas of our natural world is the so-called "estuarine zone" and that this area “protects the land from the force of the sea, moderates our weather, provides a home for water fowl and for 2/3 of all our fish and shellfish, and assists in absorbing sewage discharge by the rivers of the land”. Thus, the Legislature decided that preserving the ecological balance and preventing further deterioration of the coastal wetlands are necessary “to promote the public safety, health and welfare, and to protect public and private property, wildlife, marine fisheries and the natural environment” (New Jersey Wetlands Act of 1970; 13:9A-2).

The New Jersey Wetlands Act of 1970 defined the term of "coastal wetlands" to include banks, marshes, swamps, meadows, flat or other low land subject to tidal action in the State of New Jersey along the Delaware Bay and Delaware River, Raritan Bay, Barnegat Bay, Sandy Hook Bay, and the coastal inland waterways and inlets connected to tidal waters whose surface is at or below an elevation of 1 foot above local extreme high water.

In order to provide the best protection to New Jersey (NJ) coastal wetlands, it is necessary to acquire knowledge of their long-term history, understand the processes that contributed to their formation since the Holocene marine transgression, the natural variability and capacity to withstand the ocean force effects, and assess the changes that took place under anthropogenic impacts since the European settlement.

The salt marshes were first investigated in the 19<sup>th</sup> century when the first theories for the evolution of New Jersey lagoons from open-water to marsh-filled systems were proposed (e.g., Shaler, 1895). Many authors afterwards studied the geological processes and physical characteristics leading to the development of modern salt marshes (e.g., Knight 1934; Frey and Basan, 1978).

The Pleistocene Cape May formation (Salisbury, 1896) is overlain by the Holocene barrier and back-barrier east of the Cape May peninsula and is estimated to be 125,000 years old

(Sangamon geological stage). The presence of the Cape May Formation proves that the sea level 125,000 years ago was similar to its present-day level (Ferland, 1990). During the subsequent glaciation episodes and maximum ice loading, southern NJ was located on the forefront bulge and approximately 18,000 years ago the sea level was at levels more than 130 m below the present-day sea level (Dillon and Oldale, 1978).

Studies of stratigraphic deposits along the NJ coast suggest a continuous but fluctuating rate of rise throughout the Holocene, caused by both tectonic subsidence and eustatic sea level adjustment as the ice front receded. Rapid sea level rise (~12 mm/year) began following early Holocene glacial melting about 10,000 year ago. About 6,500 years ago, the rate of sea level rise gradually decreased. A marked decrease in sea level rise to about 2-mm/year occurred 2,000 years ago permitting the coastal wetlands to establish. Recent data provides different linear increase rates for different New Jersey locations; e.g., 4.06 mm/yr at Sandy Hook, 4.64 at Cape May; and 4.01 at Atlantic City (Kemp et al., 2013). Fluvio-deltaic sediments deposited during the marine transgression provided the foundation for intertidal sediment deposition and subsequent marsh formation.

The European settlement started in NJ as early as 1660 (The Official website for the State of New Jersey [http://www.nj.gov/nj/about/history/short\\_history.html](http://www.nj.gov/nj/about/history/short_history.html)) when the first permanent settlement was founded in Bergen. Subsequent agricultural and industrial activities induced changes in the environmental conditions that affected the coastal marshes, both by direct activities or indirectly through long-distance atmospheric and riverine transportation of various contaminants. The resulting increased pollution combined with the accelerated sea level rise over the last century, estimated from 3-3.2 mm/year to 4.4 mm/year as recorded at Atlantic City between 1912-1980, (Hicks et al., 1983; Miller et al., 2013; Kopp et al., 2014) are sources of continuous stress on modern day coastal wetlands. Consequently, restoring, enhancing, and maintaining the sustainability of our wetland assets has become the focus of wetland management programs. To be successful, these programs require knowledge of reference (background) conditions of coastal wetlands. Reasonable and achievable restoration targets can be set through the understanding of reference conditions and correlation of rates of ecosystem change over time and through natural and anthropogenic events.

The U.S. Environmental Protection Agency (EPA) approved New Jersey Wetlands Protection Plan (NJWPP) identifies the lack of knowledge on reference wetland conditions as a gap. Knowledge to fill this gap can be acquired through long-term monitoring programs. Unfortunately, these programs are sparse, relatively new, and introduced after the wetlands were impacted. The reconstruction of wetland systems based on investigations of sediment archives (cores) is a valuable tool to comprehend and quantify the magnitude of anthropogenic and natural impacts, thus filling the knowledge gap. In this project, we are using information obtained from sediment cores from four New Jersey coastal areas to track the impact of human activities since European settlement and provide quantitative information on reference conditions of NJ coastal wetlands. This information is essential to provide restoration targets that are historically meaningful, achievable, and can be employed to protect and sustain NJ wetlands. The main objectives of this study are: 1) assess wetland reference conditions and impact of anthropogenic activities; 2) assess the impact of climate and natural events (storms) on wetland characteristics; 3) refine the use of diatom (microscopic algae) species as indicators of coastal wetland ecological condition; and 4) inform future coastal wetland restoration targets.

## **PROJECT DESCRIPTION**

To meet project objectives, we are using information from sediment cores to track long-term environmental variations and the impact of human activities since the European settlement on NJ wetlands. In the absence of long-term monitoring data, the reconstruction of past environmental conditions based on investigations of sediment archives (cores) can provide a valuable tool to substitute for the absence of historical records. In this project, we are using biogeochemical proxies preserved in sediment cores, such as diatoms, pollen, and organic and inorganic contaminants, to reconstruct reference conditions and the impact of human and natural perturbances.

Investigation of such proxies preserved in sediment cores provide information necessary to understand how an ecosystem has changed over time, knowledge of natural reference conditions, and the magnitude of anthropogenic and natural perturbances. Whilst ongoing monitoring is essential to assess modern environmental conditions, current monitoring records in NJ extend back only a few decades, thus precluding a long-term assessment of these systems, and

only after they have been impacted by human disturbances. Hence, at present we are unable to establish a reliable assessment of the full range of natural variability and reference conditions, or the effects caused by anthropogenic pollution or extreme weather events (e.g., storms). Without this knowledge, it is difficult to produce metrics necessary to assist managers in identifying and quantifying causes of impairments, which in turn limits the establishment of restoration targets and protection goals that approach ecosystem equilibrium. Fortunately, in the absence of historical records, sediment archives can be used as a surrogate for environmental variability of the wetlands.

In this project we investigated sediment archives from a set of New Jersey wetlands from urban areas (e.g., Raritan Bay, northern Barnegat Bay) to the less developed areas of Great Bay, Cape May, and the Delaware Estuary. Reconstruction of reference conditions from urban areas will be of particular interest as they provide managers with specific information necessary to establish realistic restoration goals and implement programs to mitigate conditions as close as possible to those prior to human perturbations. Reconstruction of reference conditions for less developed areas will help to identify the impacts and rates of change observed in other wetland systems (e.g., Delaware Bay, Cape May, Great Bay). This information is critical to stakeholders to build, refine, and support programs for urban coastal wetlands restoration.

By providing information on wetland reference conditions and metrics based on biological indicators this project will inform and guide the following components of the EPA *Core Elements of an Effective State and Tribal Wetland Program* (<https://www.epa.gov/wetlands/core-elements-effective-state-and-tribal-wetlands-programs>):

Element 1: Monitoring and assessment, by providing a) quantitative information on natural, reference wetland condition (e.g., nutrient concentrations, salinity fluctuations, type of vegetation, etc.); b) a historical context and better understanding of the magnitude and direction of anthropogenic impacts affecting tidal wetland, littoral and riparian systems; and c) knowledge necessary to identify gaps in monitoring.

Element 3: Voluntary restoration and protection. This project will enhance integrated management and decision making based on more comprehensive knowledge of wetland systems degree of impairment necessary for developing restoration and conservation programs.

Element 4: Wetland specific water quality standards. This project will quantify

reference water quality parameters necessary to derive standards that are specific for different types of wetlands spanning a gradient of land-use types of various degrees of impairment. Thus, managers will be provided with information necessary to establish restoration goals to address impairments specific to urbanization as well as wetlands impacted by other types of natural and human factors.

The information gained through this project has the goal to inform and guide many of the NJWPP goals and objectives but will be of particular interest for : Core Element 1, Monitoring and Assessment, Objective 2 *Action 3: Establish reference condition – activities “Define reference condition (the gradient from unimpaired to impaired)”*; “*determine process for measuring reference standard condition; select reference sites using a systematic approach*” and by providing site-specific information that has the potential to strongly contribute to Objective 3, Actions 3 and 4, “*Improve the site-specific management of wetland resources*” and “*Develop geographically-defined wetland protection, restoration, and management plans*”.

We hope that our findings on human and natural impacts and wetland reference conditions will help guide future activities and can be incorporated in the NJWPP Core Element 2: Regulation; Core Element 3: Voluntary wetland restoration, creation, enhancement and protection and improved coastal shoreline resiliency; and core element 4: Water quality standards for wetlands. This project will provide the ability to “*Clearly and consistently define restoration and protection goals*” (Core Element 3, Objective 1); “*gathering information that would inform standards development*” (Core Element 4, Objective 1). We also hope that other objectives and core elements of the NJWPP may indirectly benefit and build upon the information yielded by this project.

## **PROJECT METHODS**

A plethora of research over the past few decades has demonstrated that aquatic sediments can faithfully archive indicators of environmental conditions prior to the onset of monitoring campaigns and modern anthropogenic disturbances. Indeed, paleoenvironmental reconstructions from sediment cores can extend our knowledge of baseline environmental conditions back decades to millennia (Fig. 1), and thus provide critical information to wetland managers pertaining to the longer-term behavior of these ecosystems.

Wetland sediments continuously accumulate and archive a rich population of biological and geochemical indicators that, with appropriate field, laboratory, and data analysis tools, can provide both quantitative and qualitative reconstructions of past ecosystem conditions. Like the pages of a history book, these sediment archives can be ‘read’ stratum by stratum and analyzed for preserved markers of ecosystem change. Each sedimentary layer preserves the ecosystem characteristics at the time of deposition. Therefore, a sediment core can provide a continuum of data reflecting conditions *before* and *after* disturbances, and as such, help to quantify the direction and magnitude of environmental changes prior to the instrumental records (Smol, 2008). For example, diatom species that live in clean environments are different from those that live in stressed (polluted) environments. Thus, the relative proportions of these species can be used as a proxy for past environmental conditions. In addition, other biogeochemical proxies preserved in such sediments (e.g. stable isotopes, organic biomarkers) can also be used to provide information on past environmental conditions.

Following the collection of a sediment core from the sites of interest, they were subsampled in successive intervals; radioactive isotopes (e.g., Cs-137, Pb-210, C-14) were used to provide core dating so that proxy-based inferences (see below) could be placed on an absolute time scale. Typically, quantitative inferences require two steps: (1) calibration, in which relationships between proxies (e.g. biota such as diatoms) and measured environmental parameters (e.g. nutrients) of interest are modeled using transfer functions; and (2) reconstruction of past parameters (e.g., nutrient concentrations) ‘down core’ using the model derived in step (1) inferred from the species composition and abundance of sub-fossil biological proxies (e.g., diatoms). Thus, a multiproxy paleoecological investigation (Fig. 2), coupled with examination of available data records and modeling efforts, can provide a comprehensive evaluation of the system examined (e.g., Rowell et al., 2016).

Standard paleoenvironmental methods (e.g., Smol, 1992) were used in this study. These include: coring marsh sediments; dating sediment intervals using radiocarbon and Pb-210/Cs-137; identification and enumeration of microfossils, such as diatoms and pollen; and reconstruction of past environmental changes using numerical techniques, such as transfer functions (Potapova et al., 2017) developed using standard biostatistical methods (Gotelli & Ellison, 2004; McCune et al., 2002).

## **Study area and field sampling**

Five sampling sites (sediment cores) were selected to cover specific areas of interest in regard to types of human impact. The selected wetland sites cover areas encompassing a human development gradient from the urban developed northern Raritan Bay and northern Barnegat Bay, to less developed/agricultural backbarrier wetlands from southern Barnegat Bay, Great Bay and Cape May, to the undeveloped and erosion prone Delaware Estuary northern shore wetlands (Fig. 3).

When available, data obtained from previous investigations (e.g., Nikitina et al., 2014 for the Sea Breeze site; Kemp et al., 2013 for Cape May; Kemp and Horton, 2013 for northern Barnegat Bay; and the diatom nutrient inference model developed by Potapova et al., 2017) were used to provide additional information to enhance the outcomes of this project. This ensured a cost-effective and more thorough investigation to add crucial ecological information to the existing body of knowledge on these wetland sites. Collectively, the combined data provided a network of coastal wetlands spanning the urban Raritan Bay and Barnegat Bay, to the less developed Great Bay, Cape May, and Delaware Bay. This allowed for the establishment of evaluated responses of varied types of wetlands in New Jersey to natural and anthropogenic change by comparing the modern and historic states of unprotected wetlands on the north shore of Delaware Bay (Seabreeze, Fortesque), with back-barrier wetlands on the Atlantic coast (Cape May, Great Bay, Barnegat Bay), and with wetlands along the urbanized coast of Raritan Bay (Cheesequake). These sites represent a variety of land-use histories, geomorphic settings, and differing socio-economic communities.

Cheesequake State Park is a protected preserve of 1,284 acres of parkland comprised mostly of tidal wetlands along Cheesequake Creek and low hilly forested uplands. The Cheesequake wetlands are unique in that the transitional zone from lower marsh to upland forest spans just a few yards in places. They are the site of mixing brackish sea water from Raritan Bay with freshwater run-off from the upland forest and developed land. Previous sediment core investigations by Psuty (1986) estimated the Cheesequake marsh to be at least 7,000 years old.

Urban development surrounds this park, that also has a long history of human activity. Early settlers developed and farmed the hills around the creek, which was navigable for

approximately two miles landward. Several industrial plants, primarily for the manufacturing of ceramics and housing material (Sim and Clement, 1944) existed within the park area in the mid-19th Century to early 20th Century. These human activities left a lasting legacy of hazardous chemical waste. On the north side of the park, a large brush covered hill is a closed landfill considered a superfund site. Additional impacts to the area include drainage channels to reduce mosquito infestations, and construction of NJ Route 35 and the Garden State Parkway (1946-1957) that cross the Cheesequake wetlands and have changed the natural tidal current circulation.

The Barnegat Bay-Little Egg Harbor wetlands are located along the central New Jersey coastline in the Atlantic Coastal Plain province. Barnegat Bay is a barrier beach/back-barrier lagoon system from Point Pleasant south to Little Egg Inlet. The variety of highly productive shallow water and adjacent upland habitats found in this system include barrier beach and dune, submerged aquatic vegetation beds, intertidal sand and mudflats, salt marsh islands, fringing tidal salt marshes, freshwater tidal marsh, and palustrine wetlands.

The Barnegat Bay-Little Egg Harbor watershed covers an area of approximately 1,700 km<sup>2</sup> and has been extensively developed over the past 70 years. The population of the watershed has increased substantially from the 1940s (40,000) to over 570,000 year-round residents (US 2010 Census Reports). During the height of the summer season the population can rise to approximately 1,000,000 (Potapova et al., 2014).

The Great Bay is located south from the Little Egg Harbor and is connected to the ocean via the Little Egg Inlet. In comparison to the Barnegat Bay-Little Egg Harbor estuary, the Great Bay watershed is considerably less developed. The Great Bay constitutes the estuary of the Mullica River, a large, relatively pristine, unaltered estuarine system comprised of open water, intertidal marshes, mudflats and sandflats. It is believed to be the cleanest estuary in the corridor from Boston to Washington, D.C., owing in large part to the fact that the majority of the watershed is protected by the Pinelands National Reserve, and includes several large federal and state wildlife management areas and state forests. For these reasons, this coring site was selected to represent current 'reference conditions' in contrast to samples from the Barnegat Bay-Little Egg Harbor and Cheesequake that have considerably more developed watersheds. This productive estuary supports a high diversity of aquatic and terrestrial habitats and species, with rare brackish and freshwater tidal wetland communities, plants, and invertebrates (Potapova et al., 2013).

The Cape May Courthouse coring site is located on the Cape May peninsula. This site also displays little evidence of modern human modification, and was previously investigated by Kemp et al. (2013) for its history of sea level fluctuations and recent high rate of sea level rise. The coring site is represented by a vegetated wetland with *Spartina alterniflora* (tall form) along the tidal channel, followed inland by high salt marsh *Spartina patens* and *Distichlis spicata*, and a water-logged brackish environment marking the transition of the salt marsh to the upland habitat (Meyerson, 1972).

Sea Breeze and Fortescue coring sites are located on the north shore of Delaware Bay. These areas are more prone to erosion, as the area transitions from a predominantly barrier beach coast of the SW Delaware Bay to wetlands (Pijanowski, 2016). The salt-marsh sediments preserved beneath these coastal wetlands are of particular interest for the fact that they provide a 2,500-year history of wetlands development and response to land-falling storms and other environmental changes. The salt marsh at the Fortescue project site is located south of the Fortescue Wildlife Management Area, at a distance of 20-km south of the Sea Breeze wetland coring site. These sites are currently affected by erosion as evidenced by the retreat of their shorelines as well as subsidence marked by conversion of functioning vegetated salt marshes to open water. The lack of beach protection has resulted in erosion events induced by past storms/hurricane land falls which have been preserved in the wetland sediment record as abrupt depositional changes (Nikitina et al., 2014). For these reasons, these coring sites have been selected to investigate wetland response and recovery to climate disturbances.

The exact location of the coring sites was selected in close consultation with all project collaborators and is presented in Table 1 and Figure 3. An additional coring site that was initially planned for Union Beach (Raritan Bay) has been cancelled because preliminary finding of sediment perturbation and mixing induced by the high energy system of this coastal area.

Sediment cores were collected using an Eijkelkamp coring system (Fig. 4), which allows for compaction-free samples from tidal wetlands (<https://en.eijkelkamp.com/products/augering-soil-sampling-equipment/peat-sampler.html>). We obtained cores at least 1-m long to be able to reach the pre-European settlement time period. This estimated core length is based upon previous work performed on sediment cores from Delaware River and Barnegat Bay wetlands which found approximately 5 to 10 year/cm sediment-accumulation rates (Velinsky et al., 2011). This

implies that 1-m long cores should encompass approximately a 500 to 1,000 year time interval. In addition, longer cores were collected in 50 cm increments using a peat sampler, extending to a depth of ~ 2 m or to the base of the Holocene sequence. Core samples were stored in halved PVC pipe and carefully wrapped in polyurethane to minimize exposure to air and drying of sediments. Replicate cores were collected within a 1 m<sup>2</sup> area to ensure stratigraphic consistency between replicate cores and to enable sufficient recovery of material for all laboratory analyses.

In addition to the Eijkelkamp coring an interdepartmental collaboration with the New Jersey Geological and Water Survey (NJGWS) allowed for extraction of sediment cores from Cheesequake with a truck-mounted Geoprobe<sup>®</sup> (performed by Gregg Steidl, NJGWS). Using the Geoprobe<sup>®</sup>, precision samples were collected using hydraulic direct push technology. A truck mounted Geoprobe<sup>®</sup> 540 employing the Macro-Core Four (4) foot open tube sampler allowed recovery of the entire Holocene sediment sequence, which was used to produce lithological profiles for this study area (Appendix 1).

### **Core subsampling**

The sediment cores were brought to the Rutgers University laboratory and sliced into 1-2 cm-long stratigraphic intervals depending on the sediment type and consistency. A subsampling protocol was established in each core for the various proxies analyzed. From specific intervals, according to the subsampling protocol, 1 or 2 cubic centimeters (CC) were subsampled for each diatom and pollen analysis and the remaining sediment was used for chemical and chronological analyses. The samples were stored according to the parameter of interest (diatoms, pollen or chemical components) and prepared according to the procedures described below.

### **Core chronology: Carbon-14, Pb-210, and Cs-137 dating**

Carbon-14 analyses were done on sediment core recognizable organic matter (plant macrofossils) by the National Ocean Science Accelerator Mass Spectrometry (NOSAMS) facility at Woods Hole <http://www.who.edu/nosams/radiocarbon-data-calculations>. Plant macrofossils were cleaned under a microscope to remove any contaminant sediment particles and then dried at 50 degrees Celsius. Radiocarbon ages from NOSAMS were calibrated using

CALIB (Stuiver and Reimer, 1993) and the IntCal09 calibration data set (Reimer et al., 2011). An age-depth model was produced using the Bchron package in the software R (Haslett and Parnell, 2008; Parnell et al., 2008). Bchron uses a Bayesian model to incorporate prior assumptions with provided radiocarbon results to estimate age for every 1 cm in a core with a 95% uncertainty interval.

$^{210}\text{Pb}$  and  $^{137}\text{Cs}$  activities were measured via gamma spectroscopy (661.7 keV photopeak). First, the sediment samples were dried at 60 °C in an oven until constant weight and then dry bulk density and water content were determined. Samples were then homogenized by grinding, packed into standardized vessels, and sealed for >30 days before counting for at least 24 hours. Gamma counting was conducted on low-background, high-efficiency, high-purity Germanium detectors coupled with a multi-channel analyzer. Detectors were calibrated using natural matrix standards (IAEA-300, 312, 314) at each energy of interest in the standard counting geometry for the associated detector. Activities are corrected for self-adsorption using a direct transmission method (Cutshall et al., 1983; Cable et al., 2001). Excess  $^{210}\text{Pb}$  activities were determined by subtracting total  $^{210}\text{Pb}$  (46.5 keV) from that supported by  $^{226}\text{Ra}$ .  $^{226}\text{Ra}$  was determined indirectly by counting the gamma emissions of its granddaughters,  $^{214}\text{Pb}$  (295 and 351 keV) and  $^{214}\text{Bi}$  (609 keV), in secular equilibrium with  $^{226}\text{Ra}$ . Sedimentary processes are complex and there is not a unique model to provide a chronology based on excess  $^{210}\text{Pb}$ . The simple model (Robbins, 1978) and the constant rate of supply model (CRS; Appleby and Oldfield, 1978) were used in this project.

### **Total Petroleum Hydrocarbons: PAHs, PCBs and OCPs**

Sediment sample analyses followed SW-846 procedures. Sediment samples were extracted by Accelerated Solvent Extractor (ASE) (DIONEX ASE 100). ASE is a Pressurized Fluid Extractions (PFE) device (Method 3545). About 0.5 g sediment sample and ~16 g baked Prep Diatomaceous Earth (Prep DE) (baked in furnace for 4 hrs. at 450°C) were added into a baker to ensure the sediment sample was dry.

After sample extraction, all sediment samples being analyzed for semi-volatile organics were subjected to Method 3640, Gel Permeation Chromatography (GPC). Florisil cleanups (Methods 3620) were performed for analyses of pesticides and PCBs.

Sample extracts were analyzed for the 16 PAHs by Agilent 6890N gas chromatography and 5975 inert mass spectrometer (GC/MS) operating in the selected-ion-monitoring (SIM) mode, using a 30m Agilent HP-5MS (or equivalent) and an Agilent 5975 detector (or equivalent), according to MERI SOP #1030 (<http://meri.njmeadowlands.gov/lab/>). PAH compounds were quantified using the internal standard method. Chromatographic resolution was achieved with 30m x 250 $\mu$ m x 0.25  $\mu$ m HP-5MS capillary column (Agilent, Palo Alto, CA) with helium carrier gas. PAHs were quantified by GC-MSD using SIM and the method of internal standards. The PAHs analyzed in this study are listed along with the primary and secondary ions from their mass spectra (Table 2). The analytical quality of data were determined using field blank and recoveries of surrogate standards and a series of performance standards including internal standards.

### **Trace metals**

All sediment samples were digested using the modified EPA method 3051 for microwave-assisted acid digestion. First, 10 ml HNO<sub>3</sub> was added to the 0.5 g sediment sample. After pre-digestion for two hours at room temperature, vessels were sealed and placed in the MiniWAVE microwave digestion system (SCP Science, Canada). After digestion, samples were diluted with ultrapure DI water to 50 ml. Samples were subsequently stored in polypropylene sample tubes at 4 °C until further analysis. An Inductively Coupled Plasma-Mass Spectrometer (ICP-MS; Agilent 7700X, Palo Alto, CA) was used for measurement of metal and other element concentrations in the sample digests. All samples for these analyses were stored frozen until sample digestion started. The metal species list and associated methods and Method Detection Limit (MDL) are listed in Table 3.

PAH results are reported in micrograms per kilogram ( $\mu$ g/kg) and metal results in milligrams per kilogram (mg/Kg) on a dry weight basis. Lab analyses were performed by the Meadowlands Environmental Research Institute (<http://meri.njmeadowlands.gov/lab/>), a NJDEP certified analytical laboratory.

## **Sediment nitrogen**

Sediment total nitrogen (TN) was analyzed by Dr. Michael Griffiths laboratory at William Paterson University using a Perkin Elmer Series II 2400 CHNS/O Analyzer. Prior to analysis, ~3 g of sediment was placed in a porcelain dish, pre-treated with 20% HCL, and heated for 3 hours at 75°C to remove carbonates. Samples were then wrapped in Sn capsules before being analyzed on the Perkin Elmer CHNS/O analyzer. The analyzer was calibrated daily to compensate for any changes in pressure. Blanks, standards, and k-factors (Acetanilide) were run every 10-20 samples to calculate uncertainty. Instrumental drift was assessed using an internal standard. Detection limit for the instrument is ~0.05%.

## **Diatom analysis**

Protocols for diatom samples preparation and analysis are described on the USGS NAWQA sample analysis protocols. Sediment sample digestion for diatom analysis is described in the ANSP protocols (<http://diatom.ansp.org/nawqa/Protocols.aspx>) to make quantitative slides. Samples were digested using strong acid in a specifically designed microwave (CEM model MDS-2100) with enclosed vessels, temperature and pressure monitoring and control systems. The cleaned samples were rinsed at least 6 times using distilled deionized water before the slurry is allowed to evaporate. Diatom-coated coverslips were mounted on glass slides using Naphrax<sup>®</sup> mounting medium. Two slides were made for each sediment sample processed. Except for very sparse samples, at least 400 diatom valves were identified and counted from each of the samples at a magnification of 1,000X or higher. Identifications were made to the lowest taxonomic level (e.g., variety) and followed the taxonomy system developed by Dr. Potapova & N. Desianti, Ph.D. student, for the NJ-funded Barnegat Bay diatom indicators project (Potapova et al., 2013; 2014; Potapova and Desianti, 2015). Scanning electron microscopy was used in many instances to confirm taxonomic identifications.

A total of 600 species were identified, one third of them being new to science, for development of transfer functions. The identification of diatom species in sediment cores from this project is consistent with the data generated for the calibration set from previous projects (Potapova et al., 2013, 2014), as the same principle investigators conducted the counts and identifications.

A total of 402 diatom samples were analyzed (369 samples by N. Desianti, and 33 by M. Enache) within this project, about three times more than what was initially planned. The high number of diatom samples analyzed allowed for the development of a new calibration set for quantitative inferences (Desianti, 2017, in preparation), and provided more detailed information on natural variability in study sites and impacts from anthropogenic and natural disturbances. All diatom data will be contributed to the NEOTOMA Paleocology Database and Community (<https://www.neotomadb.org/>) after project completion and publication of results.

### **Pollen analyses**

Pollen extraction from sediment samples was done at USGS by Chris Berhardt and analyzed by Jennifer Clear at Rutgers University by following the standard technique of Faegri and Iversen (1989) with cover slips mounted using clear nail polish. Lycopodium was used as a marker for calculation of pollen species absolute abundances. Identification of pollen grain was based on published pollen catalogues in McAndrews et al. (1973) and Moore et al. (1991). Pollen morphology of the *Ambrosia* pollen grain (a genus of the *Asteraceae* family) is echinate, tricolporate, and varies in size between 16-27 microns (Kapp et al., 2000). The major two morphological characteristics to identify the grains are 1) short spines on the surface of the exine surface and 2) the presence of three cavities in proximal and distal views of the grain's surface. These two morphological characteristics make the grain very distinct from other pollen grains. Once identified, all grains were compared with images provided in pollen keys and online resources. Further, each grain was carefully examined under 40x magnification to verify the presence of the extexine foot layer. Counts were done by systematically starting at the upper left-hand corner and proceeding to the right-hand corner horizontally. The sharp increase in abundance of *Ambrosia* pollen was used to identify the timing of European settlement marked by extensive forest clearing and expansion of the *Ambrosia* weed. A total of 46 samples were analyzed for pollen across all study cores. The *Ambrosia* pollen results were incorporated in the age-depth model (see above).

## **Land-use data**

Historical land-use analysis of the selected study areas has been performed. Historic land-use data was acquired by digitizing and classifying aerial photography from as early as the 1930s. Land-use profiles for buffers around each coring station were generated based on aerial photography from 2012, 1974, and early 1930 (NJGIN; 1930 to 2015 data). The NJDEP 2012 land-use/land-cover data (NJDEP, OIRM, BGIS 2015) was generated from the 2012 imagery. The 1974 land-use profiles were developed by using the NJDEP 1986 LULC data (NJDEP, OIRM, BGIA 1998) as the starting point for cover reclassification. The 1930 land-use profiles were developed by using the created 1974 land-use data and reclassifying polygon classes as necessary. Land-use/land-cover classes included forest lands, wetlands, water, barren land, agriculture, and altered/urbanized land. Profiles summarized the sum and percent of each class in buffers extending to five and ten km from the core location. Land-use categories included forest, wetlands, water, urban (developed) land, agriculture, and barren land.

Data editing and land-use/land-cover reclassification assignments were completed using ArcView 10.4 Geographic Information System (GIS) software (ESRI Inc., Redlands, California). During reclassification, a new attribute field was created to hold the new land-use class. During editing, each polygon was either merged with similar land-use polygons or modified and reclassified to fit the shape and category of the land usage as depicted on the aerial imagery. Interpretation was done using a variable scale of 1:4,000 – 1:10,000.

Each land-use layer was then intersected with the buffers to determine how much of each land-use type made up the area within each of the buffer areas. Polygon geometry was recalculated after the intersection. The data were summarized to show the amount and percentage of each land-use type in each buffer. The combined percentage of forest, wetlands, and water was also determined for each site within each buffer for each of the three time periods.

The temporal land-use profiles developed for each of the study areas were related to shifts in diatom communities in effort to explain ecological changes in diatom species.

## **Data Analysis: Reconstruction of past environmental changes**

Diatom-based transfer functions were generated through a three-year Barnegat Bay project and additional surface samples collected during the 2017 spring season from New Jersey wetlands. These tasks were all performed by PhD student Nina Desianti under the supervision of Dr. Potapova at the Academy of Natural Sciences of Drexel University (ANSDU) (Desianti, 2017, in preparation). The diatom-based transfer functions and the down core quantitative reconstructions were performed using the C2 software (Juggins 2003) or R platform. Inferred values were generated for salinity and nutrient concentrations (N) and compared with contaminants in core samples and the percentage of land use in the surrounding landscape. Paleolimnological studies have determined that this approach is ecologically realistic, statistically robust, and numerically accurate (ter Braak and van Dam, 1989; Birks et al., 1990; Dixit et al., 1999).

Series of radiocarbon and Pb-210 and/or Cs-137 dated stratigraphic profiles were generated for diatoms and measured sediment contaminants, as well as diatom-inferred values for past nutrients, salinity, and marsh habitat. Records of past human-induced events in the proximity of sampling sites are also considered. Biogeochemical characteristics inferred in pre-European stratigraphic intervals are used to provide information on reference conditions and wetland natural variability.

## **RESULTS AND DISCUSSION**

### **Core chronology**

The age-depth model for the Cheesequake State Park, New Jersey site location revealed a 2,000-year sequence through 2.4 meters of sediment. Accumulation of sediment occurred at a mean rate of 1.2 mm/year through this time period. The Cape May County, New Jersey site spans 1,300 years in 2 meters of sediment. Organic sediment accumulation began around 700 AD; between 700 AD and 1850 AD, sediment accumulation was approximately 1.3 mm/year, which increased to 3.9 mm/year after 1850 AD. In Sea Breeze (Delaware Bay), 4 meters of sediment provided a 2,200-year record. Therefore, the mean rate of sediment accumulation was 1.8 mm/year.

C-14 results for the Cheesequake core are presented in Table 4. The age-depth model created based on composite chronology calculated from AMS  $^{14}\text{C}$  together with pollution history,  $^{210}\text{Pb}$ , and the  $^{137}\text{Cs}$  gamma spectroscopy produced a multi-decadal temporal precision (Fig 5).

For the Cape May core, C-14 dating results are presented in Table 5 and the age-depth model is illustrated in Fig. 6

The chronologies of Barnegat Bay and Great Bay cores were based on  $^{210}\text{Pb}$ ,  $^{137}\text{Cs}$ , gamma spectrometry and  $^{14}\text{C}$  dates performed at the bottom interval of each core and are described in Velinsky et al. (2011) and Potapova and Desianti (2015) report to NJDEP (<http://nj.gov/dep/dsr/barnegat/final-reports/>). Briefly, Core BB1, the northern most site extends back in time to 1630 common era (CE); BB2 produced a sediment record starting in the early 15<sup>th</sup> century; core BB4 stratigraphic sequence extends back in time to 1670 CE; and the Great Bay core goes back in time to 1832 (Potapova et al., 2014).

Chronologies for the Sea Breeze and Fortescue cores SB30, F9 and F11 were established using  $^{14}\text{C}$  and  $^{210}\text{Pb}$ ,  $^{137}\text{Cs}$  and pollutant history (Pb fallout from un-leaded gasoline peaked in 1979) for dating the upper part of the SB30 core (Figs 7, 8 and 9). All storm events from Sea Breeze (SB-30) and Fortescue (F11 and F9) cores were dated using  $^{14}\text{C}$  (Table 6).

### **Delaware Bay litho-stratigraphy of storm erosion events**

Sea Breeze stratigraphy (Figs 8, 9). Six lithostratigraphic units were recognized in the sediment underlying the Sea Breeze salt marsh. These six units and associated erosive boundaries were correlated across the Sea Breeze area from core logs described in Nikitina et al. (2014). Briefly, the Sea Breeze salt marsh is uniformly underlain by pre-Holocene fluvial deposits of gray sand, overlain by a paleosol constituted of black, humic sandy mud. A dark brown to black basal peat with fragments of *Schoenoplectus* spp. follows in the majority of cores at elevations below  $-2.5$  m NAVD88, dated 290 BC  $\pm$  40 years. The authors considered that this peat was likely deposited in a brackish environment at the transition between the salt marsh and freshwater upland; and is similar to the modern transitional environment at Sea Breeze. A gray-brown, fibrous peat with *Spartina patens* and *Distichlis spicata* macrofossils indicating that it accumulated in a high salt-marsh environment overlies the paleosol and brackish saltmarsh

deposits. Above the high salt-marsh peat units, a gray mud occurs at different stratigraphic levels and represents tidal-flat and low salt-marsh depositional environments. Vertical stems of *S. alterniflora* deposited above the tidal mud illustrate colonization by low salt-marsh vegetation. Finally, a last unit represented by gray-brown muddy peat with abundant *S. alterniflora* fragments was described as deposited in a low salt-marsh environment (Nikitina et al., 2014).

The contacts between the high saltmarsh peat and overlying mud are sharp (~1 mm), suggesting an abrupt change in the sedimentation regime and environment of deposition, which were interpreted as marsh erosion caused by powerful storm events. These erosion events were enumerated 1 to 8, from oldest (lowest in core) to the youngest storm event; the 8<sup>th</sup> event was not recorded in all core sequences (Nikitina et al., 2014, 2015).

In this project, we used core SB-30A to improve our understanding of erosional boundaries and timing of the events and the changes in nutrient concentration and salinity associated with these disturbance events. Four sequences were recognized in core SB-30, the bottom sequence that extends from 307 cm to 231 cm, was interpreted as the erosional sequence produced by two storms and corresponded to sequences 2 and 3 in the original publication of Nikitina et al. (2014). The other sequences were documented but the time of their occurrence were poorly dated. In this study, we constrained the occurrence of the events by dating the sediments immediately below erosional contacts. For sequences 2 and 3, it was established that the erosion occurred between AD 679 and AD 1012. During this period the high marsh was eroded and the exposed surface was infilled with sub-tidal mud. *S. alterniflora*, a low-salt marsh plant colonized the tidal flat at the depth of 254 cm below the surface, and *S. patens* a high marsh plant established at the depth of 244 cm by AD 893-1012. Sequence 5 from 183 cm to 116 cm was produced by storm events between AD 1324-1644.

We analyzed for changes in diatom assemblages and associated environmental conditions associated with the storm erosion event located at 183 cm depth and dated 1324 AD. Forty-four (44) cm of high marsh sediments were eroded during this event, the space was infilled, the low marsh environments were established by AD 1516-1644, and subsequent high marsh was established by AD 1665. The upper part of the core was analyzed for the assessment of anthropogenic impacts and was analyzed for diatoms, organic and inorganic pollutants.

Fortescue stratigraphy (Fig 8). Two cores from the Fortescue study area were retrieved and analyzed for this study. Six lithologic units were identified in both cores: fine to medium sand, dark brown to black compacted peat, gray mud, organic rich mud with fragments of *S. alterniflora*, grey-brown muddy peat with *S. alterniflora* and *S. patens*, brown peat with *S. patens*. These lithologic units were interpreted as pre-Holocene fluvial sand deposits, basal peat, sub-tidal mud deposits, low-marsh organic rich sediments (peat/mud), high-marsh peat.

The stratigraphy documented several abrupt changes in the sediment deposition, similar to Sea Breeze stratigraphy described in Nikitina et al. (2015). In core F-9F five sequences were documented at the depth of 276-250 cm, 250-220 cm, 220-132 cm, 132-70 cm and above the abrupt contact at 70 cm below the surface. The sequence above the abrupt contact at 220 cm correlates well with Sea Breeze sequence 2/3 at the depth of 307-244 cm and possibly were produced by similar storm events that occurred between AD 679-943.

Stratigraphy of core F11-A documents erosional contact at the depth of 191 cm that overlays high-marsh basal peat unit. Post erosion deposition includes 28 cm of mud overlaid by 33 cm of low marsh sediments and high-marsh peat at the depth of 130 cm. The estimated time period for the erosion was between AD 594-1269. The time span for marsh recovery from vegetation of tidal flat with *S. alterniflora* to high marsh was ~168 years.

## **Pollution histories**

Results for the organic pollutants are available for Cheesequake, Cape May and Sea Breeze cores and are presented in Figures 10-12.

### **Cheesequake**

In the Cheesequake sediment core the Polycyclic Aromatic Hydrocarbons (PAHs) were analyzed in 15 sub samples between 0 – 70 cm at 3 cm intervals between 0 and 21 cm, 6 cm intervals between 21 and 57 cm, and 12 cm interval from 58 to 70 cm representing a total of 379 years for a time period extending from 2015 to 1636 CE. Total PAH values ranged from 4,010 µg/kg in 1636 to 7,976 µg/kg in 2006. The maximum PAH values for all 16 PAHs were recorded in 2015.

A general trend observed in 4 PAHs; Acenaphthene (Acy), Fluorene (F), Phenanthrene (P) and Anthracene (Ant) suggest organic pollution was low until early 1900's with the exception of a temporary rise in Acy, P and Ant at approximately 1726 CE. This could be indicative of burning biomass associated with the early 1700's settlement activities. After 1921, there is a declining trend in PAHs observed until 1952, when PAH values begin to rise until the present day. One exception to rising PAHs is a decline observed during mid-1970s, potentially due the Environmental Movement leading to Federal legislation e.g. Clean Air Act (1970) and Water Pollution Control Act (1974). The P:Ant ratio of 0.97 – 1.0 throughout the record indicates that combustion, i.e. biomass burning and vehicle emissions, is the dominant source of PAHs.

Naphthalene (N) is present from the late 1600's with values ranging from 0 – 285 µg/kg. Values of 0 µg/kg (absence) are recorded in 1866 and 1974. A rise in N around 1900 is followed by a decline from 1931, potentially linked to the Great Depression between 1929 and 1939. Since 1974 there has been a steady rise in N to the present day (2015). N is a by-product of coal tar and petroleum refining and is still used in many household products.

Acenaphthylene (Acy) a PAH indicative of combustion (biomass burning and vehicle emissions) values range between 425 – 817 µg/kg. There are two declines in Acy; a dip at 1906 and prolonged decline between 1931 and 1974, but sharp increase afterwards.

Fluoranthene (Fl) and Pyrene (Py) are only present in 1931, 1952 and 2015 and the Fl:(Fl+Py) ratio sum of 0.44 – 0.5 indicates industrial combustion. Benz(a)anthracene, Chrysene, Benzo(b)fluoranthene, Benzo(k)fluoranthene and Benzo(a)pyrene are all present in 1931 with Benzo components still present in 1952.

### Cape May Courthouse

For the Cape May Courthouse core, a total of 16 individual Polycyclic Aromatic Hydrocarbons (PAHs) were analyzed in 15 sub samples at approximately 5 cm intervals between 2 and 73 cm. The time period extends approximately 300 years, between 1698 and 2016 CE. Total PAH values ranged from 2290 – 5814 µg/kg with maximum PAH values in 1978. There are two periods of increased PAHs; the first at approximately 1850 CE during the onset of the

Industrial Revolution and the second peak in PAHs between 1964 and 1978, during the Great Acceleration.

A general trend was observed in five PAHs; Acy, Ace, F, P and Ant rise after 1949 CE, and peak at 1969 – 1978 CE. The P:Ant ratio sum of 0.98 – 1.0 throughout the record indicates that combustion i.e. biomass burning and vehicle emissions is the dominant source of PAHs (Yunker et al 2002). Other components, Fl and Py are only present in 1949 and 1957 CE. The Fl:(Fl+Py) ratio sum of 0.47 in 1949 indicates industrial combustion. Carcinogenic benzo[a]pyrene is only present in samples during the years of 1949 CE (82 µg/kg) and 1998 CE (105 µg/kg) potentially due to the increase in war-time industry and the rise in the use of diesel automobiles, respectively. Naphthalene is present from the mid 1800's during the industrial revolution, then values increase two-fold post-world war II, and peak at a maximum of 256 µg/kg in 1998 CE. Sources of Naphthalene include the distillation of coal tar (oil contains approx. 50% naphthalene) and petroleum refining. Naphthalene is the only PAH to rise between 1978 and 1998 CE and is still used in many auto, household and pesticide products (Bailey et al, 2015).

### Sea Breeze

For the Sea Breeze core 30A a total of 16 individual Polycyclic Aromatic Hydrocarbons (PAHs) were analyzed in 8 sub samples at 8 cm intervals between 1 (2016 CE) and 57 (~1945 CE) cm (Fig. 12). Total PAH values range between 1,985 – 5,515 µg/kg with maximum PAH values at 9 cm, and minimum recorded at 1 cm. There are two periods of increased PAHs; at 9 cm (~2009) and at 41 cm (~1965).

This trend is observed in 3 PAHs; Acenaphthylene (Acy) Acenaphthene (Ace) and Fluorene (F) suggesting a common source likely combustion of fossil fuel. Further trends observed in Phenanthrene (P) and Anthracene (Ant) peak at 41 cm (~1965 CE) with a declining pollution signal throughout the rest of the core. Both Fluoranthene (Fl) and Pyrene (Py) are only present at 57 cm and 41 cm. A peak in Naphthalene (N) of 159 µg/kg at 49 cm (~1955) is the only presence of N throughout the core and occurs when all other PAH values record a minimum or absence.

Trace metals were measured along with the organic pollutants in the cores from the same study sites. A total of 50 trace metals were measured in the Cheesequake core, 51 in Cape May Courthouse, 52 in Barnegat Bay core BB1, and 21 in Sea Breeze. Changes in select metals through time and depth in the cores are presented in Figures 13-16. Minimum, Maximum, Average, Median and 90<sup>th</sup> percentile for each measured trace metal are presented in Tables 7-10. Contrary to PAHs which are only of anthropogenic origin, metals can be present due to both natural and anthropogenic sources (Morais et al. 2012). Wetland sediments become a repository for metal loads via watershed runoff, as well as deposition of airborne contaminants. Thus, the examination of pollutants in sediment cores can provide a long-term integrated source of information for the wetland environmental quality.

Metals that are considered of concern for human health are As, Cd, Cr, Cu, Pb, Ni, Se and Zn (Mugdall et al. 2010). Increased metal concentrations can originate from various sources, both local and regional. In most cases high metal concentrations in soil and sediments are related to industrial activities occurring after the industrial revolution of mid-19<sup>th</sup> century. Other sources are the application of biosolids from waste water treatment and other by-products used as fertilizer in agriculture. Elevated Pb concentrations are mainly caused by gasoline emissions prior to 1980 or paint from old houses. Anthropogenic arsenic (As) is mainly caused by pesticides use in agriculture or leaching from pressure treated lumber. In order to protect human health and ecosystems, the US EPA (2002) established screening levels for use in soils to guide cleanup efforts. More stringent values may be used by states (e.g., NYS DEC 2006).

The most abundant metals found in the Cheesequake core were Na, Fe, Al, Ca, and Mg. In Barnegat Bay BB1 and Cape May Courthouse cores, Al, Na, Fe, K, Mg dominated while in the Sea Breeze core, Fe, Al, Zn, and Ti were the most abundant metals. Concentrations that exceeded the EPA (2002) published soil screening levels were found in the Cheesequake core for As (3-44 mg/Kg) exceeding the 0.4 mg/Kg EPA value; Cd (0.03-0.61 mg/Kg) exceeding 0.43 mg/Kg maximum level for unrestricted use; Cu (4.1-310 mg/Kg) exceeding the maximum 270 mg/Kg EPA guidance level; and Pb (4-224 mg/Kg) exceeding the 200 mg/Kg EPA value. Similarly, in the Barnegat Bay BB1: As (2.2-13.13mg/Kg) and Cd (0.03-0.73 mg/Kg); Cape May Courthouse core: As (3.4-14 mg/Kg) and Cd (0.04-0.47); and Sea Breeze core: As (3.9-38.4mg/Kg) and Cd (0.2-1.39 mg/Kg) are exceeding the EPA screening levels at various intervals throughout the cores and are associated with the post-industrial activities (Figs 13-16).

Trends in sediment metal contaminants recorded in the cores strongly reflect the human activity history associated with the European settlement, especially in the areas with intense post-settlement activities, such as the Raritan Bay and northern Barnegat Bay. However, metal increases were also recorded in areas that were less impacted by direct industrial activities, such as Great Bay, Cape May and Delaware Bay.

In Cheesequake, extensive beds of clays exist close to Raritan Bay and Cheesequake Creek; these were used by the early European settlers as the main sources of raw material for the stoneware industry. In 1770 the Morgan pottery was founded, and Cheesequake became an epicenter of the colonial stoneware industry, with two potteries manufacturing salt-glazed stoneware (Morgan and Warne & Letts) considered among the most important historically for their role in fostering the growth of the domestic stoneware industry. The stoneware manufacture industry started to decline early 19<sup>th</sup> century and lasted nearly three-quarters of a century by the time it closed in 1835 (Branin, 1988; Sim and Clement, 1944).

Concurrent increases in Al, Fe, Ni, and Cd (Fig. 13) in the stratigraphic record during that time period appear to be related to smelting. Furthermore, sharp increases in metals (Cu, As, Hg, Pb) may reveal the impacts from chemical dumps, fly ash, and landfills resulting from the growing industrial activities associated with the post-1850s industrial revolution. Spikes in Zn, Cd, Ni around 20-cm depth in the core (late 1930's) could be related to the use of waste incineration in NY (Walsh et al., 2001) that ceased in 1970. A spike in Zn in 1653 occurred prior to the European arrival and could not be related to human activities. A similar temporal spike in Zn was recorded in the Cape May Courthouse core and it is possible that this spike was related to a regional signal from increased volcanic activity worldwide after 1640 (Newhall and Self, 1982; Briffa et al., 1998).

In Barnegat Bay BB1 core, background metals values are occurring up to the 1700s, followed by concurrent increases in Mg, Cr, Mn, Fe, Co, Cd, and Ni, also reflecting impacts from the early settlement mining and smelting activities. These trends mirror similar increases recorded in the same time period at the Cheesequake site. After declining in mid-1800's, inputs of these elements to the Barnegat Bay wetland increased again after the industrial revolution (Fig. 14).

Although less industrialized and mostly retaining rural status after the European settlement, increases in metal concentration are also exhibited by Cape May and Sea Breeze sediment cores. Spikes in Al, Ti, and Co were already present in the late 1700's – early 1800's, but the most marked changes in metal inputs were related to the post-1850 industrial revolution marked by higher levels of Cd, Zn, Ni, and Fe. A drop in Fe is visible during the first half of the 19<sup>th</sup> century. This could be related to the extensive bog iron mining of limonite ore naturally occurring in the Pinelands area. The high levels of Fe present in the pre-European sediment intervals indicate that this element was likely a natural source to the wetlands. Similar to the other cores, trends related Pb from the use of leaded gasoline are present until 1980 (Figs 15, 16).

Decreases in many metal concentrations are displayed in all cores after the EPA implementation of pollution control regulations in the 1970s. However, some metals of concern to human health are showing consistent increases over the last few decades, such as Cu, Zn, and As, e.g., in Barnegat Bay. Despite the fact that industrial activities exerted less impacts after the 1970s EPA regulations, the population growth in urban areas is now considered a strong contributor to non-point source emissions over the last few decades. For example, Cu, Zn, and Pb were shown to increase due to urban traffic via tire and brake wear (Hwang et al., 2006). This is supported by the strong increase in urban population over the last few decades in all sites, except for Delaware Bay sites, occurring concurrently with these increases in metal concentrations.

The 1-m long Sea Breeze stratigraphic record encompassed only the last 130 years; thus, we could only assess changes in trace metals over this time frame and values for reference concentrations are not available. Increases in As, Cd, Co, and other metals visible in the stratigraphic record up to approximately 1970 are likely related to industrial activities. The most notable feature is a marked increase in Hg since the early 2000's.

Al and Fe are normally found in high quantities naturally and considered reference metals that are used to normalize the concentration of anthropogenically sourced metals (Hwang et al., 2006). In our cores, both elements displayed fluctuations through time that could be related to both industrial activities and watershed transportation processes. Such variations would be important to consider while using these elements for ambient estimates of metal enrichment in modern samples.

Background metal values prior to 1700, post settlement (1700-1970) and post 1970 values are shown in Table 11.

## **Diatom analysis**

Sediment core changes in diatom assemblages are presented in study sites from northern to southern NJ wetlands, and include results from the Barnegat and Great Bay cores analyzed previously through a NJDEP-funded project. Stratigraphic plots of diatom species enumerated in each core are presented in Figures 17-26.

Cheesequake State Park core. Diatoms were counted in 69 samples from 0 to 250 cm depth in the Cheesequake core, with every 1 cm-thick sample analyzed in the upper 20-cm section. CONISS identified two diatom zones in the core. The first zone covering the depth from 250 cm up to 44 cm, maintained a remarkably uniform diatom assemblage dominated by *Diploneis smithii*, *Navicula peregrina*, *N. hanseatica*, *Caloneis bacillum*, *Rhopalodia musculus*, *Decussata placenta*, *Paralia sulcata* and *Cyclotella striata*. These diatoms are commonly found in intertidal habitats in the absence of nutrient enrichment. The transfer functions also indicated stable diatom assemblage with respect to nitrogen concentration and absence of sharp salinity fluctuations.

The transition to the second diatom zone at 44 cm depth (~CE 1760) was also identified as a major shift by the change-point analysis. This transition was mostly caused by the loss or sharply decreased abundance of *Decussata placenta*, *Navicula peregrina*, *Cyclotella striata*, *Paralia sulcata* and proliferation of nitrogen-tolerant species *Nitzschia microcephala*, *Navicula* sp. 63 and *Planorbulina cf. frequentissimum*. Application of the nitrogen transfer function shows sharp nitrogen increase over the course of the 19<sup>th</sup> century (from an average 0.4 to 1.1 mg/g), which may be caused by eutrophication of Raritan Bay during that time.

Another zone of considerable change in diatom assemblage composition occurs at the depth of 14-16 cm (CE 1930-1940). At this time, there was a decrease in abundance of *Nitzschia microcephala* and increase of *Chapmaepinnularia* aff. *begeri*, *Diploneis smithii*, *Luticola mutica* and *Navicula isabelensiminor*. Species characteristic of subtidal and lower intertidal zones increase in abundance in the upper portion of the core corresponding to the last 50-60 years as

reflected by the increase of reconstructed salinity values and drop in reconstructed nitrogen values (Fig. 17). While this shift may indeed be linked to increased tidal inundation because of sea level rise, the loss of nitrogen is possibly due not to an improvement in water quality, but rather to the overall loss of organic matter inputs due to increased impervious surfaces associated with the recent urban development.

Barnegat Bay cores. A summary of changes in diatom assemblages in the Barnegat Bay cores is presented below.

Core BB1 was sectioned into 2-cm intervals and diatoms were counted in 20 samples covering the depth from 0 to 94 cm, with every sample analyzed in the upper 26-cm portion of the core. The CONISS identified three diatom zones in the core (Fig. 18). The first zone spanning the depth of 18 – 94 cm, which corresponds approximately to CE 1630 – 1940, is dominated by *Fragilaria cassubica*, *Denticula subtilis*, *Stauroforma exiguiformis*, *Chamaepinnularia* aff. *begeri*, *C. sp. 8.*, *Navicula antverpiensis*, and *N. sp. 63*. There were considerable fluctuations in the salinity and marsh elevation during this time as evidenced by the shifts from assemblages dominated by higher marsh and lower salinity indicators, such as *Stauroforma exiguiformis* and *Cavinula variostrata* to assemblages where diatoms characteristic for lower marshes and mudflats, such as *Cocconeis stauroneiformis*, *Paralia sulcata*, *Fallacia pygamea* and *Planothidium delicatulum* increased in abundance. Some of these fluctuations may have been caused by the openings and closures of the inlets that influenced hydrological regime of the Barnegat. Diatom-based salinity reconstructions accurately tracked salinity fluctuations induced by inlet changes, providing additional evidence for the diatom-based model performance Bay (see Fig. 19).

The 18-cm depth (~ CE 1940) is identified by the CONISS as the point of a major transition in diatom assemblage. The change-point analysis dates this transition by 1957. Around this time, the diatom assemblage shifted towards dominance by pollution-tolerant species, such as *Planothidium* cf. *frequentissimum*, *Nitzschia frustulum* and *Chamaepinnularia* aff. *begeri*. The nitrogen transfer function estimates a considerable increase of species associated with higher nitrogen concentrations. This apparent eutrophication has not been countered by an increase in tidal flushing and salinity indicated by the salinity reconstruction. The diatom assemblage

composition somewhat changed again at about 1986 CE (depth 6 cm), but pollution-tolerant species such as *Planothidium frequentissimum* still dominate in the upper third zone of the core. The loss of *Luticola mutica* and the increase of *Fragilaria amicorum* in this zone are signs of declining marsh elevation that has been previously demonstrated for this core by Kemp et al. (2013).

Core BB2 was sectioned into 2 cm intervals and diatoms were counted in 19 samples covering the depth from 0 to 80 cm, with every sample analyzed in the upper 26 cm portion of the core. CONISS identified three diatom zones in the core. The first zone spanning the depth of 64 – 80 cm, which corresponds approximately to CE 1416 – 1603, is dominated by *Pseudostaurosira subsalina*, *Pinnularia viridis*, *Planothidium delicatulum*, *Paralia sulcata*, *Nitzschia scalpelliformis*, *N. cf. perversa*, *Navicula jonssonii*, and *Diploneis smithii*. This assemblage indicates an unpolluted brackish marsh regularly inundated by tidal water. The second diatom zone covers the depth from 8 to 54 cm corresponding to the age interval of CE 1678-1953. The dominant diatom species in this zone are *Chamaepinnularia aff. begeri*, *Denticula subtilis*, and *Navicula antverpiensis*, all species associated with elevated nitrogen content of sediments. The advent of *Planothidium cf. frequentissimum* in the second zone also indicates some nutrient enrichment. The third diatom zone extends from the depth of 8 cm to the surface and covers the age interval from 1953 to 2015. Diatoms indicate a sharp increase in nitrogen concentration with the dominant species being *Luticola mutica*, *Denticula subtilis*, *Navicula antverpiensis*, *N. sp. 63* and *Planothidium cf. frequentissimum* (Fig. 20).

Core BB4 was sectioned into 2 cm intervals and diatoms were counted in 21 samples covering the depth from 0 to 96 cm, with every sample analyzed in the upper 22 cm portion of the core. CONISS identified two diatom zones in the core. The first zone spanning the depth of 24 – 96 cm, which corresponds approximately to CE 1670 – 1920, is dominated by *Denticula subtilis*, *Navicula cf. microcari*, *N. sp. 63* and *Paralia sulcata*. Starting from approximately 1870, there is an increase in abundance of *Planothidium frequentissimum* and *Navicula antverpiensis* indicative of slight nitrogen enrichment. The nitrogen transfer function also signals the beginning of eutrophication starting at the same time. The second diatom zone extending from 22 cm of depth to the surface is characterized by the further increase in diatoms associated with elevated nitrogen levels. The dominant diatom species in this zone are *Chamaepinnularia*

aff. *begeri*, *Denticula subtilis*, *Navicula antverpiensis*, *N. microcari*, *N. perminuta* and *Planothidium* cf. *frequentissimum*. The transfer function confirms the continuing trends towards eutrophication (Fig. 21).

Unlike other cores, Great Bay (GB2) Core was taken from a salt pan located in a marsh modified by ditching. Therefore, the diatom assemblage composition in this core is characteristic for a mudflat rather than vegetated marsh. The Great Bay watershed is much less developed than the Barnegat Bay area to the north and therefore was expected to be less nutrient-enriched. The upper 15-cm portion of the core was sectioned into 1 cm-thick intervals and diatoms were counted in each of the upper 11 samples. The lower portion of the core was sectioned into 2 cm-thick samples. A total of 25 samples covering the depth from 0 to 95 cm were analyzed. CONISS identified three diatom zones in the core. The first zone spanning the depth of 12 – 95 cm, which corresponds approximately to CE 1832 – 1989, is dominated by *Cyclotella choctawatcheana*, *Amphora* sp. 6, *Halamphora aponina*, *H. acutiuscula*, *H. tenerrima* and *Nitzschia* sp. 1. This assemblage is characteristic for a mudflat or a sparsely vegetated low marsh. The occurrence of *Cyclotella choctawatcheana* indicates that Great Bay received nutrient inputs from mid-Atlantic coastal waters as early as 1832, as this planktonic species is an indicator of nutrient enrichment (Cooper 1995). The second diatom zone covers the depth from 5 to 11 cm (CE 1993-2002) and is characterized by an increase of *Halamphora coffeaeformis*, *Navicula flautica* and *Nitzschia* sp. 1. The transfer function shows an increase in salinity, which continues in the upper third zone of the core. In this zone, which extends from 5 cm depth to the surface (CE 2002-2014), *Amphora* sp. 6 and *Nitzschia pusilla* rose to prominence, while *Navicula flautica* and *Nitzschia* sp. 1 declined. The diatom-based transfer function did not reveal any consistent trend in nitrogen content, which is consistent with relatively low development in the area around Great Bay (Fig. 22).

Diatom assemblages in cores BB1, BB2, BB4, and GB2 have been described previously in the Potapova et al. (2014) report to NJDEP (<http://nj.gov/dep/dsr/barnegat/final-reports/>). Quantitative reconstructions of past nutrient, salinity, and changes in marsh habitat/elevation are based on new transfer functions computed through this project.

Diatoms from the Cape May Courthouse core were counted in 102 samples from 0 to 270 cm depth, with every 1 cm-thick sample analyzed in the upper 30-cm section. CONISS identified four diatom zones in the core (Figure 23). The first zone extends from 270 to 220 cm depth, which corresponds to an age interval covering several hundred years before 630 CE. The dominant diatoms in this zone are *Diploneis smithii*, *Caloneis bacillum*, *Rhopalodia musculus*, *Navicula antverpiensis* and *Paralia sulcata*. This assemblage is characteristic for a vegetated salt marsh, but presence of *Eunotia exigua* in two samples indicates an influx of water from a freshwater wetland or a stream. The next zone covering the depths from 220 to 74 cm is rather similar to the first, with lower abundances of *Paralia sulcata*, *Caloneis bacillum* and *Diploneis smithii*, but higher numbers of *Denticula subtilis*, *Navicula hanseatica* and *N. microcari*.

The transition from the second to the third zone at the depth of 74 cm, which corresponds to the early 1700s is also identified as a major shift in diatom assemblage composition by the change-point analysis. The nitrogen transfer function shows that this transition is caused by the increased abundance of nitrogen-tolerant species, such as *Navicula* sp. 63 and *Nitzschia microcephala* at the expense of such nitrogen-sensitive species as *Navicula digitoconvergens*. This shift is interpreted as a sign of early nutrient enrichment probably caused by European settlers developing the whaling industry in the Cape May area.

The CONISS identified the boundary between the third and the fourth diatom zones at the depth of 22 cm (approximately at CE 1960) as another major transition in diatom assemblage. The dominant diatoms in the fourth zone (0-22cm depth) are *Navicula antverpiensis*, *Denticula subtilis*, *Chamaepinnularia* aff. *begeri*, *Nitzschia frustulum* and *Planothidium* cf. *frequentissimum*, the species that appear to be indicative of eutrophication in mid-Atlantic salt marshes. The nitrogen transfer function shows a sharp increase of N-tolerant species in this zone of the core. Another feature of the upper zone is the consistently increased abundance of *Planothidium delicatulum*, which is likely a consequence of decreasing marsh elevation as this species is more abundant in subtidal and lower intertidal zones than in the higher elevations. Reconstruction of salinity using a previously developed transfer function confirms an earlier finding (Kemp et al., 2013) that this marsh does not keep up with the increasing rate of sea level rise over the last decades (Fig. 23).

Fortescue Core F9. Diatoms were counted in 48 samples from 0 to 291 cm depth in the F9E core, with every 1 cm-thick sample analyzed in the upper 21-cm section. CONISS identified two diatom zones in the core (Figure 24). The first zone covering the depth from the bottom of the core to 41 cm was dominated by typical salt marsh diatoms *Denticula subtilis*, *Luticola mutica*, *Nitzschia microcephala* and *Pseudostaurosira subsalina*. In several intervals (120-121 cm, 230-241 cm, 260-271 cm) diatoms characteristic for open-water and subtidal habitats, such as *Paralia sulcata*, *Cyclotella striata*, *Melosira nummuloides* and *Nitzschia granulata* increased in abundance, indicating a higher degree of marsh inundation. Two of these intervals (120-121 cm and 260-271 cm) corresponded to deposition of clastic sediments and may correspond to the periods of marsh degradation caused by storm events. The second diatom zone extending from 41 cm to the surface is dominated by *Navicula antverpiensis*, *Planothidium cf. frequentissimum*, *Chamaepinnularia aff. begeri* and *Denticula subtilis*, which are mostly indicative of nutrient enrichment. Compared to the intervals just below this zone, there is some increase in planktonic (*Cyclotella striata* and *Paralia sulcata*) and mudflat (*Planothidium delicatulum*) diatoms likely associated with some elevation loss in this marsh in the recent times (Fig. 24).

Fortescue Core F11. Diatoms were counted in 30 samples from 0 to 206 cm depth in the F11A core, with every 1 cm-thick sample analyzed in the upper 20-cm section. CONISS identified two main diatom zones in the core (Figure 25). The first zone covering the depth from the bottom of the core to 130 cm was dominated by diatoms characteristic for mudflats, such as *Skeletonema* spp., *Planothidium delicatulum*, *Thalassiosira proschkiniae*, *Cyclotella striata* and *Paralia sulcata*. In the upper portion of this zone some diatoms indicating a higher marsh elevation, such as *Denticula subtilis*, became more abundant. This sequence corresponds to the increasing marsh elevation and accumulation of organic material. The second zone is subdivided in a sub-zone that includes two intervals (50-51 and 100-101 cm) represented by higher marsh diatoms such as *Navicula antverpiensis*, *N. isbelensiminor*, and *Denticula subtilis*, while diatoms indicative of lower elevations disappear. In the upper sub-zone (20-0 cm) there are fluctuations of nitrogen-tolerant diatoms and species associated with increased inundation. Similar to the Cheesequake core, there is a peak of *Nitzschia microcephala* at the depth of 16-19 cm, a species associated with low salinity and high nitrogen content (Fig. 25) representing modern times.

Seabreeze core SB-30 A total of 33 intervals have been analyzed in this core, with high resolution sampling for the upper 20 cm in the core, and more spaced intervals down core. Two main zones and six sub-zones have been delimited by CONISS (Figure 26). The bottom of the core up to 41 cm-depth is dominated by a more diverse association of species indicative of pristine wetland species such as *Cyclotella striata*, *Thalassionema nitzschioides* and *Nitzschia brevisissima* present in the 177-185 cm intervals, which represent the transition from a high marsh to a mud flat, considered an infill following a storm event. The mud flat unit is inhabited by open-water and subtidal diatoms such as *Pseudostaurosira subsalina* and *Karayevia submarina*. indicating a higher degree of marsh inundation up to 139 cm core depth, corresponding to the early 1700s. The species composition becomes more diverse in the following 121-135 interval likely indicating nutrient enrichment related to the low marsh interval. High species diversity is maintained up to 41 cm except for the 91-92 cm interval represented by *P. subsalina* dominant at more than 80% relative abundance. The upper core zone is represented by high abundances of planktonic *Thalassiosira proschkiniae*, and *Skeletonema* spp., together with less abundant *Cyclotella striata*, *Cymatosira belgica* and *Minidiscus* spp. which may be indicative of a period with more inundation and likely associated with the recent sea level rise (Fig. 26).

### **Land-use changes**

Land-use land-cover in the vicinity of the seven cores was summarized for three time periods, early 1930s, 1974, and 2012. Characteristics were summarized within a 5-km and 10-km buffer around each core location (Table 12). Over the nearly eighty-year span from the early 1930s to 2012, forest and wetlands decreased substantially at Cheesequake, while water remained the same or increased. Loss of unaltered land was mainly due to conversion to developed land. Developed land accounted for over 40% of the cover by 2012, as compared to only 11-12% in 1930. Agriculture decreased from 19-20% in 1930 to 1-3% in 2012 for the two buffer zones.

Land-use profiles in the Barnegat Bay area show similar changes at BB1 and BB2 with forest and wetlands converted to developed land within both a 5- and 10-km buffer. Comparatively, BB1 had a higher percentage of developed land than BB2 where BB1 showed

34% developed land and BB2 showed 16% in the largest buffer area by 2012. There was an approximate 6-fold increase in developed land from 1930 to 2012.

The BB4 core maintained a consistent profile through time at the 5- and 10-km buffers. BB4 is dominated through time by forest, water, and wetlands. A small percentage of developed land is present within the buffers but increased from 1-3% in 1930 to 7-13% by 2012.

The core at Great Bay 2 has a similar profile to BB4. Through time, a small percentage of unaltered land, mostly forest and wetlands, was lost to the developed land class. Developed land increased from 1% in 1930 to 5-10% in 2012 for the two buffer zones.

The Cape May Courthouse core is dominated by unaltered lands with a small proportion of developed land in recent periods. Agriculture in the area surrounding this core has decreased from about 10% in the early 1930s to 1 or 2% (depending on buffer distance) in the most recent period. Developed land increased from 3-5% in 1930 to 15-19% in 2012.

As with the other cores, the Sea Breeze core is dominated by unaltered cover but open water dominates (58-63%). A small proportion through time of the 10-km area is classified as agriculture (decrease of 12% to 9%).

Barren land and agriculture are very small components of the land-use/land-cover profiles of each of the cores except at Cheesequake where in the 1930s agriculture was estimated to be up to 20% of the cover in the buffer areas.

## **Reference conditions**

The sediment core investigations provided long-term records that reached to the time before the European settlement period. The data provided by the analyses of core intervals representing this time period represent reference conditions for the study sites. Pollen analyses displayed a peak in Ambrosia pollen around 1860, marking the maximum extent of forest clearance by the European settlers (Potapova et al., 2014). However, the sediment core analyses revealed that the environmental changes started after the arrival of settlers in New Jersey in the 1700s. Changes are first marked by subtle increases in nutrient concentrations (sediment N) and inputs of metals produced by mining and smelting during the 18<sup>th</sup> century.

Prior to the 1700s, diatom-based transfer functions revealed that salinity varied across all study sites, providing a natural range of variation that is specific to each study site (Table 13). These variations are linked to natural changes in rates of sea level and tide amplitude, storm events, as well as opening and closing of inlets (e.g., Fig. 19, northern Barnegat Bay). During two centuries prior to 1700, Cheesequake and Cape May wetlands recorded high salinity variations in the range of ~ 19-30 psu. Lower salinity values were inferred in the Barnegat Bay cores, with minima reaching 15 and maxima 20 psu. However, in the Barnegat Bay cores, a smaller number of intervals reached the pre-European time, thus the entire natural range may not be covered. The Great Bay core didn't reach the pre-European period and values for reference conditions are not available for this site. The inferred salinity varied between 19-25 psu throughout the core.

Sediment nitrogen values, as inferred based on diatom transfer functions, were consistently low across the study sites prior to 1700's, with average values of 0.27% in southern Barnegat Bay BB4 core, and 0.63% in BB2. Low sediment N concentrations were also inferred in Cheesequake and Cape May (Table 13).

Background metal concentrations were consistently low for the metals of concern for human health prior to the arrival of European settlers (Table 11).

### **Anthropogenic impacts**

The sediment core investigation revealed that marked environmental changes took place across the study sites after the European settler's arrival. These changes are reflected by diatom-inferred salinity and nitrogen concentrations, as well as measured organic and inorganic contaminants in the sediment cores. The diatom reconstructions reveal slight increases in nitrogen concentration associated with the early European settlement during the 18<sup>th</sup> century. The nitrogen contents are strongly increasing in the second half of the 19<sup>th</sup> century reaching values about 5-times higher than in the pre-1700 time period. Even after the 1970's implementation of EPA regulations, concentrations of sediment N remain high, or even higher than prior to the regulations in the case of Cape May, and the Barnegat Bay sites of cores BB1 and BB4. However, decreases in N were recorded in Cheesequake although nitrogen values are still above the reference values (Table 13).

Sharp increases recorded by inorganic contaminants reveal the impacts from the 18<sup>th</sup> century mining and smelting activities, followed by chemical dumps, fly ash, and landfills resulting from the growing industrial activities and increased population associated with the post-1850s industrial revolution (Figures 13-16). Although the metals of concern remain at high concentrations in modern samples, a decrease in total metals, including the naturally occurring Al and Fe are a consistent feature across all sites.

Most of the PAHs displayed the highest increases during the 20<sup>th</sup> century, and especially after the second world war, reaching the highest values in Cheesequake (~8,000 µg/Kg), and much lower values in Cape May and Delaware Bay (Sea Breeze). High values similar to Cheesequake were found in the Barnegat Bay BB1 core with maximum values of more than 7,000 µg/Kg (Velinsky et al., 2011; Potapova et al., 2014). Decreases in PAHs were recorded over the last few decades in Cape May and Sea Breeze, possibly reflecting the consequence of the implementation of the Clean Air Act (1970) and the closure of many industrial facilities in the region.

Changes in land-use patterns since the 1930s revealed a sharp increase in urban development in both Cheesequake and BB1 study sites (Table 12). These two sites also showed the highest recorded anthropogenic influence. Cheesequake and northern Barnegat Bay (BB1) recorded the highest increases in organic and inorganic contaminants. Diatom-based inferences also show the highest impacts for these highly urbanized sites: highest sediment nitrogen concentrations, coupled with high salinity fluctuations, which are uncharacteristic of the pre-European settlement period.

The coring sites from Great Bay, Cape May, and the Delaware Bay are representative of less impacted coastal wetlands. However, the sediment core investigations revealed that they were also impacted by nutrient enrichment, organic and inorganic contaminants although to a lesser extent than the more developed Raritan and northern Barnegat Bay sites. This is most likely indicative of indirect sources of pollutants from regional and long-distance transportation via atmospheric deposition, tidal transport, and/or sediment resuspension due to storm events.

## **Climate impacts - storm events**

Diatom species and diatom-based salinity and nitrogen inferences were used to evaluate changes induced by the erosive storm events identified in sites from Fortescue and Sea Breeze (Delaware Bay). These storm events eroded the existing marshes at various times producing abrupt patterns in the core lithology (Figure 9). The investigation of diatom species changes and inferred nutrients and salinity revealed that changes in habitat, nutrients and salinity associated with these erosional events are significant and site-specific. The storm events were associated with salinity increase of ~ 3 psu after the storm episodes in the F9 and F11 Fortescue sites. The storm events also induced decreases in nitrogen levels, which dropped to about half the N values preceding the storm events. Highest N content was noted when the wetland recovers to a high marsh (Table 14).

Contrary to the Fortescue wetlands, the Sea breeze site received more fresh water inputs associated with the storm erosion events, and also exhibited higher nitrogen contents in the mudflat episode following storm erosion (Table 14). This suggests that the Sea Breeze marsh dynamics differs from those at Fortescue. In Fortescue, erosive events are accompanied with marine erosion and intrusion processes, while the Sea Breeze erosion events bear the signature of fresh water flooding with nutrient inputs, possibly related to the proximity of the Cohansey River. These changes reflect the natural variability of the marsh systems and can provide a benchmark to evaluate recent wetlands changes with potential for future monitoring of these wetlands.

## **Refining the use of diatom species as coastal wetland ecological indicators**

Portions of this paleoecological investigations depended upon the utilization of diatom-based transfer functions developed from a 100-site calibration set in Barnegat Bay (Potapova et al., 2014). However, poor analogs were found between the Barnegat Bay calibration dataset and sub-fossil diatoms from cores collected during this project. In order to explore the ecological significance of wetland diatoms, additional surface sediment samples were collected across elevation and wetland type gradients and a new calibration set was developed based on 171 sites (Tables 15, 16). This new data set improved the similarity between the diatom calibration set and the diatom assemblages found in sediment cores evaluated for this project (Desianti, 2017, work in progress). This new data set greatly improved the ability to reconstruct past environmental

conditions (N, salinity), fluctuations in marsh habitat and elevation over the past few thousand years. Indicator diatom species that can be used in future monitoring for N, salinity, type of habitat, and indicators for reference conditions are provided in Tables 17 and 18.

### **Informing future coastal wetland restoration targets**

This project provides coastal managers and stakeholders with a set of diatom species that can be utilized as indicators for reference and polluted conditions, quantitative models computed based on diatom response to sediment nitrogen content and salinity, and reconstructions of reference (pre-European settlement) conditions. Information on wetlands changes induced by storm perturbances and the subsequent wetland response and recovery are also provided.

The indices developed based on diatom species offer a yet untapped possibility to incorporate diatoms for holistic assessments of coastal wetlands ecological status and application in future wetland monitoring.

The project findings stress the importance of acquiring knowledge of wetlands reference conditions and highlights long-term variability and sources of pollutants in an effort to understand the potential for coastal systems to accommodate natural and human perturbations. The sediment core investigations are relatively rapid, cost-effective, and provide knowledge that allow development of efficient wetlands conservation and restoration programs

Up to now, long-term quantitative reconstructions based on multi-proxy sediment core investigations, that go beyond the existing monitoring records, have not been considered by the New Jersey coastal wetland stakeholders. It is anticipated that results from this study will outline the potential for practical applications for New Jersey (and other states) wetland ecosystems. We would also like to stress the great potential that such investigations have in the understanding and protection of these fragile, but extremely important, coastal ecosystems and encourage their incorporation into future wetland management tools.

## **CONCLUSIONS**

Based upon the findings of this sediment-core paleoenvironmental investigation, coastal wetland managers and stakeholders are provided with a thorough investigation of reference conditions and long-term impacts from human activities, climate and human perturbations across a human development gradient, from heavily impacted locations in the northern coastal region to less developed ‘reference’ sites along the southern New Jersey coast.

Reference conditions have been assessed for wetlands from urban (Cheesequake, Raritan Bay; northern Barnegat Bay) and rural settings (Great Bay, Cape May, northern shore of Delaware Bay) with regard to nutrient, salinity, and habitat changes through time based on diatom-derived models established by using a 171-site calibration data set from New Jersey wetlands and Barnegat Bay (Tables 13, 17, and 18). In addition, information on reference and historical concentrations of organic (PAHs) and inorganic (trace metals) (Table 11) in core sediments have been provided.

Storm event perturbations induced site-specific responses in wetlands, which are described for the Sea Breeze and Fortescue sites. Marsh recovery times following storm events varied across sites and through time.

The sediment cores reveal the impacts associated with the European settlement, notably the post-1950 industrial revolution, by increases in organic and inorganic pollutants, sediment nitrogen, and changes in salinity. These inputs, linked to the post-settlement human activities, continue to increase in some cases even after federal and state agencies enacted environmental regulations to limit emissions and protect the environment. While the anthropogenic impacts are more regional in character, the variability of reference conditions is site-specific. A thorough assessment of the wetland conditions prior to implementation of restoration projects would be optimal to ensure a cost-effective and lasting success of such projects.

## **ACKNOWLEDGEMENTS**

We thank the Environmental Protection Agency for funding this project through grant number 96284800. We also thank Dr. Michael Griffiths, William Paterson University, his students

Ksawery Biskup and Austin Degen, and lab technician Mike DaSilva, for the in-kind contribution of laboratory analyses of wetlands sediments; Peter Zampella, New Jersey Department of Environmental Protection (NJDEP) for GIS analyses; Dr. Dan Milleman (NJDEP) for support in the field; Tonia Wu, Librarian, NJDEP; and Bruce Ruppel (NJDEP), Dr. Lee Lippincot (NJDEP), Dr. Paul Sanders (NJDEP), and Metthea Yepsen (NJDEP) for providing insight into sediment core findings. We thank Dr. Gary Buchanan (NJDEP) for support throughout the project.

## REFERENCES

- Appleby PG, Oldfield F. 1978. The calculation of lead-210 dates assuming a constant rate of supply of unsupported 210-Pb to the sediment. *Catena* 5: 1-8.
- Birks HJB, Juggins S, Line JM. 1990. Lake surface-water chemistry reconstructions from palaeolimnological data. In B.J. Mason (ed.), *The Surface Waters Acidification Programme*. Cambridge University Press. 301-313.
- Branin, M.L. 1988. *The Early Makers of Handcrafted Earthenware and Stoneware in Central and Southern New Jersey*. Associated University Press, Cranbury, New Jersey.
- Briffa KR, Jones PD, Schweingruber FH, Osborn TJ. 1998. Influence of volcanic eruptions on Northern Hemisphere summer temperature over the past 600 years. *Nature* 393: 450-455.
- Cable J, Burnett W, Moreland., Westmoreland J. 2001. Empirical assessment of gamma ray self-absorption in environmental analyses. *Radioactivity and Radiochemistry* 12: 30-39.
- Corbett DR and Walsh JP. 2015. <sup>210</sup>Pb and <sup>137</sup>Cesium, in *Handbook of Sea-Level Research* (eds I. Shennan, A. J. Long and B. P. Horton), John Wiley & Sons, Ltd, Chichester, UK. doi: 10.1002/9781118452547.ch24.
- Cutshall NH, Larsen IL, Olsen CR. 1983. Direct analysis of <sup>210</sup>Pb in sediment samples: self-absorption corrections. *Nuclear Instruments and Methods* 206: 309-312.
- Desianti N. 2017. Ph.D. thesis in preparation. Drexel University.
- Dillon WP and Oldale RN. 1978. Late Quaternary Sea-Level Curve: Reinterpretation Based on Glaciotectonic Influence. *Geology* 6: 56-60.

- Dixit SS, Smol JP, Charles DF, Hughes RM, Paulsen SG, Collins GB. 1999. Assessing lake water quality changes in the lakes of the northeastern United States using sediment diatoms. *Canadian Journal of Fisheries and Aquatic Sciences* 56: 131-152.
- Faegri K, Iversen J, Kaland PE, Krzywinski K. 1989. Textbook of pollen analysis. Blackburn Press. Caldwell, New Jersey. 328 pp.
- Ferland MA. 1990. Holocene depositional history of the southern New Jersey Barrier and Backbarrier regions. Technical Report CERC-90-2 prepared for the Department of The Army Corps of Engineers.
- Frey RW and Basan PB. 1978. "Coastal Salt Marshes," in *Coastal Sedimentary Environments*, R. A. Davis, Ed., Springer-Verlag, New York. pp 101-159.
- Gotelli N. and Ellison AM. 2004. A primer of ecological statistics. Sunauer Associates. Sunderland, MA. 492 pp.
- Haslett J. and Parnell A. 2008. A simple monotone process with application to radiocarbon-dated depth chronologies. *Journal of the Royal Statistical Society: Series C (Applied Statistics)* 57(4): 399-418.
- Hicks SD, Debaugh HA, Hickman LE. 1983. "Sea Level Variations for the United States, 1855-1980," US Department of Commerce, National Oceanic and Atmospheric Association/NOS. Vol I, pp 151-153
- Hwang H-M, Green PG, Higasi RM, Young TM. 2006. Tidal salt marsh sediment in California, USA. Part 2: Occurrence and anthropogenic input of trace metals. *Chemosphere* 64: 1899-1909.
- Juggins S. 2003. *C<sup>2</sup> User guide*. Software for ecological and paleoecological data analysis and visualization. University of Newcastle, Newcastle upon Tyne, UK. 69pp
- Kapp RO, Davis OK, and King JE. 2000. *Guide to Pollen and Spores*. American Association of Stratigraphic Palinologists. 279 pp.
- Kemp AC, Sommerfield CK, Vane CH, Horton BP, Chenery S, Anisfeld S, Nikitina D. 2012. Use of lead isotopes for developing chronologies in recent salt-marsh sediments. *Quaternary Geochronology* 12: 40-49

- Kemp AC, Horton BP, Vane CH, Bernhardt CE, Corbett DR, Engelhart SE, Anisfeld SC, Parnell AC, Cahill N. 2013. Sea-level change during the last 2500 years in New Jersey, USA. *Quaternary Science Reviews* 81:90-104
- Kemp AC and Horton BP. 2013. Contribution of relative sea-level rise to historical hurricane flooding in New York City. *Journal of Quaternary Science* 28(6): 537-541.
- Kopp RE, Horton RM, Little CM, Mitrovica JX, Oppenheimer M, Rasmussen DJ, Strauss BH, Tebaldi C. 2014. Probabilistic 21st and 22<sup>nd</sup> century sea-level projections at a global network of tide-gauge sites, *Earth's Future* 2: 383–406, doi:10.1002/2014EF000239.
- Knight JB. 1934. "A Salt-Marsh Study," *American Journal of Science* 28(165): 161-181.
- Lathrop RG. 2004. Measuring land use change in New Jersey: land use update to year 2000. Rutgers University, Grant F. Walton Center for Remote Sensing and Spatial Analysis, New Brunswick, NJ, CRSSA Report#2007-04.
- Lathrop RG and Haag S. 2007. Assessment of Land Use Change and Riparian Zone Status in the Barnegat Bay and Little Egg Harbor Watershed: 1995-2002-2006. Rutgers University, Grant F. Walton Center for Remote Sensing and Spatial Analysis, New Brunswick, NJ, CRSSA Report#2007-04.
- Long ER, MacDonald DD, Smith SL, Calder FD. 1995. Incidence of adverse biological effects within ranges of chemical concentrations in marine and estuarine sediments. *Environmental Management* 19: 81-97.
- McAndrews JH, Berti AA, Norris G. 1973. Key to the Quaternary Pollen and Spores of the Great Lakes Region. Royal Ontario Museum Life Sciences Miscellaneous Publication: Toronto, Ontario, Royal Ontario Museum, 61 p.
- McCune B, Grace JB, Dean LU. 2002. Analysis of ecological communities. MjM Software Design, Portland, 304 pp.
- Meyerson AL. 1972. Pollen and paleosalinity analyses from a Holocene tidal marsh sequence, Cape May County, New Jersey. *Marine Geology* 12: 335-357.

Miller KG, Robert E. Kopp RE, Horton BP, Browning JV, and Kemp AC. 2013. A geological perspective on sea-level rise and its impacts along the U.S. mid-Atlantic coast. *Earth's Future* 1: 3–18, doi:10.1002/2013EF000135.

Moore PD, Webb JA, Collinson ME. 1991. *Pollen analysis*. 2<sup>nd</sup> Edition. Blackwell Scientific Publications. Oxford, 217 pp.

Morais S, Garcia F, Costa FG and Pereira ML. 2012. *Heavy Metals and Human Health, Environmental Health - Emerging Issues and Practice*, Prof. Jacques Oosthuizen (Ed.), ISBN: 978-953-307-854-0, InTech, Available from: <http://www.intechopen.com/books/environmental-health-emerging-issuesand-practice/heavy-metals-and-human-health>

Mudgal V, Madaan N, Mudgal A, Singh RB and Sanjay M. 2010. Effect of Toxic Metals on Human Health. *The Open Nutraceuticals Journal* 3: 94-99

Newhall CG and Self S. 1982. The volcanic explosivity index: An estimate of explosive magnitude for historical volcanism. *Journal of Geophysical Research* 87: 1231-1238.

New Jersey Wetlands Act of 1970. N.J.S.A. 13:9A-1 ET SEQ. Updated through P.L. 2016, ch.32, and JR 3 of 2016.

New Jersey Wetland Program Plan 2014-2018. First iteration 2013. Prepared by: New Jersey Department of Environmental Protection (NJDEP) pursuant to The United States Environmental Protection Agency (EPA) Enhancing State and Tribal Programs (ESTP) Initiative.

New Jersey Department of Environmental Protection (NJDEP), Office of Information Resources Management (OIRM), Bureau of Geographic Information and Analysis (BGIA). 1986. 1986 Land Use/Land Cover. <http://www.nj.gov/dep/gis/lulcshp.html>

New Jersey Department of Environmental Protection (NJDEP), Office of Information Resources Management (OIRM), Bureau of Geographic Information Systems (BGIS). 2012. NJDEP 2012 Land Use/Land Cover Update 2/17/15. <http://www.nj.gov/dep/gis/lulc12.html>

New Jersey Geographic Information Network. 2017. New Jersey Orthophotography for various years. Available at [https://njgin.state.nj.us/NJ\\_NJGINExplorer/jviewer.jsp?pg=wms\\_instruct](https://njgin.state.nj.us/NJ_NJGINExplorer/jviewer.jsp?pg=wms_instruct).

NYS DEC. 2006. New York State Brownfield Cleanup Program Development of Soil Cleanup Objectives Technical Support Document. New York State Department of Environmental

Conservation and New York State Department of Health, Albany, NY.

<http://www.dec.ny.gov/chemical/34189.html>

Nikitina DL, Kemp AC, Horton BP, Vane CH, van de Plassche O, Engelhart SE. 2014. Storm erosion during the past 2000 years along the north shore of Delaware Bay, USA, *Geomorphology* 208: 160-172. <http://dx.doi.org/10.1016/j.geomorph.2013.11.022>

Nikitina D, Kemp AC, Engelhart SE, Horton BP, Hill DF, Kopp RE. 2015. Sea-level change and subsidence in the Delaware Estuary during the last ~2200 years. *Estuarine, Coastal and Shelf Science* 164:506-519.

Parnell AC, Haslett J, Allen JRM, Buck CE, Huntley B. 2008. A flexible approach to assessing synchronicity of past events using Bayesian reconstructions of sedimentation history. *Quaternary Science Reviews* 27(19-20): 1872-1885.

Pijanowski K 2016. Patterns and rates of historical shoreline change in the Delaware Estuary. Published by ProQuest LLC 10191317.

Potapova M, Desianti N, Velinsky D, Mead J. 2013. Barnegat Bay nutrient inference model (Year 1). Report to NJDEP.

Potapova M, Potapova M, Desianti N, Velinsky D 2014. Barnegat Bay nutrient inference model (Year 2). Report to NJDEP.

Potapova M, Desianti N 2015. Barnegat Bay nutrient inference model (Year 3). Report to NJDEP.

Potapova M, Desianti N, Enache M, Belton T, Velinsky D, Thomas R, and Mead J. 2017. Sediment diatoms as environmental indicators in New Jersey coastal lagoons. *Journal of Coastal Research Special Issue* 78: 127-140.

Psuty NP. 1986. Holocene sea level in New Jersey. *Physical Geography* 7:156-167.

Reimer, P.J., Baillie, M.G.L., Bard, E., Bayliss, A., Beck, J.W. Weyhenmeyer, C.E. 2011. IntCal09 and Marine09 radiocarbon age calibration curves, 0-50,000 years cal. BP. *Radiocarbon* 51: 1111-1150.

- Robbins, J.A., Edgington, D.N., Kemp, A.L.W. 1978. Comparative  $^{210}\text{Pb}$ ,  $^{137}\text{Cs}$ , and pollen geochronologies of sediments from Lakes Ontario and Erie. *Quaternary Research* 10(2): 256-278.
- Rowell HC, Enache MD, Quinlan R et al. 2016. Quantitative paleolimnological inference models applied to a high-resolution biostratigraphic study of lake degradation and recovery, Onondaga Lake, New York (USA). *Journal of Paleolimnology* 55: 241-258. DOI 10.1007/s10933-015-9877-8.
- Salisbury R.D. 1896. Annual Report of the State Geologist of New Jersey, Geological Survey of New Jersey.
- Sim RJ and Clement AW. 1944. The Cheesequake potteries. *Magazine Antiques* 44:122-125.
- Shaler NS 1895. Beaches and Tidal Marshes of the Atlantic Coast, National Geographic Monography Vol I: 151-153.
- Smol, J.P. 1992. Paleolimnology: An important tool for effective ecosystem management. *Journal of Aquatic Ecosystem Health* 1:49-58.
- Smol JP. 2008 *Pollution of Lakes and Rivers: a Paleoenvironmental Perspective* 2nd Edition. Blackwell Publishing, Oxford. 383 pp.
- Stuiver, M. and Reimer, P.J. 1993. Extended data base and revised CALIB 3.0  $^{14}\text{C}$  age calibration program. *Radiocarbon* 35(1): 215-230.
- ter Braak, C.J.F. and van Dam, H. 1989. Inferring pH from diatoms: a comparison of old and new calibration methods. *Hydrobiologia* 178: 209-223.
- United Nations Scientific Committee on the Effects of Atomic Radiation (UNSCEAR). (2000). Sources and effects of ionizing radiation. UNSCEAR 2000 report to the General Assembly.
- US EPA Strategic Plan. <https://www.epa.gov/grants/epa-order-57007a1-epas-policy-environmental-results-under-epa-assistance-agreements> accessed 12-19-2017.
- US EPA. 2002. Supplemental guidance for developing soil screening levels for superfund sites. Office of Solid Waste and Emergency Response, Washington DC. <http://www.epa.gov/superfund/health/conmedia/soil/index.htm>
- Vane, C.H., Rawlins, B.G., Kim, A.W., Moss-Hayes, V., Kendrick, C.P., Leng, M.J. 2013. Sedimentary transport and fate of polycyclic aromatic hydrocarbons (PAH) from managed

burning of moorland vegetation on a blanket peat, South Yorkshire, UK. *Science of The Total Environment* 449: 81-94.

Vane, C.H., Kim, A.W., Moss-Hayes, V., Snape, C.E., Diaz, M.C., Khan, N.S., Engelhart, S.E., and Horton, B.P. 2013. Degradation of mangrove tissues by arboreal termites (*Nasutitermes acajutlae*) and their role in the mangrove C cycle (Puerto Rico): Chemical characterization and organic matter provenance using bulk  $\delta^{13}\text{C}$ , C/N, alkaline CuO oxidation-GC/MS, and solid-state  $^{13}\text{C}$  NMR. *Geochemistry, Geophysics, Geosystems*, 14(8): 3176-3191.

Velinsky D, Sommerfield C, Enache MD, Charles D. 2011. Nutrient and Ecological Histories in Barnegat Bay, New Jersey (PCER Report No. 10-05). Prepared for Mr. Thomas Belton New Jersey Department of Environmental Protection – Science and Research.

Walsh DC, Chillrud SN, Simpson HJ, Bopp RF. 2001. Refuse incinerator particulate emissions and combustion residues for New York City during the 20<sup>th</sup> century. *Environmental Science & Technology* 35:2441-2447.

Yunker M. B., Macdonald R. W., Vingarzan R., Mitchell R. H., Goyette D., Sylvestre S. 2002. PAHs in the Fraser River basin: a critical appraisal of PAH ratios as indicators of PAH source and composition. *Organic Geochemistry*. 33:489–515. doi: 10.1016/S0146-6380(02)00002-5

## LIST OF TABLES

**Table 1** Location of coring sites. \*Cores from a previous NJDEP study (see text)

**Table 2** PAH target compounds and their monitored ions

**Table 3** Metal species, associated methods and Method Detection Limit (MDL)

**Table 4** C-14 dating results for the Cheesequake core. Age and age error are years BP

**Table 5** C-14 dating results for the Cape May core. Age and age error are years BP

**Table 6** C14 Dating results for Sea Breeze, and Fortescue cores. Age and age error are years BP

**Table 7** Variations in trace metal data measured in the Cheesequake core. Values in mg/Kg

**Table 8** Variations in trace metal data measured in the Barnegat Bay BB1 core. Values in mg/Kg

**Table 9** Variations in trace metal data measured in the Cape May Courthouse core. Values in mg/Kg

**Table 10** Variations in trace metal data measured in the Sea Breeze core. Values in mg/Kg

**Table 11** Comparison of average metal concentrations (mg/Kg) for the time periods pre-1700, 1700-1970; and 1970-present.

**Table 12** Summary of land-use land-cover in the vicinity of coring sites for three time periods: early 1930s, 1974, and 2012. Characteristics are summarized within a 5-km and 10-km buffer around each core location

**Table 13** Variations of diatom inferred salinity and sediment nitrogen for the time periods pre-1700, 1700-1970; and 1970-present.

**Table 14** Variations in diatom-inferred salinity and sediment nitrogen in storm post-erosion and recovery marsh sequences from Sea Breeze and Fortescue cores

**Table 15** Performance statistics for WA-PLS- inference models. Reported statistics are root mean square error of prediction (RMSEP), coefficient of determination ( $r^2$ ), and maximum bias (Max. bias).

**Table 16** Percentage of samples with ‘good’ modern analogue and ‘close’ modern analog in the 100 sites and 171 sites calibration dataset; ‘good’ and ‘close’ are defined as the 5th and 20th percentiles respectively, of Bray-Curtis dissimilarity values for the modern samples.

**Table 17** Optima and tolerances for salinity and nitrogen content in the sediment of diatom taxa most common in New Jersey coastal wetlands and sediment cores or highly indicative of reference conditions (in bold). CQ = Cheesequake, BB = Barnegat Bay, GB = Great Bay, CMC = Cape May Courthouse, Fort = Fortescue, SB = Sea Breeze

**Table 18** Summary of reference (pre-1700) vs present-day conditions assessed by presence/absence of indicator diatom species, and the diatom-inferred nitrogen and salinity in study sites. Sites are grouped as high-developed wetlands (HD; >30% developed land) - Cheesequake and Barnegat Bay BB1; medium-developed wetlands (MD; 10-30% developed land in 2012) - Barnegat Bay BB2, BB4, and Cape May; and low-developed wetlands (LD; < 10% developed land) - Great Bay GB 2 and Delaware Bay Fortescue and Sea Breeze sites.

## LIST OF FIGURES

**Figure 1** Environmental monitoring – a matter of time scales. The time scales shown in the figure to the left are on a logarithmic scale; the figure to the right shows a more realistic representation of the relative amount of information potentially available from sedimentary deposits (Modified from Smol 2008)

**Figure 2** Sediment core multi-proxy data is used to provide quantitative reconstructions of environmental parameters necessary to evaluate the ecological condition of wetland ecosystems. Figure courtesy of Dr. JP Smol, Queen’s University, Canada

**Figure 3.** Locations of sediment cores studied in this project. The Barnegat Bay and Great Bay cores were analyzed for diatoms through a previous NJDEP project (Potapova et al., 2014), while the remaining 5 cores were analyzed during this project

**Figure 4.** a) Eijkelkamp Peat-coring system (<https://en.eijkelkamp.com/products/augering-soil-sampling-equipment/peat-sampler.html>); and b) sediment core increment obtained at the Cheesequake State Park site

**Figure 5.** Cheesequake State Park Core chronology based on C-14, Cs-137 and pollution markers. The age-depth model was produced using the Bchron package in R (Haslett and Parnell, 2008)

**Figure 6.** Cape May Courthouse Core chronology based on C-14, Cs-137, pollution markers and Ambrosia pollen. The age-depth model was produced using the Bchron package in R (Haslett and Parnell, 2008)

**Figure 7.** Sea Breeze SB-30 core chronology based on C-14, and Cs-137. The age-depth model was produced using the Bchron R statistical package in R (Haslett and Parnell, 2008)

**Figure 8.** Storm events lithology and C-14 chronology for the Sea Breeze and Fortescue cores. Radiocarbon ages were calibrated using CALIB (Stuiver and Reimer, 1993) and the IntCal09 calibration data set (Reimer et al., 2011)

**Figure 9.** Dating of the Sea Breeze upper part core SB-30 using Cs-137 gamma spectrometry; modified from Nikitina et al. (2014)

**Figure 10.** Stratigraphic profile of PAHs distribution in the Cheesequake sediment core

**Figure 11.** Stratigraphic profile of PAHs distribution in the Cape May sediment core

**Figure 12.** Stratigraphic profile of PAHs distribution in the Sea Breeze core

**Figure 13.** Stratigraphic profile of select trace metals distribution in the Cheesequake core

**Figure 14.** Stratigraphic profile of select trace metals distribution in the Barnegat Bay BB1 core

**Figure 15.** Stratigraphic profile of select trace metals distribution in the Cape May Courthouse core.

**Figure 16.** Stratigraphic profile of select trace metals distribution in the Sea Breeze core.

**Figure 17.** Diatom stratigraphy plot for Cheesequake core showing relative abundances of taxa that reached at least 10% in at least one sample, Principal Component (PC1 and PC2) sample scores, diatom-based reconstruction of salinity (Inf\_Salinity) and nitrogen content in the sediment (Inf\_Nsed) with a loess smoother fitted to reconstructed values and calculated 95% confidence intervals (grey area), and a dendrogram illustrating depth-constrained cluster analysis of diatom data (CONISS). Green dotted lines separate two diatom zones identified by CONISS.

Star symbol shows the major transition in the diatom assemblage composition identified by the STARS algorithm. Both STARS algorithm and CONISS identified a major transition at ca. 1760.

**Figure 18.** Diatom stratigraphy plot for Barnegat Bay core 1 showing relative abundances of taxa that reached at least 5% in at least one sample, Principal Component (PC1 and PC2) sample scores, diatom-based reconstruction of salinity (Inf\_Salinity) and nitrogen content in the sediment (Inf\_Nsed) with a loess smoother fitted to reconstructed values and calculated 95% confidence intervals (grey area), and a dendrogram illustrating depth-constrained cluster analysis of diatom data (CONISS). Green dotted lines separate three diatom zones identified by CONISS.

**Figure 19.** Diatom assemblages in the BB1 core, inferred salinity and nitrogen, and maps of historical records of inlet opening/closing in the vicinity of core BB1 that are reflected in salinity fluctuations.

**Figure 20.** Diatom stratigraphy plot for Barnegat Bay core 2 showing relative abundances of taxa that reached at least 5% in at least one sample, Principal Component (PC1 and PC2) sample scores, diatom-based reconstruction of salinity (Inf\_Salinity) and nitrogen content in the sediment (Inf\_Nsed) with a loess smoother fitted to reconstructed values and calculated 95% confidence intervals (grey area), and a dendrogram illustrating depth-constrained cluster analysis of diatom data (CONISS). Green dotted lines separate three diatom zones identified by CONISS.

**Figure 21.** Diatom stratigraphy plot for Barnegat Bay core 4 showing relative abundances of taxa that reached at least 5% in at least one sample, Principal Component (PC1 and PC2) sample scores, diatom-based reconstruction of salinity (Inf\_Salinity) and nitrogen content in the sediment (Inf\_Nsed) with a loess smoother fitted to reconstructed values and calculated 95% confidence intervals (grey area), and a dendrogram illustrating depth-constrained cluster analysis of diatom data (CONISS). Green dotted lines separate two diatom zones identified by CONISS.

**Figure 22.** Diatom stratigraphy plot for Great Bay core showing relative abundances of taxa that reached at least 5% in at least one sample, Principal Component (PC1 and PC2) sample scores, diatom-based reconstruction of salinity (Inf\_Salinity) and nitrogen content in the sediment (Inf\_Nsed) with a loess smoother fitted to reconstructed values and calculated 95% confidence

intervals (grey area), and a dendrogram illustrating depth-constrained cluster analysis of diatom data (CONISS). Green dotted lines separate three diatom zones identified by CONISS.

**Figure 23.** Diatom stratigraphy plot for Cape May Courthouse core showing relative abundances of taxa that reached at least 10% in at least one sample, Principal Component (PC1 and PC2) sample scores, diatom-based reconstruction of salinity (Inf\_Salinity) and nitrogen content in the sediment (Inf\_Nsed) with a loess smoother fitted to reconstructed values and calculated 95% confidence intervals (grey area), and a dendrogram illustrating depth-constrained cluster analysis of diatom data (CONISS). Green dotted lines separate four diatom zones identified by CONISS. Star symbol shows the major transition in the diatom assemblage composition identified by the STARS algorithm. Both STARS algorithm and CONISS identified a major transition at ca. 1675.

**Figure 24.** Diatom stratigraphy plot for Fortescue core 9E showing relative abundances of taxa that reached at least 10% in at least one sample, Principal Component (PC1 and PC2) sample scores, diatom-based reconstruction of salinity (Inf\_Salinity) and nitrogen content in the sediment (Inf\_Nsed) with a loess smoother fitted to reconstructed values and calculated 95% confidence intervals (grey area), and a dendrogram illustrating depth-constrained cluster analysis of diatom data (CONISS). Green dotted line separates two diatom zones identified by CONISS.

**Figure 25.** Diatom stratigraphy plot for Fortescue core 11A showing relative abundances of taxa that reached at least 5% in at least one sample, Principal Component (PC1 and PC2) sample scores, diatom-based reconstruction of salinity (Inf\_Salinity) and nitrogen content in the sediment (Inf\_Nsed) with a loess smoother fitted to reconstructed values and calculated 95% confidence intervals (grey area), and a dendrogram illustrating depth-constrained cluster analysis of diatom data (CONISS). Green dotted line separates two diatom zones identified by CONISS.

**Figure 26.** Diatom stratigraphy plot for Sea Breeze core showing relative abundances of taxa that reached at least 5% in at least one sample, Principal Component (PC1 and PC2) sample scores, diatom-based reconstruction of salinity (Inf\_Salinity) and nitrogen content in the sediment (Inf\_Nsed) with a loess smoother fitted to reconstructed values and calculated 95% confidence intervals (grey area), and a dendrogram illustrating depth-constrained cluster analysis of diatom data (CONISS). Green dotted lines separate six diatom zones identified by CONISS.

Table 1 Location of coring sites. \*Cores from a previous NJDEP study (see text)

Sampling site	Coordinates	Core length (cm)
<b>Barnegat Bay BB1*</b>	N 40.029883; W 74.079950	94
<b>Barnegat Bay BB2*</b>	N 39.847583; W 74.147283	80
<b>Barnegat Bay BB4*</b>	N 39.627361; W 74.260222	96
<b>Cape May Courthouse (CMC)</b>	N 39.08585; W 74.81043	270
<b>Cheesequake State Park (CQ)</b>	N 40.43861; W 74.27347	250
<b>Fortescue (F11A)</b>	N 39.22642; W 75.16589	206
<b>Fortescue (F9E)</b>	N 39.2243; W 75.1655	291
<b>Great Bay GB 2*</b>	N 39.513178; W 74.413011	95
<b>Sea Breeze (SB30A)</b>	N 39.316167; W 75.315333	185

Table 2 PAH target compounds and their monitored ions

Retention Order	PAH	Primary	Secondary	Molecular weight
1	Naphthalene	128	129	128.18
2	Acenaphthene	152	153	152.20
3	Acenaphthylene	153	154	154.20
4	Fluorene	166	165	166.23
5	Phenanthrene	178	176	178.24
6	Anthracene	178	176	178.24
7	Fluoranthene	202	101	202.26
8	Pyrene	202	101	202.26
9	Benz[a]anthracene	228	114	228.30
10	Chrysene	228	114	228.30
11	Benzo(b)fluoranthene	252	126	252.32
12	Benzo(k)fluoranthene	252	126	252.32
13	Benzo[a]pyrene	252	126	252.32
14	Indeno[1,2,3-cd]pyrene	276	138	276.34
15	Dibenzo[a,h+a,c]anthrac	278	139	278.35
16	Benzo[g,h,i]perylene	276	138	276.34

Table 3. Metal species list, associated methods, and Method Detection Limit (MDL)

Metals (trace and major)	Method (Preparation/Analysis)	Method Detection Limit (ug/L)	Manufacture, Instrument Model
Ag	EPA 3051/EPA 200.8	0.018	Agilent 7700X ICPMS
Al	EPA 3051/EPA 200.8	0.059	Agilent 7700X ICPMS
As	EPA 3051/EPA 200.8	0.012	Agilent 7700X ICPMS
Ba	EPA 3051/EPA 200.8	0.00092	Agilent 7700X ICPMS
Be	EPA 3051/EPA 200.8	0.039	Agilent 7700X ICPMS
Ca	EPA 3051/EPA 200.8	5.6	Agilent 7700X ICPMS
Cd	EPA 3051/EPA 200.8	0.0017	Agilent 7700X ICPMS
Co	EPA 3051/EPA 200.8	0.0035	Agilent 7700X ICPMS
Cr	EPA 3051/EPA 200.8	0.034	Agilent 7700X ICPMS
Cu	EPA 3051/EPA 200.8	0.0038	Agilent 7700X ICPMS
Fe	EPA 3051/EPA 200.8	0.31	Agilent 7700X ICPMS
Hg	EPA 3051/EPA 200.8	0.0039	Agilent 7700X ICPMS
K	EPA 3051/EPA 200.8	6.1	Agilent 7700X ICPMS
Mg	EPA 3051/EPA 200.8	6.8	Agilent 7700X ICPMS
Mn	EPA 3051/EPA 200.8	0.003	Agilent 7700X ICPMS
Mo	EPA 3051/EPA 200.8	0.013	Agilent 7700X ICPMS
Na	EPA 3051/EPA 200.8	4.8	Agilent 7700X ICPMS
Ni	EPA 3051/EPA 200.8	0.0011	Agilent 7700X ICPMS
Pb	EPA 3051/EPA 200.8	0.042	Agilent 7700X ICPMS
Sb	EPA 3051/EPA 200.8	0.023	Agilent 7700X ICPMS
Se	EPA 3051/EPA 200.8	0.019	Agilent 7700X ICPMS
Sr	EPA 3051/EPA 200.8	0.0073	Agilent 7700X ICPMS
Th	EPA 3051/EPA 200.8	0.62	Agilent 7700X ICPMS
Ti	EPA 3051/EPA 200.8	0.0039	Agilent 7700X ICPMS
U	EPA 3051/EPA 200.8	0.2	Agilent 7700X ICPMS
V	EPA 3051/EPA 200.8	0.22	Agilent 7700X ICPMS
Zn	EPA 3051/EPA 200.8	0.68	Agilent 7700X ICPMS

Table 4. C-14 dating results for the Cheesequake core. Age and age error are years BP

Sample	Depth (cm)	Age	Age Error
CQ15/1C 62	62	155	15
CQ/15/81	81	380	15
CQ/15/93	93	605	20
CQ15/1C 122	122	315	20
CQ/15/132	132	545	15
CQ/15/134	134	1,500	20
CQ/15/141	141	795	15
CQ/15/145	145	1,290	20
CQ/15/157	157	1,080	15
CQ/15/161	161	1,470	20
CQ/15/164	164	935	15
CQ15/1C 170	170	1,600	20
CQ/15/189	189	1,650	20
CQ/15/203	203	1,770	20
CQ/15/210	210	1,030	20
CQ/15/227	227	1,910	20
CQ15/1C 239	239	2,010	15

Table 5. C-14 dating results for the Cape May core. Age and age error are years BP

Sample ID	Depth (cm)	Age	Age error
14C10	76	120	30
14C12	82	230	25
14C4	86	250	40
14C11	94	285	30
14C8	111	400	25
14C5	122	520	40
14C1	135	770	30
14C2	145	865	25
14C6	160	960	40
14C3	171	1100	30
14C13	180	1120	25
14C7	194	1190	35
14C9	208	1350	30

Table 6. C14 Dating results for Sea Breeze, and Fortescue cores. Age and age error are years BP

Sample ID	Depth (cm)	Age	Age error
F11A	130	685	20
F11A	163	795	20
F9E	194	1170	20
F9E	205	1160	15
SB30	116	165	25
SB30	244	1090	25

Table 7. Variations in trace metal data measured in the Cheesequake core. Values in mg/Kg

Metal	Min	Max	Avg	Median	90th percentile
Ag	0.03	1.27	0.29	0.09	0.87
Al	5500	13400	7955	7500	10080
As	3.00	44.00	15.69	9.00	34.60
B	20.00	60.00	41.14	40.00	60.00
Ba	11.00	31.00	18.78	17.00	29.60
Be	0.40	0.80	0.57	0.60	0.70
Bi	0.06	2.46	0.35	0.16	0.78
Ca	1900	10600	5662	5800	6800
Cd	0.03	0.61	0.18	0.12	0.40
Ce	13.90	32.40	20.42	19.40	26.68
Co	1.40	14.90	3.99	3.10	6.44
Cr	10.00	85.00	20.91	18.00	33.00
Cs	0.56	1.21	0.82	0.77	1.14
Cu	4.10	310	50.78	11.80	183
Fe	6800	23100	13480	12900	17700
Ga	1.60	4.70	2.81	2.50	4.16
Ge	<0.1	<0.1	NA	NA	NA
Hf	0.06	0.13	0.08	0.07	0.12
Hg	0.01	0.70	0.17	0.05	0.50
In	0.02	0.25	0.07	0.04	0.18
K	1600	3800	2551	2600	2960
La	6.70	14.00	9.44	9.20	12.06
Li	7.00	47.00	17.36	14.00	30.40
Lu	0.05	0.12	0.08	0.07	0.10
Mg	3400	10100	8160	8300	9760
Mn	30.00	324.00	65.18	55.00	100.00
Mo	2.66	11.80	6.34	5.97	8.92
Na	9500	49600	32593	32200	41460
Nb	0.41	0.96	0.68	0.64	0.92
Ni	6.50	40.50	16.14	13.70	30.44
P	410.00	1840	686	650	942
Pb	4.00	224.00	50.70	17.80	162.00
Rb	7.20	18.90	11.52	10.60	17.86
S	9900	39500	26268	26800	34000
Sb	0.18	7.41	1.63	0.81	4.26
Sc	1.20	3.50	2.00	1.80	3.12
Se	1.00	13.00	3.11	2.00	6.60
Sn	0.30	26.70	3.95	0.90	13.10
Sr	48.10	141.00	103.72	105.00	130.60
Ta	0.08	0.08	0.08	0.08	0.08
Tb	0.21	0.47	0.29	0.28	0.38
Te	0.05	1.70	0.43	0.21	1.28
Th	0.30	3.60	1.04	0.80	2.32
Ti	50.00	200.00	88.89	100.00	160.00

Table 7 (contnd) Variations in trace metal data measured in the Cheesequake core. Values in mg/Kg

Metal	Min	Max	Avg	Median	90th percentille
Tl	0.04	0.38	0.10	0.08	0.14
U	3.08	10.90	5.06	4.50	7.80
V	17.00	73.00	30.58	28.00	54.60
W	0.10	1.00	0.48	0.40	0.88
Y	5.13	10.50	7.06	6.66	9.08
Yb	0.40	0.90	0.57	0.50	0.76
Zn	12.00	233.00	52.02	41.00	103.40
Zr	1.10	6.60	2.65	2.80	3.90

Table 8. Variations in trace metal data measured in the Barnegat Bay BB1 core. Values in mg/Kg

Metal	Min	Max	Avg	Median	90th percentile
Ag	0.01	0.35	0.09	0.04	0.24
Al	28100	58847	39976	38026	51253
As	2.20	13.13	6.10	6.02	10.35
Ba	160.66	436.51	268.89	251.10	386.69
Be	0.67	2.09	1.24	1.21	1.59
Bi	0.05	0.46	0.17	0.12	0.35
Ca	5814	11135	7921	7833	9219
Cd	0.03	0.73	0.24	0.16	0.55
Ce	32.72	65.80	46.07	44.18	57.14
Co	2.89	11.75	5.41	4.77	8.32
Cr	43.09	74.22	55.69	54.19	65.38
Cs	1.87	3.53	2.59	2.60	3.05
Cu	5.15	75.95	16.97	8.59	50.72
Dy	1.90	3.58	2.63	2.59	3.20
Er	1.07	1.97	1.46	1.42	1.77
Eu	0.61	1.25	0.89	0.89	1.06
Fe	10290	43727	22550	19888	35446
Ga	6.97	14.00	10.04	9.60	12.66
Gd	2.37	4.85	3.38	3.32	4.10
Hf	1.13	2.27	1.56	1.49	1.99
Ho	0.36	0.73	0.51	0.50	0.61
K	10014	20617	14214	13318	18275
La	15.45	31.81	21.90	21.16	27.48
Li	25.12	52.67	35.53	35.76	42.36
Lu	0.14	0.24	0.19	0.19	0.22
Mg	7813	12011	9858	9645	11031
Mn	96.04	296.17	161.12	143.58	212.28
Mo	2.35	22.94	7.24	5.20	15.23
Na	27655	49819	36983	35927	45438
Nb	4.53	8.80	6.26	5.98	7.72
Nd	15.79	31.41	22.46	22.10	26.97
Ni	12.55	34.67	19.44	18.65	26.21
Pb	7.91	164.38	39.11	13.70	99.71
Pr	4.02	7.83	5.63	5.46	6.84
Rb	39.38	82.85	56.91	54.24	72.04
Sb	0.09	1.63	0.52	0.24	1.37
Sm	3.03	5.88	4.27	4.24	5.14
Sn	0.94	5.84	2.19	1.34	4.58
Sr	116.22	223.82	161.00	160.67	193.05
Ta	0.33	0.64	0.44	0.42	0.54
Tb	0.35	0.70	0.49	0.49	0.59
Th	4.41	7.98	5.99	5.85	7.20
Ti	1500	2924	2035	1924	2598
Tl	0.23	0.51	0.35	0.35	0.43
Tm	0.15	0.28	0.20	0.20	0.24
U	3.04	19.77	7.25	4.82	16.71

Table 8 (contnd) Variations in trace metal data measured in the Barnegat Bay BB1 core. Values in mg/Kg

Metal	Min	Max	Avg	Median	90th percentille
V	55.06	89.56	71.82	70.64	82.54
W	0.35	1.17	0.56	0.51	0.83
Y	9.73	18.75	13.25	12.83	16.22
Yb	0.96	1.78	1.30	1.29	1.56
Zn	25.75	121.09	58.21	53.31	105.85
Zr	39.74	86.10	57.33	55.28	72.76

Table 9. Variations in trace metal data measured in the Cape May Courthouse core. Values in mg/Kg

Metal	Min	Max	Avg	Median	90th percentile
Ag	0.02	4.46	0.68	0.05	2.12
Al	18663	62361	39083	41489	50794
As	3.42	14.08	7.34	7.01	13.04
Ba	110	409	243	248	321
Be	0.48	1.67	1.07	1.12	1.53
Bi	0.10	0.60	0.24	0.16	0.56
Ca	3754	8375	6401	6163	7610
Cd	0.04	0.47	0.18	0.12	0.40
Ce	17.97	59.42	41.09	42.79	51.41
Co	1.44	9.94	5.35	5.42	7.84
Cr	38.96	114.86	58.83	57.92	72.65
Cs	1.14	3.89	2.38	2.46	3.31
Cu	4.77	164.04	31.35	13.22	78.20
Dy	1.12	3.52	2.40	2.50	2.93
Er	0.62	1.86	1.31	1.38	1.58
Eu	0.35	1.02	0.74	0.77	0.92
Fe	4121	34066	19220	19004	30701
Ga	4.76	16.15	9.71	9.29	12.17
Gd	1.37	4.23	2.91	3.09	3.46
Hf	0.64	2.09	1.29	1.31	1.64
Ho	0.20	0.66	0.44	0.46	0.53
K	7318	20999	13402	13337	17138
La	8.14	27.77	19.03	19.79	26.34
Lu	0.09	0.23	0.17	0.17	0.20
Mg	6802	11783	9165	9207	10781
Mn	42.25	171.76	114.93	124.41	169.81
Mo	1.89	12.79	5.13	4.78	8.23
Na	27943	53447	39117	38413	46252
Nb	3.34	9.56	5.91	5.73	7.67
Nd	9.21	27.97	19.70	21.42	23.48
Ni	7.85	50.66	25.63	23.38	44.15
Pb	10.03	86.60	31.63	21.33	74.84
Pr	2.31	7.12	4.96	5.24	5.84
Rb	24.52	92.02	54.97	55.79	75.19
Sb	0.13	1.04	0.42	0.25	0.77
Sm	1.78	5.13	3.69	3.92	4.40
Sn	0.79	7.04	2.50	1.73	5.08
Sr	84.13	189.25	136.60	137.86	162.60
Ta	0.24	0.75	0.43	0.43	0.53
Tb	0.19	0.64	0.43	0.44	0.51
Th	3.19	9.72	6.13	6.07	7.85
Ti	1048	3231	1916	1886	2448
Tl	0.13	0.50	0.31	0.32	0.42
Tm	0.08	0.25	0.17	0.18	0.21
U	2.11	8.18	4.74	4.20	7.39

Table 9 (contnd) Variations in trace metal data measured in the Cape May Courthouse core. Values in mg/Kg

Metal	Min	Max	Avg	Median	90th percentile
V	47.06	98.09	71.02	72.90	83.33
W	0.38	1.37	0.71	0.63	1.01
Y	4.78	18.80	12.04	12.05	14.92
Yb	0.61	1.56	1.17	1.21	1.42
Zn	16.56	170.80	63.91	53.90	107.22
Zr	23.72	70.18	45.77	46.53	59.50

Table 10. Variations in trace metal data measured in the Sea Breeze core. Values in mg/Kg

Metal	Min	Max	Avg	Median	90th percentile
Ag	0.04	0.87	0.37	0.40	0.53
Al	4254	5613	4860	4903	5160
As	3.93	38.43	17.32	15.05	28.54
Ba	28.7	54.7	45.0	46.2	51.2
Cd	0.15	1.39	0.58	0.48	1.04
Co	6.08	22.46	12.48	11.12	21.25
Cr	48.2	99.6	72.2	68.2	90.5
Cu	11.6	99.7	36.5	32.3	51.1
Fe	9015	34170	14639	12635	21530
Hg	0.15	1.46	0.65	0.64	0.85
Mn	205	525	315	311	416
Mo	1.95	11.05	4.03	3.52	5.91
Ni	19.7	52.4	31.7	31.7	41.1
Pb	12.3	80.6	48.1	41.2	74.0
Sb	-0.05	0.39	0.12	0.11	0.34
Se	1.40	3.31	2.28	2.21	2.87
Ti	530	1088	934	973	1049
Th	3.13	7.11	6.26	6.62	6.98
V	51.5	80.4	67.1	65.4	78.8
U	1.70	2.82	2.29	2.33	2.68
Zn	55.0	655.4	225.6	168.5	453.0

Table 11. Comparison of average metal concentrations (mg/Kg) for the time periods pre-1700, 1700-1970; and 1970-present.

Site	Metal (mg/Kg)	Pre-1700	1700-1970	Post-1970
BB1	Al	35,116	42,285	32,052
BB1	As	3.58	6.31	8.73
BB1	Cd	0.09	0.22	0.61
BB1	Cr	49.82	57.49	52.83
BB1	Cu	6.08	13.01	61.34
BB1	Fe	19,154	24,208	16,705
BB1	Ni	14.01	19.83	25.46
BB1	Pb	8.86	35.53	111.89
BB1	Zn	30.45	56.63	113.36
BB1	Total metals	124,413	140,000	115,333
CMC	Al	40,704	39,694	31,256
CMC	As	9.32	6.99	6.00
CMC	Cd	0.18	0.19	0.09
CMC	Cr	48.27	62.54	52.10
CMC	Cu	11.48	36.86	29.75
CMC	Fe	28,500	17,833	11,068
CMC	Ni	28.51	26.26	15.20
CMC	Pb	11.42	37.50	27.96
CMC	Zn	84.17	60.06	52.28
CMC	Total metals	145,612	128,934	99,936
CQ	Al	7,200	8,825	6,200
CQ	As	4.88	19.71	31.00
CQ	Cd	0.06	0.27	0.13
CQ	Cr	13.13	25.58	23.40
CQ	Cu	6.76	76.81	66.68
CQ	Fe	13,763	13,729	11,380
CQ	Ni	8.35	21.34	16.06
CQ	Pb	6.00	73.77	83.02
CQ	Zn	42.75	58.17	52.20
CQ	Total metals	109,415	93,203	84,619

BB1 - Barnegat Bay core BB1; CMC - Cape May courthouse core; CQ - Cheesequake State Park core.

Table 12. Summary of land-use land-cover in the vicinity of coring sites for three time periods: early 1930s, 1974, and 2012. Characteristics are summarized within a 5-km and 10-km buffer around each core. FWW represents sum of Forest, Wetland and Water land-cover.

Percentage of each class within each buffer and time period									
Core Location			Forest	Wetland	Water	Developed Land	Agriculture	Barren Land	FWW
<b>Cheesequake</b>									
	5 km Buffer	1930	29	26	11	11	20	2	66
		1974	23	19	11	36	6	4	53
		2012	20	18	12	46	3	2	49
	10 km Buffer	1930	23	22	22	12	19	2	67
		1974	17	20	22	34	4	4	59
		2012	13	18	22	43	1	2	54
<b>Barnegat Bay 1</b>									
	5 km Buffer	1930	12	28	54	5	1	1	93
		1974	6	12	55	25	0	1	73
		2012	4	11	56	29	0	1	70
	10 km Buffer	1930	21	19	51	6	3	1	91
		1974	11	9	51	26	1	1	72
		2012	5	8	52	34	0	1	65
<b>Barnegat Bay 2</b>									
	5 km Buffer	1930	13	27	54	3	4	0	94
		1974	12	18	54	15	1	0	84
		2012	6	16	55	22	0	0	78
	10 km Buffer	1930	24	21	50	3	1	1	95
		1974	20	17	50	10	0	2	87
		2012	16	16	51	16	0	1	82
<b>Barnegat Bay 4</b>									
	5 km Buffer	1930	4	42	49	1	4	0	95
		1974	5	40	49	4	1	1	95
		2012	4	38	51	7	0	0	93
	10 km Buffer	1930	21	26	46	3	3	1	93
		1974	20	23	47	8	0	1	91
		2012	16	23	48	13	0	1	86
<b>Great Bay 2</b>									
	5 km Buffer	1930	8	43	45	1	4	0	96
		1974	10	43	45	2	1	0	97
		2012	8	41	47	5	0	0	95
	10 km Buffer	1930	16	47	33	1	4	0	95
		1974	15	45	33	4	1	0	94
		2012	11	43	35	10	0	0	89
<b>Cape May Courthouse</b>									
	5 km Buffer	1930	23	41	21	3	11	0	85
		1974	22	41	21	12	3	1	84
		2012	16	41	22	19	1	1	79
	10 km Buffer	1930	14	37	33	5	9	1	84
		1974	14	38	33	11	3	1	85
		2012	11	38	33	15	2	1	82

Table 12 (contnd) Summary of land-use land-cover in the vicinity of coring sites for three time periods: early 1930s, 1974, and 2012. Characteristics are summarized within a 5-km and 10-km buffer around each core

Core Location			Forest	Wetland	Water	Developed Land	Agriculture	Barren Land		FWW
<b>Sea Breeze</b>										
	5 km Buffer	1930	0	35	61	0	3	0		97
		1974	0	36	61	0	2	0		97
		2012	1	35	63	0	2	0		98
	10 km Buffer	1930	2	28	58	1	12	0		87
		1974	2	28	58	1	11	0		87
		2012	2	29	59	1	9	0		90

Table 13. Variations of diatom inferred salinity and sediment nitrogen for the time periods pre-1700, 1700-1970; and 1970-present.

Site	Period	Inferred Salinity (psu)			Inferred sediment N (%)		
		Min	Max	Avg	Min	Max	Avg
CQ	pre-1700	18.87	29.52	24.07	0.19	0.81	0.38
BB1	pre-1700	15.94	19.66	17.80	0.43	0.56	0.49
BB2	pre-1700	12.35	17.29	14.98	0.36	0.89	0.63
BB4	pre-1700	NA	NA	22.99	NA	NA	0.27
CMC	pre-1700	19.77	29.14	24.86	0.14	0.64	0.42
CQ	post-1700	13.97	24.37	19.71	0.21	1.69	0.84
BB1	post-1700	14.78	26.08	20.63	0.39	0.68	0.52
BB2	post-1700	8.34	18.93	15.90	0.33	0.60	0.45
BB4	post-1700	12.07	23.77	17.45	0.19	0.87	0.58
CMC	post-1700	19.06	26.40	23.37	0.33	0.87	0.61
CQ	post-1970	22.78	27.19	24.15	0.38	0.63	0.55
BB1	post-1970	20.14	23.38	21.56	0.67	0.83	0.76
BB2	post-1970	10.61	14.53	12.49	0.57	0.59	0.58
BB4	post-1970	14.14	16.26	15.25	0.67	1.20	0.94
CMC	post-1970	22.28	26.66	24.43	0.70	0.87	0.77

BB1, BB2, BB4 - Barnegat Bay cores BB1, BB2, BB4; CMC - Cape May courthouse core; CQ - Cheesequake State Park core.

Table 14. Variations in diatom-inferred salinity and sediment nitrogen in storm post-erosion and recovery marsh sequences from Sea Breeze and Fortescue cores

Site	Inferred parameter	Storm event sequence		
		Mudflat	Low marsh	High marsh
F9	Avg salinity (psu)	28.24	27.03	25.41
F11	Avg salinity (psu)	23.74	25.88	21.70
SB30	Avg salinity (psu)	23.34	26.00	25.23
F9	Avg N (%)	0.36	0.44	0.62
F11	Avg N (%)	0.56	0.48	0.71
SB	Avg N (%)	0.70	0.35	0.27

F9 - Fortescue core F9; F11 - Fortescue core F11; SB - Sea breeze core SB30



Table 16. Percentage of samples with ‘good’ modern analogue and ‘close’ modern analog in the 100 sites and 171 sites calibration dataset; ‘good’ and ‘close’ are defined as the 5th and 20th percentiles\*, respectively, of Bray-Curtis dissimilarity values for the modern samples.

Core code	No. of samples	Samples with good modern analogue (%)		Samples with close modern analogue (%)	
		100 sites calibration dataset	171 sites calibration dataset	100 sites calibration dataset	171 sites calibration dataset
Barnegat Bay 1 (BB1)	20	0	10	15	80
Barnegat Bay 2 (BB2)	19	0	5	37	79
Barnegat Bay 3 (BB3)	21	0	0	44	69
Barnegat Bay 4 (BB4)	21	0	5	43	95
Great Bay 2(GB2)	25	0	0	68	84
Cheesequake (CQ)	69	0	20	0	42
Cape May Courthouse 8B (CMC 8B)	102	0	30	16	93
Fortescue 9E (F9E)	48	0	2	23	79
Fortescue 11A (F11A)	30	0	7	33	93
Sea Breeze 30A (SB30A)	34	35	53	65	85

\* 100 sites: cutoff for good analogue is 0.498 and for close analog is 0.660

171 sites: cutoff for good analogue is 0.492 and for close analog is 0.690

Table 17. Optima and tolerances for salinity and nitrogen content in the sediment of diatom taxa most common in NJ coastal wetlands and sediment cores or highly indicative of reference conditions (**in bold**). CQ = Cheesequake, BB = Barnegat Bay, GB = Great Bay, CMC = Cape May Courthouse, Fort = Fortesque, SB = Sea Breeze

Taxa	Salinity (ppt)		N sediment (%)		Habitat preferences				Occurrence in cores				
	Optimum	Tolerance	Optimum	Tolerance	Subtidal	Mudflats	Marsh	Upland	CQ	BB/GB	CMC	Fort	SB
<i>Adlafia sp. 3 COAST</i>	23.1	0.8	0.26	0.05	X	X	X		X	X		X	X
<i>Amphicocconeis disculoides</i>	23.8	0.8	0.14	0.03	X				X	X	X	X	X
<i>Astartiella bahusiensis</i>	22.7	0.9	0.47	0.06	X				X	X		X	X
<i>Bacillaria paradoxa</i>	16.7	1.1	0.4	0.05			X		X	X	X	X	X
<i>Berkeleya rutilans</i>	20.4	0.8	0.38	0.03	X		X		X	X	X	X	
<i>Caloneis bacillum</i>	11.7	1.1	0.45	0.13			X	X	X	X	X	X	X
<i>Chaetoceros spp.</i>	17.8	0.6	0.45	0.04	X	X				X	X	X	X
<i>Cocconeis neothumensis</i> var. <i>marina</i>	22.2	0.9	0.24	0.04	X				X	X	X		
<i>Cocconeis peltoides</i>	23.6	0.9	0.23	0.05	X				X	X	X	X	X
<i>Cocconeis cf. scutellum</i>	27.9	0.6	0.33	0.09	X				X	X	X		

Table 17 (contnd) Optima and tolerances for salinity and nitrogen content in the sediment of diatom taxa most common in NJ coastal wetlands and sediment cores or highly indicative of reference conditions (**in bold**). CQ = Cheesequake, BB = Barnegat Bay, GB = Great Bay, CMC = Cape May Courthouse, Fort = Fortesque, SB = Sea Breeze

Taxa	Salinity (ppt)		N sediment (%)		Habitat preferences				Occurrence in cores				
	Optimum	Tolerance	Optimum	Tolerance	Subtidal	Mudflats	Marsh	Upland	CQ	BB/GB	CMC	Fort	SB
<i>Cocconeis placentula</i> <i>var. lineata</i>	19.8	1.2	0.29	0.05	X				X	X	X	X	X
<i>Cocconeis</i> <i>stauroneiformis</i>	24.5	0.9	0.22	0.03	X				X	X	X	X	X
<i>Cosmioneis pusilla</i>			-	-			X	X	X	X	X	X	
<i>Cyclotella atomus</i> <i>var. gracilis</i>	21.3	1.4	0.3	0.03	X	X	X		X	X	X	X	X
<i>Cyclotella</i> <i>choctawatcheeana</i>	19.1	0.5	0.41	0.04	X	X	X		X	X		X	X
<i>Cyclotella striata</i>	18.5	1.2	0.31	0.04	X	X	X	X	X	X	X	X	X
<i>Cymatosira belgica</i>	15.9	1.8	0.19	0.05	X	X			X	X	X	X	X
<i>Denticula subtilis</i>	13.8	1.2	0.41	0.04			X	X	X	X	X	X	X
<i>Diploneis smithii</i>	17.2	1.5	-	-									
<i>Fallacia aequorea</i>	26.8	0.9	0.18	0.03	X				X	X	X		
<i>Fallacia cryptolyra</i>	19.5	1.2	0.38	0.06		X	X		X	X	X	X	X
<i>Fragilaria amicornum</i>	16.8	1.1	0.58	0.08	X	X	X			X	X	X	

Table 17 (contnd) Optima and tolerances for salinity and nitrogen content in the sediment of diatom taxa most common in NJ coastal wetlands and sediment cores or highly indicative of reference conditions (**in bold**). CQ = Cheesequake, BB = Barnegat Bay, GB = Great Bay, CMC = Cape May Courthouse, Fort = Fortesque, SB = Sea Breeze

Taxa	Salinity (ppt)		N sediment (%)		Habitat preferences				Occurrence in cores				
	Optimum	Tolerance	Optimum	Tolerance	Subtidal	Mudflats	Marsh	Upland	CQ	BB/GB	CMC	Fort	SB
<i>Frustulia creuzburgensis</i>	6.3	1.9	0.35	0.09			X	X	X	X	X	X	X
<i>Halamphora acutiuscula</i>	13.4	1.2	0.6	0.09		X	X		X	X	X	X	
<i>Halamphora aponina</i>	18.9	1.2	0.4	0.06		X	X		X	X	X	X	X
<i>Halamphora coffeaeformis</i>	23.2	1.4	0.43	0.06		X	X			X			X
<i>Halamphora staurophora</i>	22.4	0.9	0.5	0.05	X	X							
<i>Halamphora</i> sp. 6 COAST	26.8	0.8	0.39	0.06	X	X				X		X	X
<i>Melosira nummuloides</i>	14.2	1.5	0.54	0.07	X				X	X	X	X	X
<i>Navicula antverpiensis</i>	15.9	1.1	0.44	0.06			X	X	X	X	X	X	X
<i>Navicula consentanea</i>	23.4	1.2	0.39	0.06		X			X	X	X	X	X
<i>Navicula digitoconvergens</i>	19.7	1.4	0.24	0.06			X		X	X	X	X	X
<i>Navicula flantica</i>	23.5	0.8	0.33	0.03	X		X		X	X	X	X	
<i>Navicula gregaria</i>	13.4	0.9	0.52	0.08		X	X	X	X	X	X	X	X
<i>Navicula jonssonii</i>	17.1	1.3	0.49	0.06		X	X		X	X	X	X	X

Table 17 (contnd) Optima and tolerances for salinity and nitrogen content in the sediment of diatom taxa most common in NJ coastal wetlands and sediment cores or highly indicative of reference conditions (**in bold**). CQ = Cheesequake, BB = Barnegat Bay, GB = Great Bay, CMC = Cape May Courthouse, Fort = Fortesque, SB = Sea Breeze

Taxa	Salinity (ppt)		N sediment (%)		Habitat preferences				Occurrence in cores				
	Optimum	Tolerance	Optimum	Tolerance	Subtidal	Mudflats	Marsh	Upland	CQ	BB/GB	CMC	Fort	SB
<i>Navicula microcari</i>	13.2	2.2	0.43	0.05		X	X	X	X	X	X	X	X
<i>Navicula peregrina</i>	12.2	2.1	0.49	0.14				X	X	X	X	X	X
<i>Navicula perminuta</i>	18.9	0.9	0.48	0.06	X	X	X		X	X	X	X	X
<i>Navicula salinarum</i>	23.4	1.7	0.51	0.05					X	X	X	X	X
<i>Navicula salinicola</i>	27	0.7	0.33	0.04		X	X			X			X
<i>Nitzschia brevissima</i>	8.3	1.9	0.35	0.09			X	X	X	X	X	X	X
<i>Nitzschia constricta</i>	16.6	1.5	0.32	0.1			X		X	X	X	X	X
<i>Nitzschia dissipata</i>	22.4	0.9	0.39	0.04	X		X		X	X	X	X	X
<i>Nitzschia frustulum</i>	18.3	0.9	0.43	0.05	X	X	X		X	X	X	X	X
<i>Nitzschia microcephala</i>	7.7	1.9	0.7	0.11		X	X		X	X	X	X	X
<i>Nitzschia palea</i>	19.4	0.7	0.37	0.05	X	X			X	X	X	X	X
<i>Nitzschia pusilla</i>	19.7	1.2	0.66	0.09		X	X		X	X	X	X	X
<i>Nitzschia sigma</i>	12.4	2	0.29	0.05			X	X	X	X	X	X	X
<i>Nitzschia</i> sp. 3 COAST	22.9	1	0.33	0.05	X	X				X		X	X
<i>Opephora</i> sp. 2 COAST	23.6	0.7	0.32	0.04	X	X			X	X	X	X	X
<i>Opephora</i> sp. 8 COAST	22.9	0.8	0.38	0.54	X		X		X	X	X	X	

Table 17 (contnd) Optima and tolerances for salinity and nitrogen content in the sediment of diatom taxa most common in NJ coastal wetlands and sediment cores or highly indicative of reference conditions (**in bold**). CQ = Cheesequake, BB = Barnegat Bay, GB = Great Bay, CMC = Cape May Courthouse, Fort = Fortesque, SB = Sea Breeze

Taxa	Salinity (ppt)		N sediment (%)		Habitat preferences				Occurrence in cores				
	Optimum	Tolerance	Optimum	Tolerance	Subtidal	Mudflats	Marsh	Upland	CQ	BB/GB	CMC	Fort	SB
<i>Paralia sulcata</i>	20.7	1.4	0.25	0.02	X	X	X	X	X	X	X	X	X
<i>Planothidium delicatulum</i>	19.5	0.9	0.33	0.04	X	X	X		X	X	X	X	X
<i>Planothidium cf. frequentissimum</i>	14.7	1.2	0.52	0.06			X		X	X	X	X	X
<i>Planothidium rodriguense</i>	23.5	1.3	0.19	0.03	X				X	X	X	X	X
<i>Psammogramma vigoensis</i>	24.9	0.8	0.21	0.02	X				X	X			X
<i>Pseudostaurosira subsalina</i>	10.3	1.5	1.03	0.19		X			X	X	X	X	X
<i>Pseudostaurosira sp. 1</i>	20.8	1.6	0.5	0.08		X	X		X	X	X	X	X
<i>Pseudostaurosira trainorii</i>	19.7	0.9	0.52	0.07	X	X	X		X	X	X	X	X
<i>Rhopalodia musculus</i>	23.3	1.5	0.28	0.05	X	X			X	X	X	X	X
<i>Skeletonema spp</i>	16.5	1.14	0.28	0.03	X	X	X		X	X	X	X	X
<i>Thalassionema nitzschioides</i>	21.9	1.13	0.28	0.05	X		X		X	X	X	X	X

Table 17 (contnd) Optima and tolerances for salinity and nitrogen content in the sediment of diatom taxa most common in NJ coastal wetlands and sediment cores or highly indicative of reference conditions (**in bold**). CQ = Cheesequake, BB = Barnegat Bay, GB = Great Bay, CMC = Cape May Courthouse, Fort = Fortesque, SB = Sea Breeze

Taxa	Salinity (ppt)		N sediment (%)		Habitat preferences				Occurrence in cores				
	Optimum	Tolerance	Optimum	Tolerance	Subtidal	Mudflats	Marsh	Upland	CQ	BB/GB	CMC	Fort	SB
<i>Thalassiora oestrupii</i>	13.1	1.6	0.24	0.07			X	X	X	X	X	X	X
<i>Thalassiora proeckhinae</i>	21.8	0.8	0.26	0.03	X	X	X		X	X	X	X	X

Table 18. Summary of reference (pre-1700) vs present-day conditions assessed by presence/absence of indicator diatom species, and the diatom-inferred nitrogen and salinity in study sites. Sites are grouped as high-developed wetlands (HD; >30% developed land) - Cheesequake and Barnegat Bay BB1; medium-developed wetlands (MD; 10-30% developed land in 2012) - Barnegat Bay BB2, BB4, and Cape May; and low-developed wetlands (LD; < 10% developed land) - Great Bay GB 2 and Delaware Bay Fortescue and Sea Breeze sites.

Indicator	Reference conditions			Present-day conditions		
	HD	MD	LD	HD	MD	LD
Diatom species						
<i>Amphicocconeis discoloides</i>	Y	Y	Y	N	N	N
<i>Caloneis bacillum</i>	Y	Y	Y	N	Y	Y
<i>Cocconeis placentula var. lineata</i>	Y	Y	Y	N	N	N
<i>Cocconeis stauroneiformis</i>	Y	Y	Y	N	Y	N
<i>Cosmioneis pusilla</i>	Y	Y	Y	Y	N	N
<i>Cyclotella striata</i>	Y	Y	Y	Y	Y	Y
<i>Cymatosira belgica</i>	Y	Y	Y	N	N	Y
<i>Frustulia creuzburgensis</i>	Y	Y	Y	N	Y	Y
<i>Navicula digitoconvergens</i>	Y	Y	Y	Y	Y	Y
<i>Navicula peregrina</i>	Y	Y	Y	N	Y	Y
<i>Opephora sp. 2 COAST</i>	Y	Y	Y	N	N	N
<i>Paralia sulcata</i>	Y	Y	Y	Y	Y	Y
<i>Rhopalodia musculus</i>	Y	Y	Y	Y	N	N
<i>Thalassionema nitzschioides</i>	Y	Y	Y	Y	N	Y
<i>Thalassiora oestrupii</i>	Y	Y	Y	Y	N	Y
Inferred Nitrogen Min-Max (%)	0.2-0.8	0.1-0.9	0.2-2.1*	0.4-0.8	0.6-1.2	0.2-0.6
Salinity Min-Max (psu)	16-30	12-29	12-29*	20-27	11-27	25-29

\*Delaware Bay sites only; include impacts from storm events which induced high nitrogen increase and salinity fluctuations caused by wetland erosion and infill (see text)

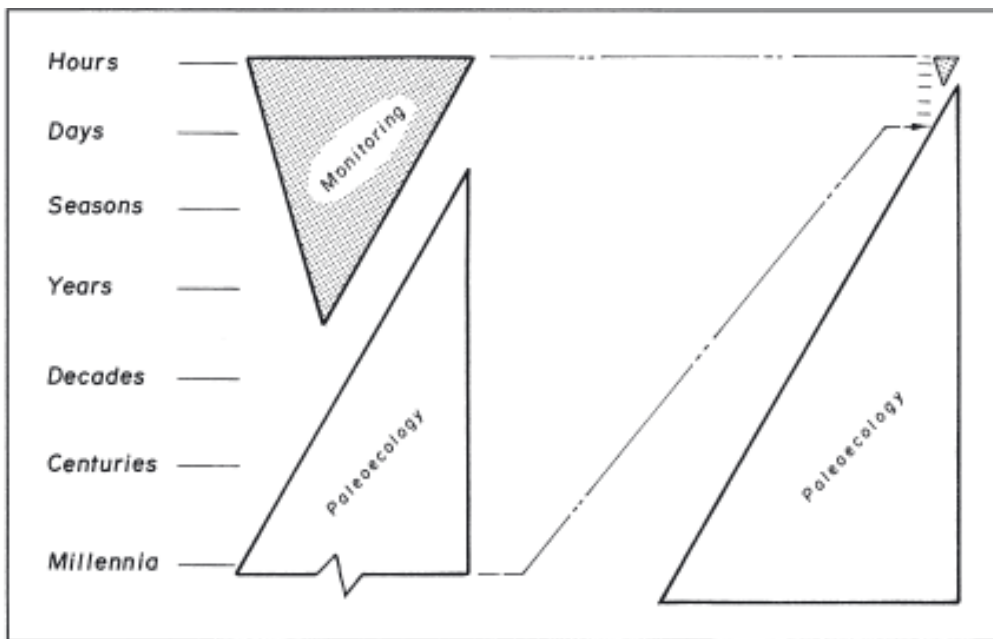


**Figure 1** Environmental monitoring – a matter of time scales. The time scales shown in the figure to the left are on a logarithmic scale; the figure to the right shows a more realistic representation of the relative amount of information potentially available from sedimentary deposits (Modified from Smol 2008)

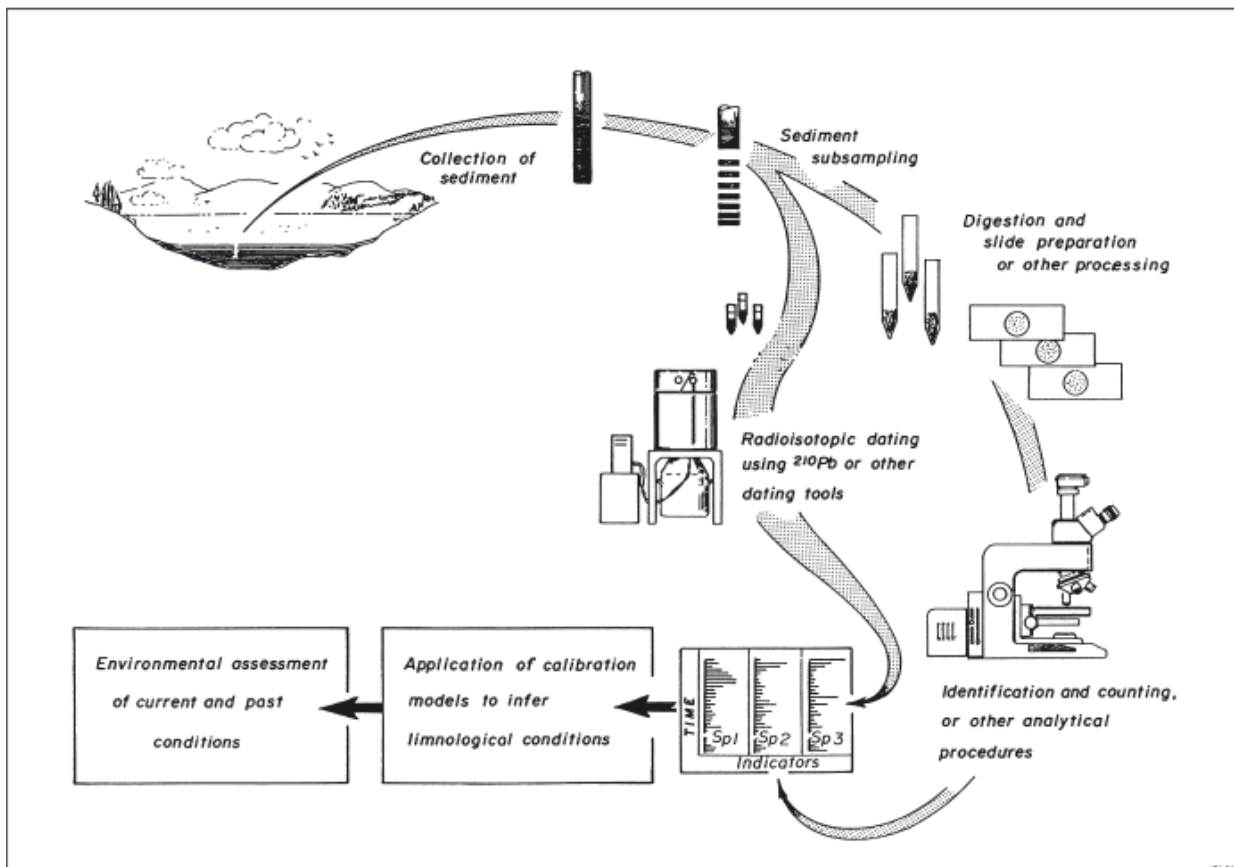


**Figure 2** Sediment core multi-proxy data is used to provide quantitative reconstructions of environmental parameters necessary to evaluate the ecological condition of wetland ecosystems. Figure courtesy of Dr. JP Smol, Queen's University, Canada

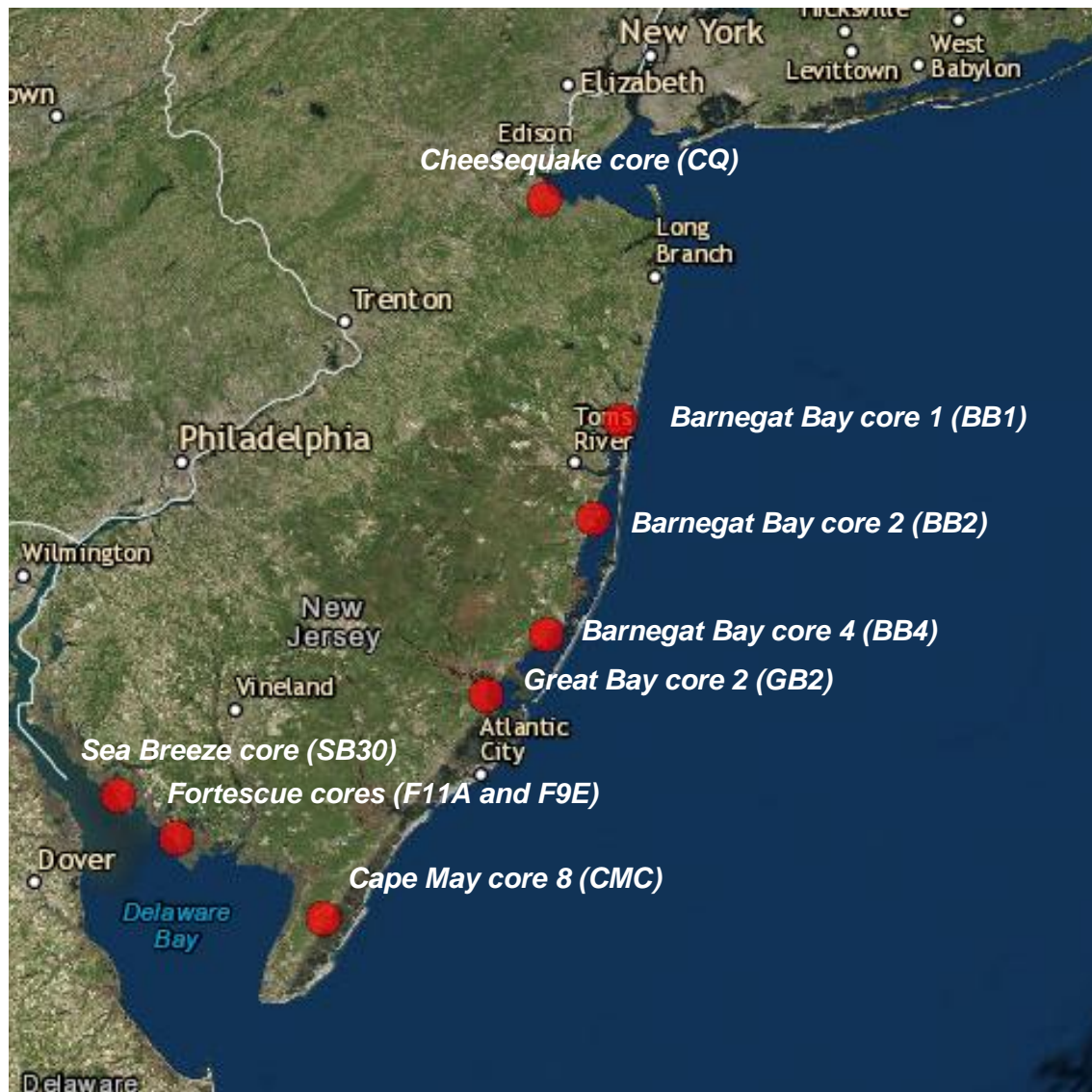


**Fig. 3.** Locations of sediment cores studied in this project. The Barnegat Bay and Great Bay cores were analyzed for diatoms through a previous NJDEP project (Potapova et al. 2017), while the remaining 5 cores were analyzed during this project.



a)



b)

Figure 4. a) Eijkelkamp Peat-coring system (<https://en.eijkelkamp.com/products/augering-soil-sampling-equipment/peat-sampler.html>); and b) sediment core increment obtained at the Cheesequake State Park site.

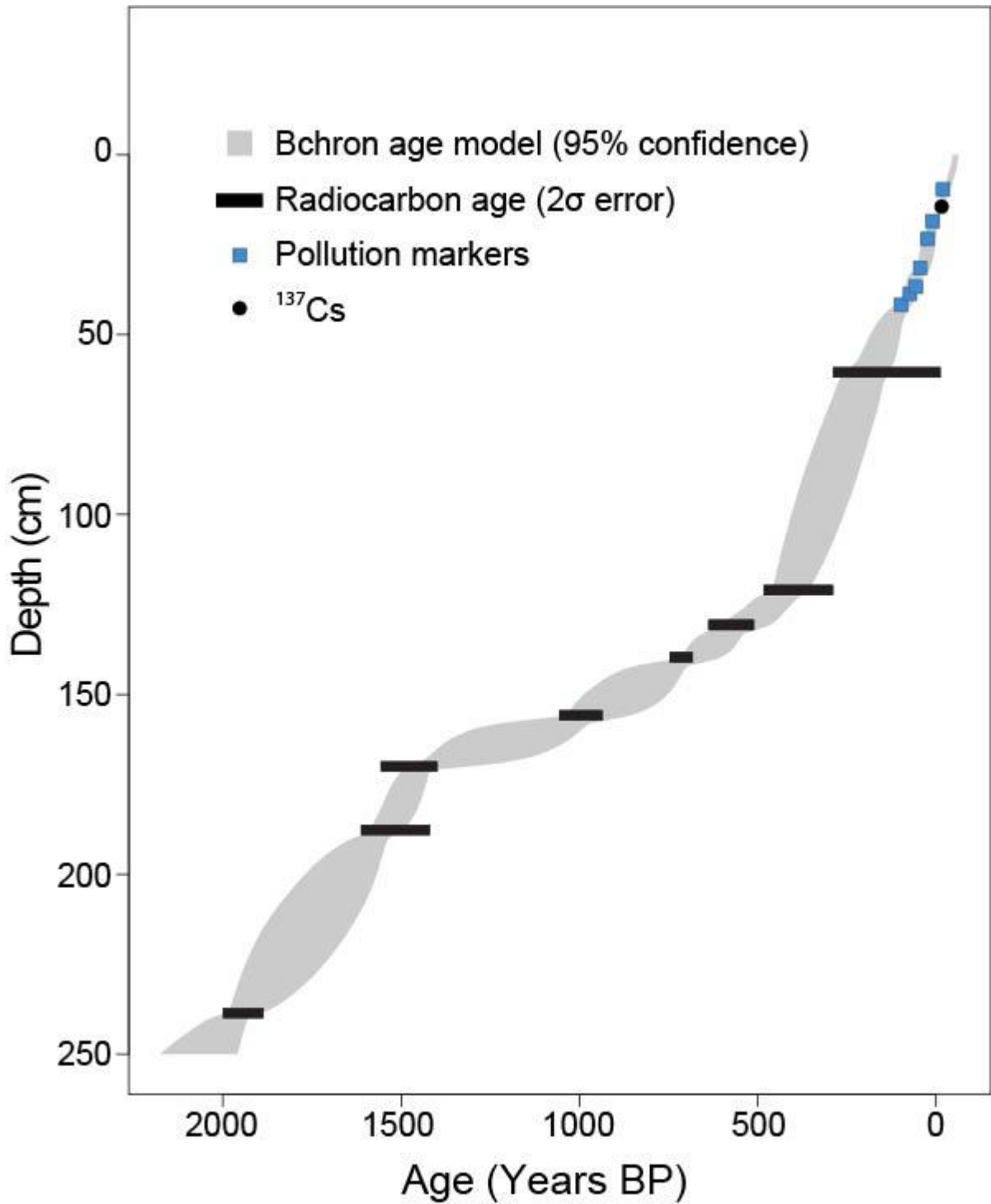


Figure 5. Cheesecake State Park Core chronology based on C-14, Cs-137 and pollution markers. The age-depth model was produced using the Bchron package in R (Haslett and Parnell, 2008)

## Cape May

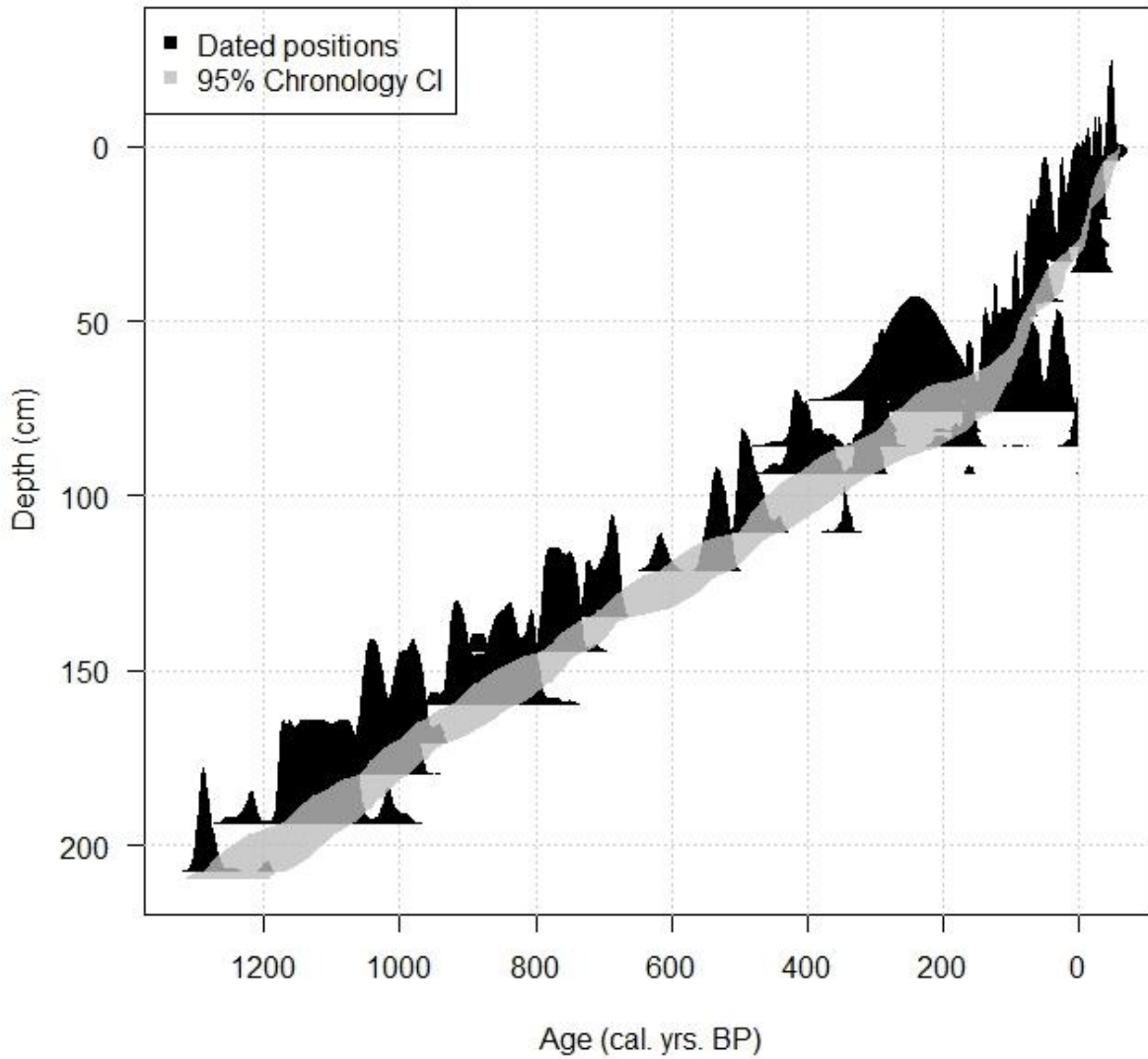


Figure 6. Cape May Courthouse Core chronology based on C-14, Cs-137, pollution markers and Ambrosia pollen. The age-depth model was produced using the Bchron package in R (Haslett and Parnell, 2008)

## Sea Breeze

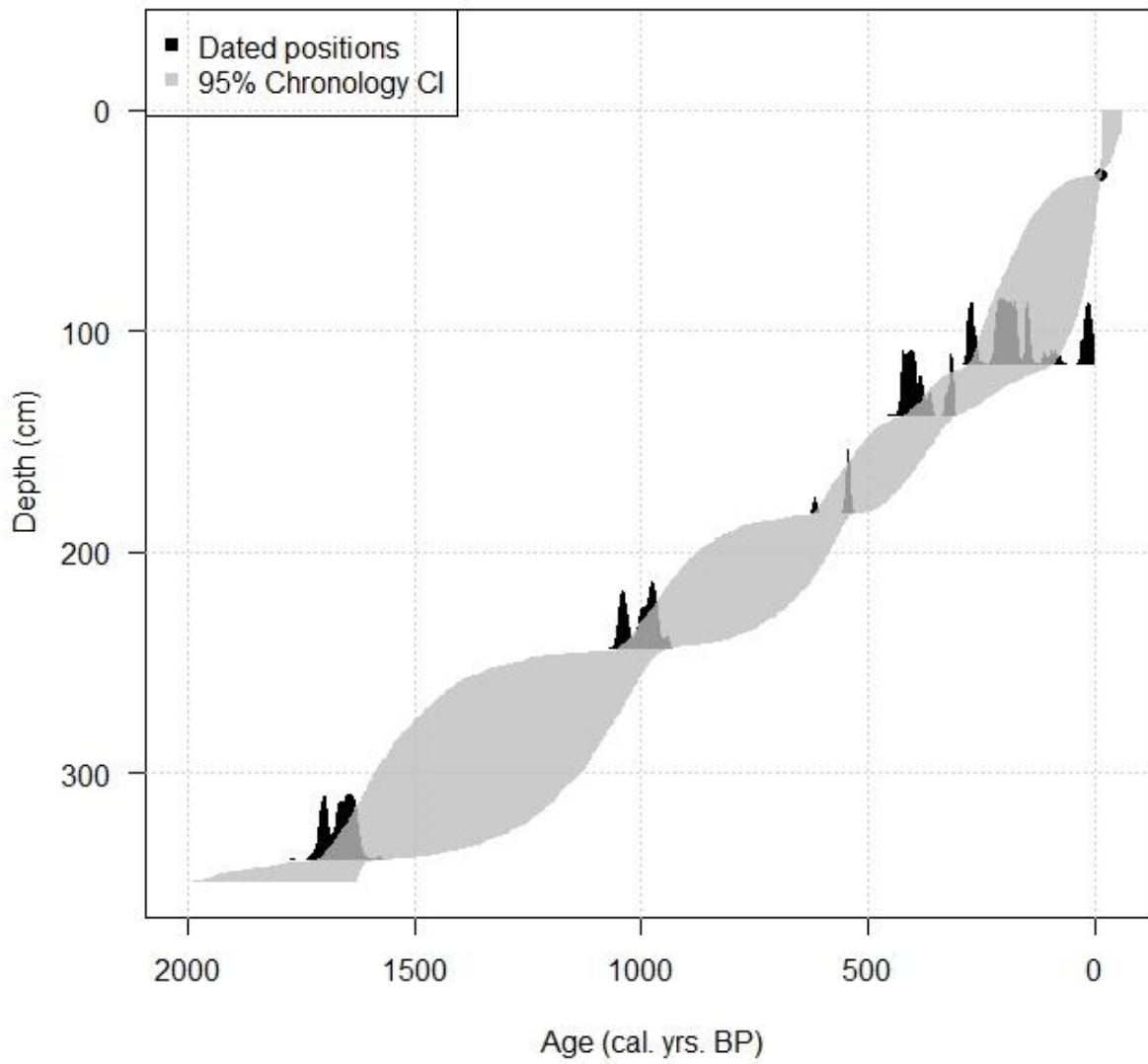


Figure 7. Sea Breeze SB-30 core chronology based on C-14, and Cs-137. The age-depth model was produced using the Bchron package in R (Haslett and Parnell, 2008)

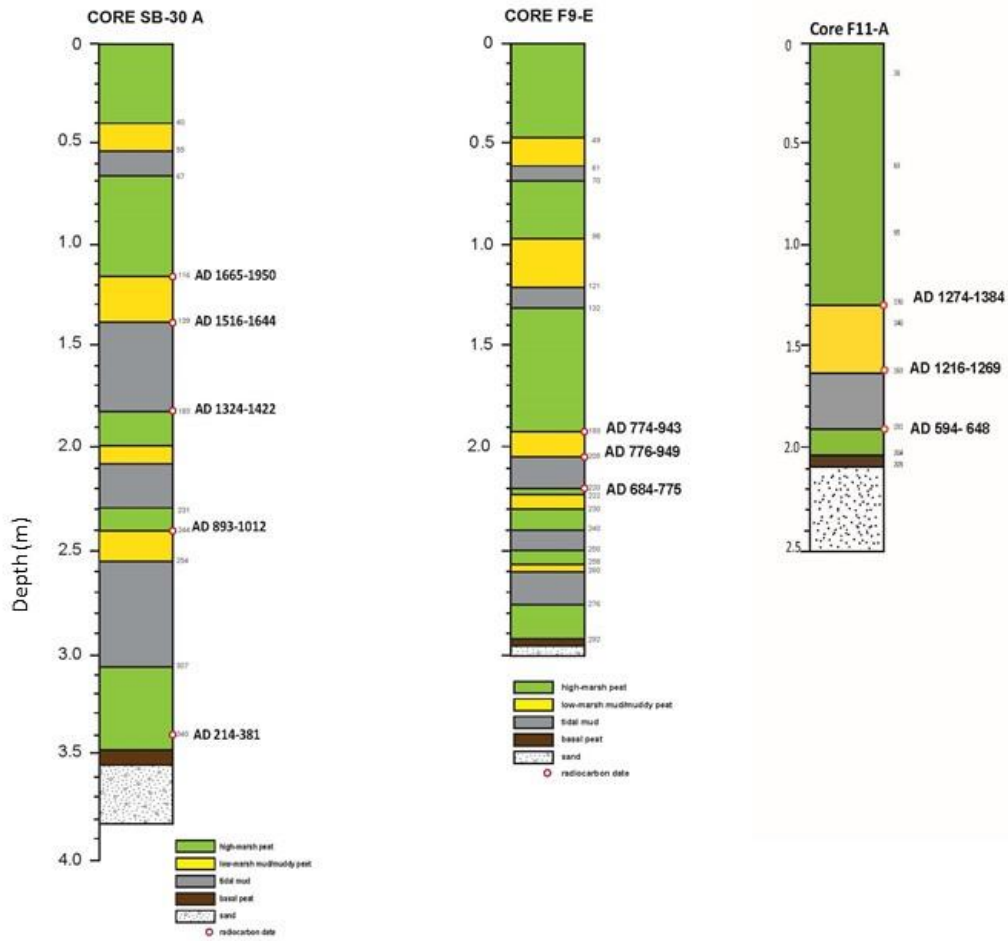


Figure 8. Storm events lithology and C-14 chronology for the Sea Breeze and Fortescue cores. Radiocarbon ages were calibrated using CALIB (Stuiver and Reimer, 1993) and the IntCal09 calibration data set (Reimer et al., 2011)

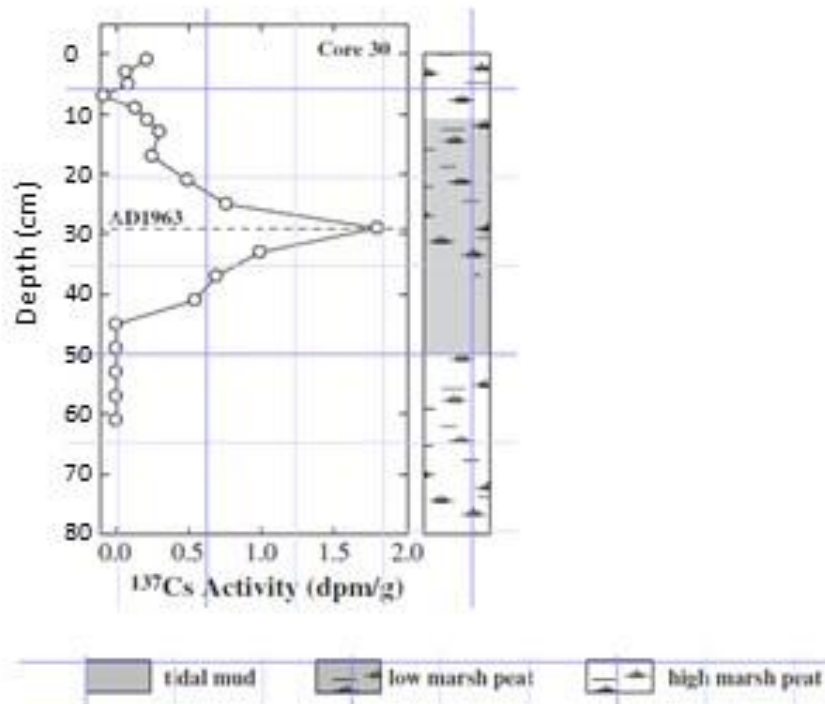


Figure 9. Dating of the Sea Breeze upper part core SB-30 using Cs-137 gamma spectrometry; modified from Nikitina et al. (2014)

Cheesequake (PAHs)

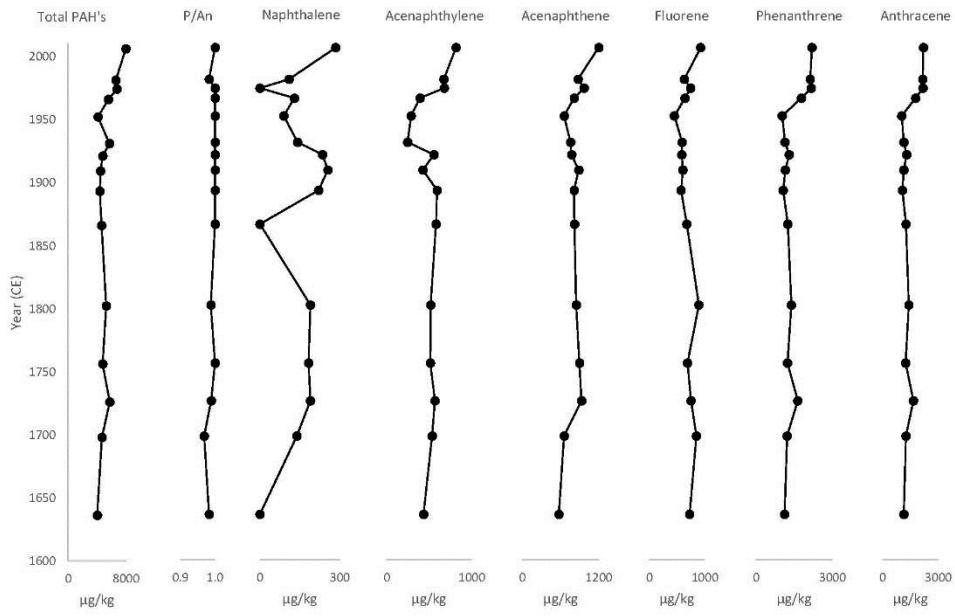


Figure 10. Stratigraphic profile of PAHs distribution in the Cheesequake sediment core

Cape May (PAH's)

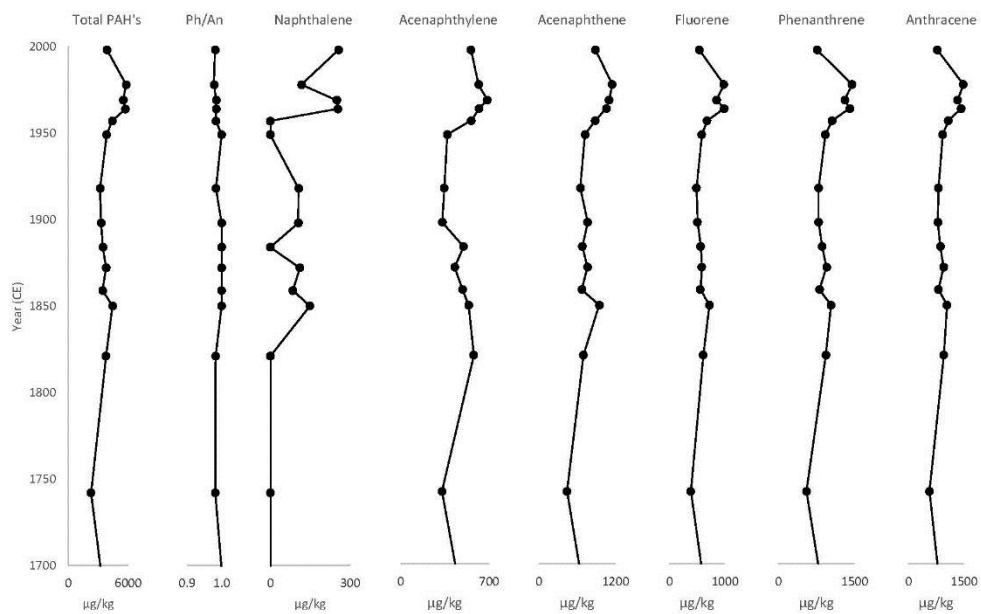


Figure 11. Stratigraphic profile of PAHs distribution in the Cape May sediment core

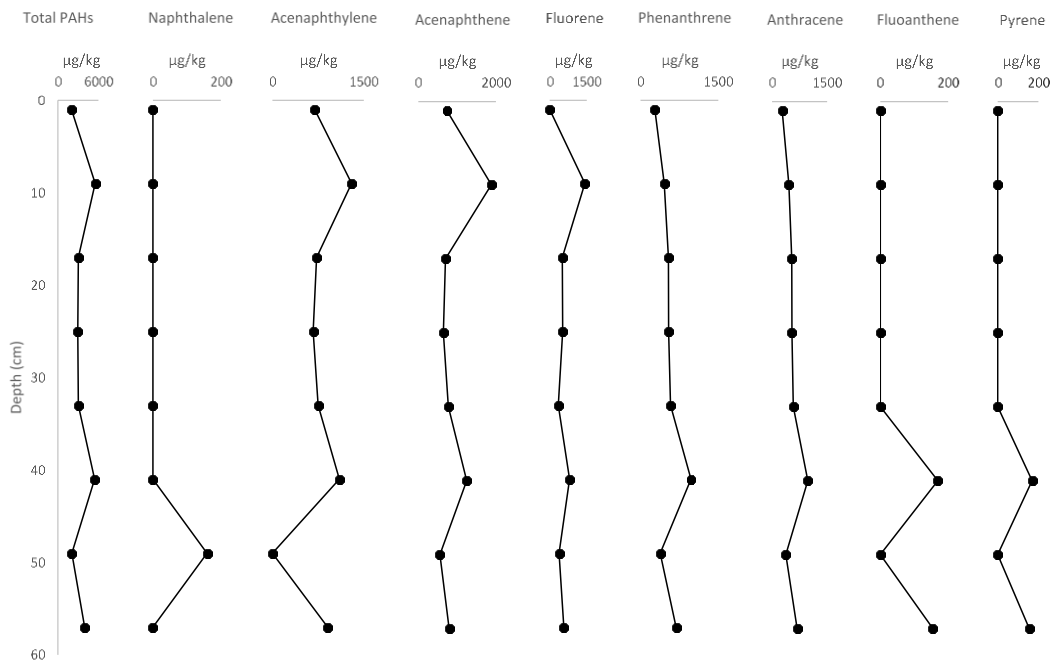


Figure 12. Stratigraphic profile of PAHs distribution in the Sea Breeze core

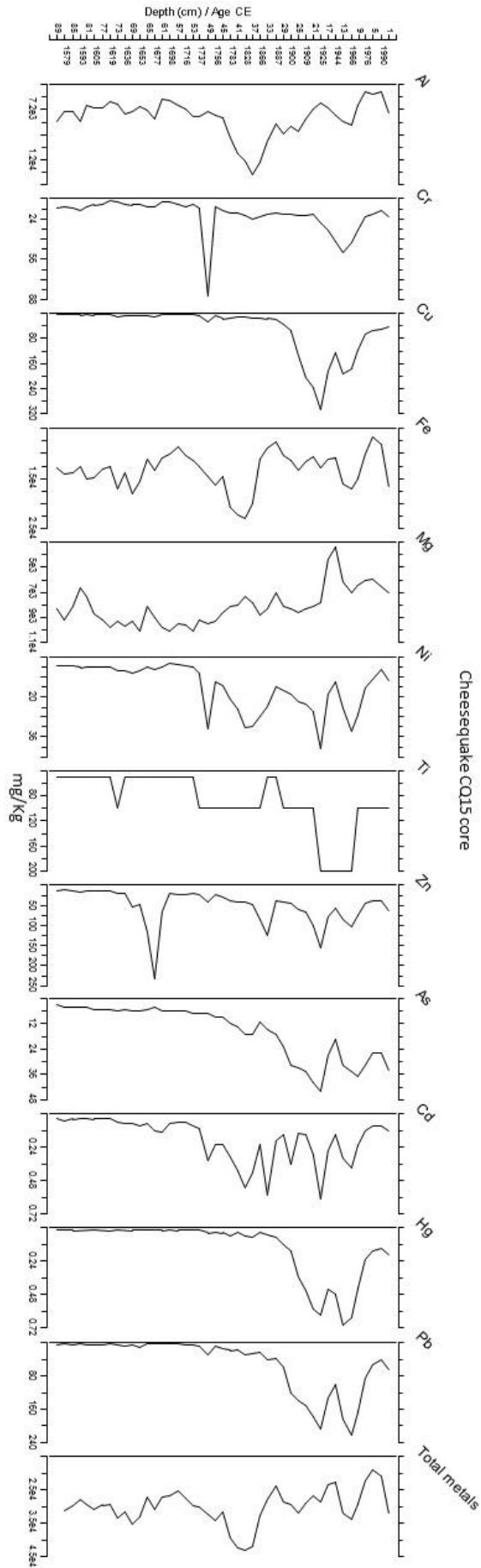


Figure 13. Stratigraphic profile of select trace metals distribution in the Cheesapeake core

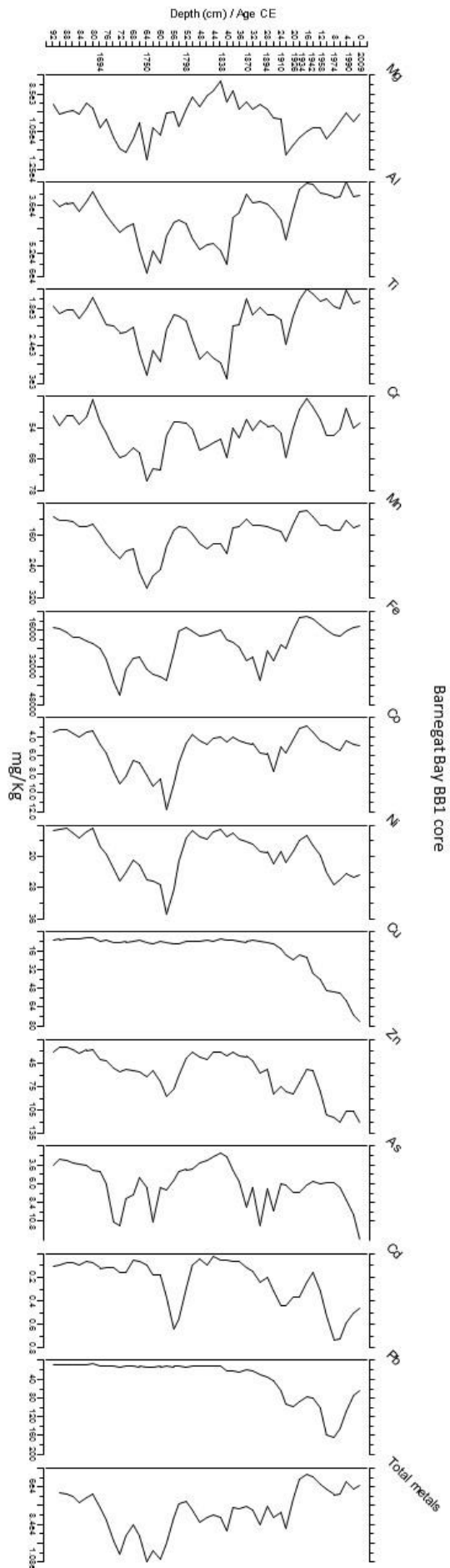


Figure 14. Stratigraphic profile of select trace metals distribution in the Barnegat Bay BB1 core

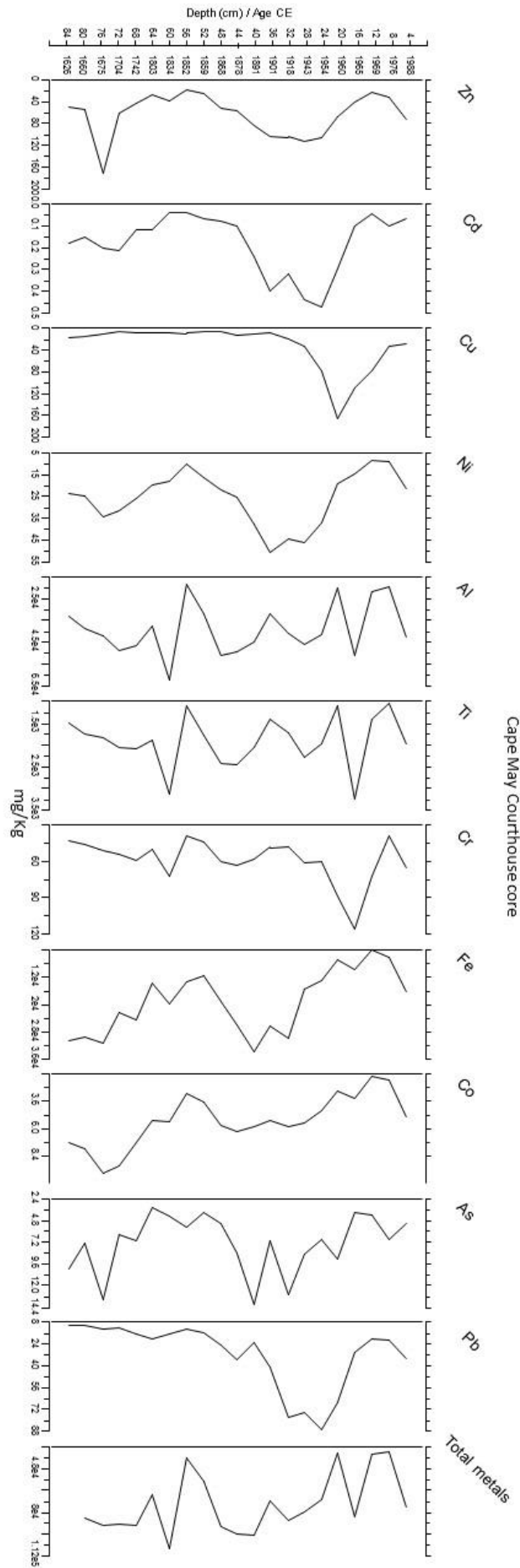


Figure 15. Stratigraphic profile of select trace metals distribution in the Cape May Courthouse core

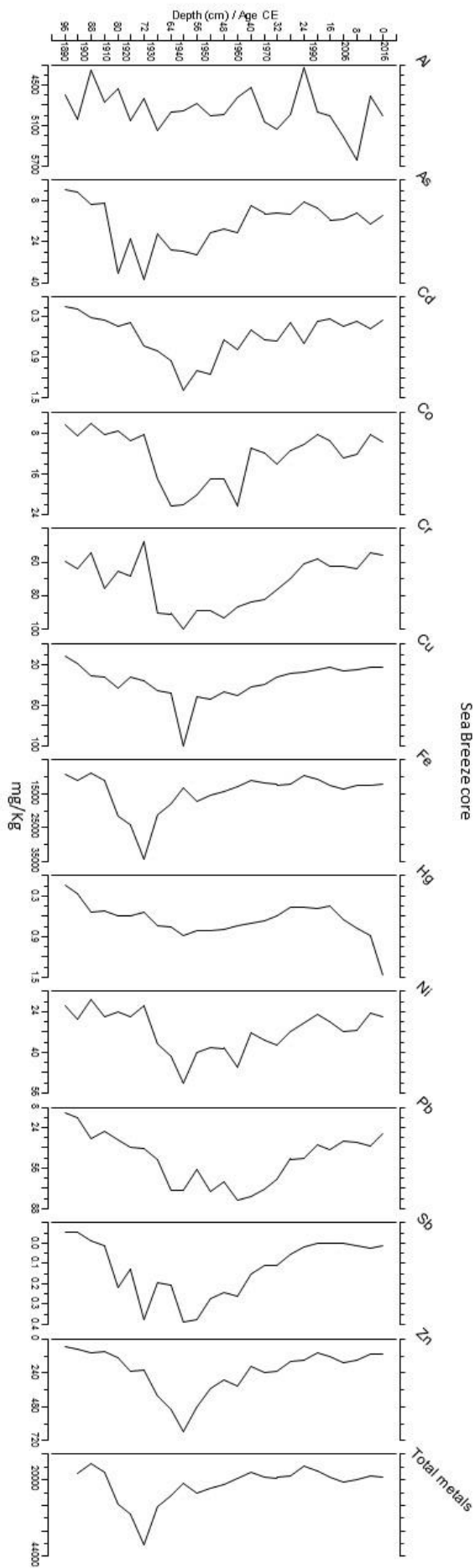


Figure 16. Stratigraphic profile of select trace metals distribution in the Sea Breeze core

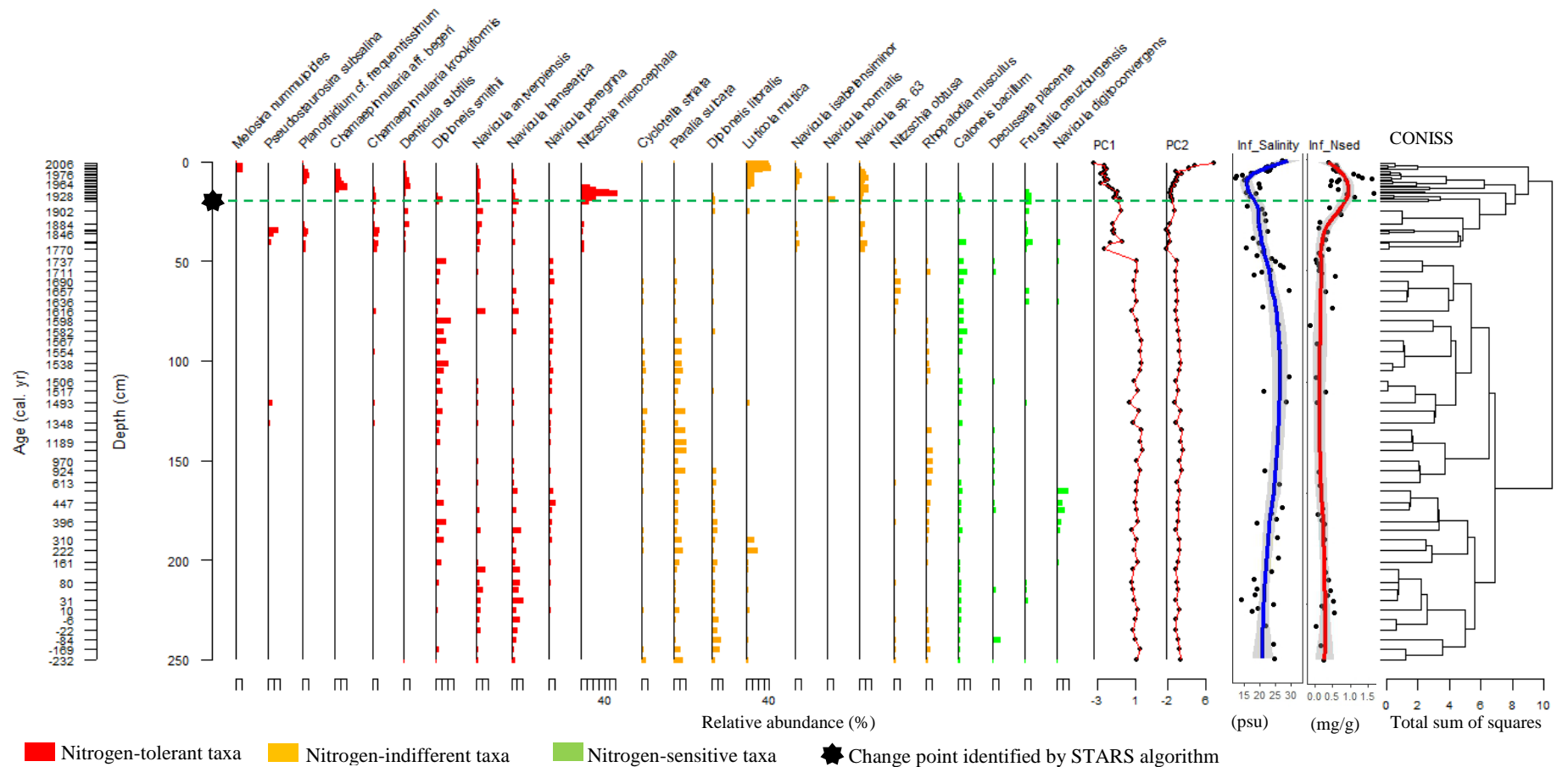


Figure 17. Diatom stratigraphy plot for Cheesequake core showing relative abundances of taxa that reached at least 10% in at least one sample, Principal Component (PC1 and PC2) sample scores, diatom-based reconstruction of salinity (Inf\_Salinity) and nitrogen content in the sediment (Inf\_Nsed) with a loess smoother fitted to reconstructed values and calculated 95% confidence intervals (grey area), and a dendrogram illustrating depth-constrained cluster analysis of diatom data (CONISS). Green dotted lines separate two diatom zones identified by CONISS. Star symbol shows the major transition in the diatom assemblage composition identified by the STARS algorithm. Both STARS algorithm and CONISS identified a major transition at ca. 1760

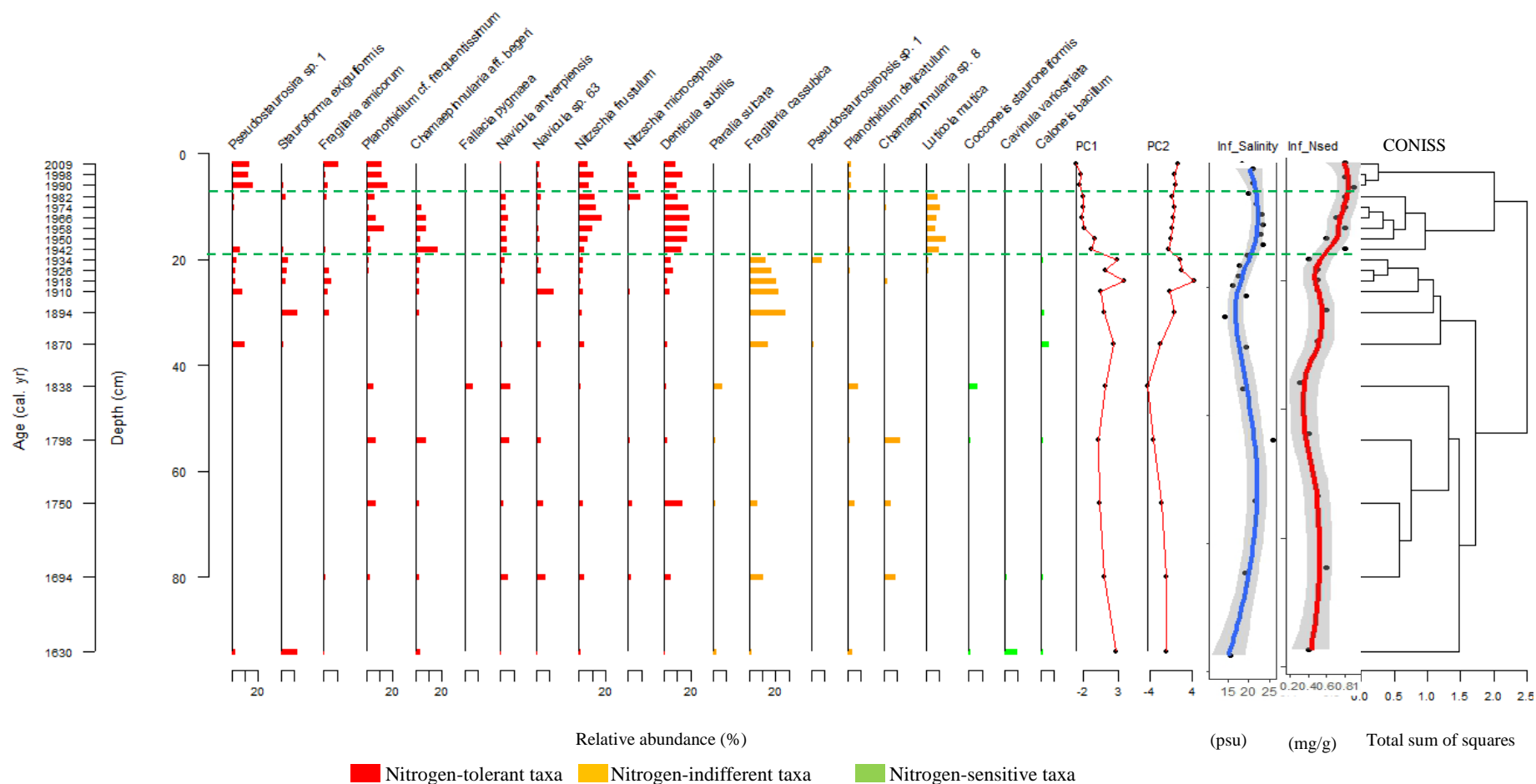
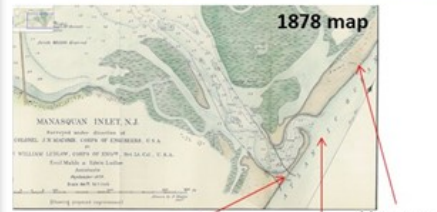
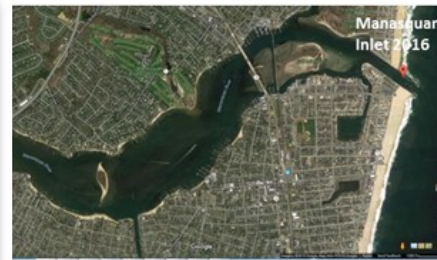
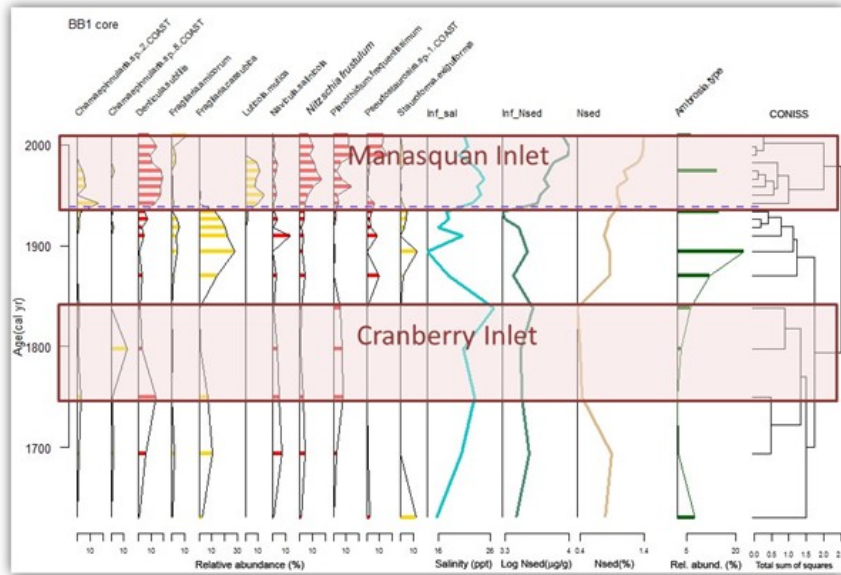


Figure 18. Diatom stratigraphy plot for Barnegat Bay core 1 showing relative abundances of taxa that reached at least 5% in at least one sample, Principal Component (PC1 and PC2) sample scores, diatom-based reconstruction of salinity (Inf\_Salinity) and nitrogen content in the sediment (Inf\_Nsed) with a loess smoother fitted to reconstructed values and calculated 95% confidence intervals (grey area), and a dendrogram illustrating depth-constrained cluster analysis of diatom data (CONISS). Green dotted lines separate three diatom zones identified by CONISS.

Core BB1: salinity and sediment Nitrogen reconstructions



Manasquan Inlet opening project started in 1930 and the inlet was completely open in 1931 until now (2016)

Manasquan Inlet 1878

Manasquan Inlet 1868

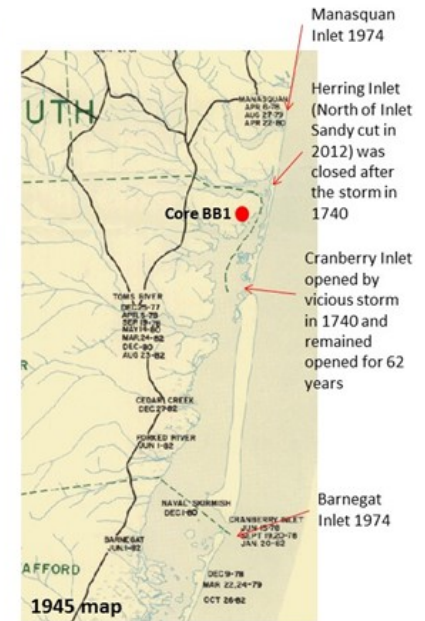


Fig. 19. Diatom assemblages in the BB1 core, inferred salinity and nitrogen, and maps of historical records of inlet opening/closing in the vicinity of core BB1 that are reflected in salinity fluctuations.

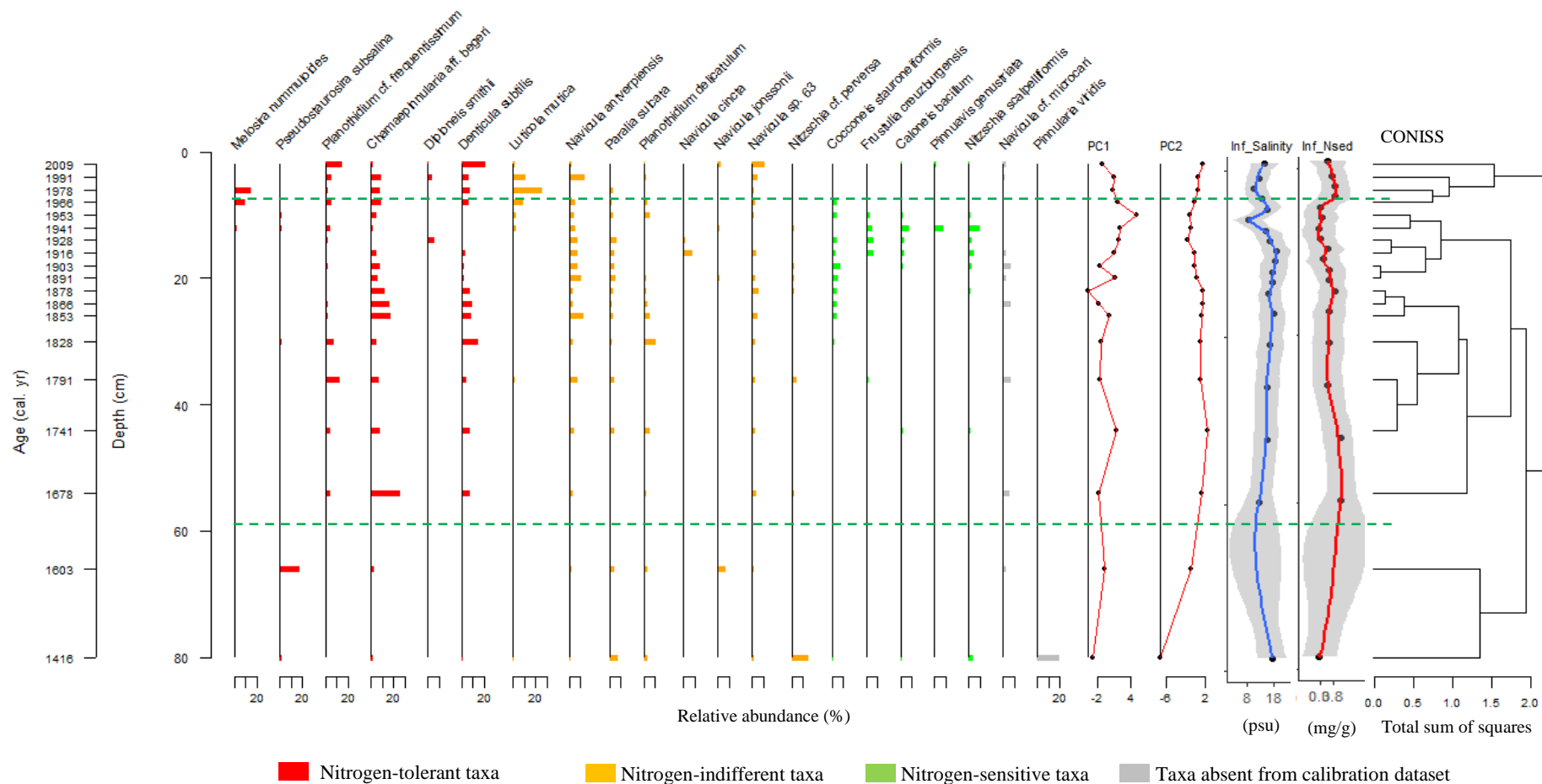


Figure 20. Diatom stratigraphy plot for Barnegat Bay core 2 showing relative abundances of taxa that reached at least 5% in at least one sample, Principal Component (PC1 and PC2) sample scores, diatom-based reconstruction of salinity (Inf\_Salinity) and nitrogen content in the sediment (Inf\_Nsed) with a loess smoother fitted to reconstructed values and calculated 95% confidence intervals (grey area), and a dendrogram illustrating depth-constrained cluster analysis of diatom data (CONISS). Green dotted lines separate three diatom zones identified by CONISS.

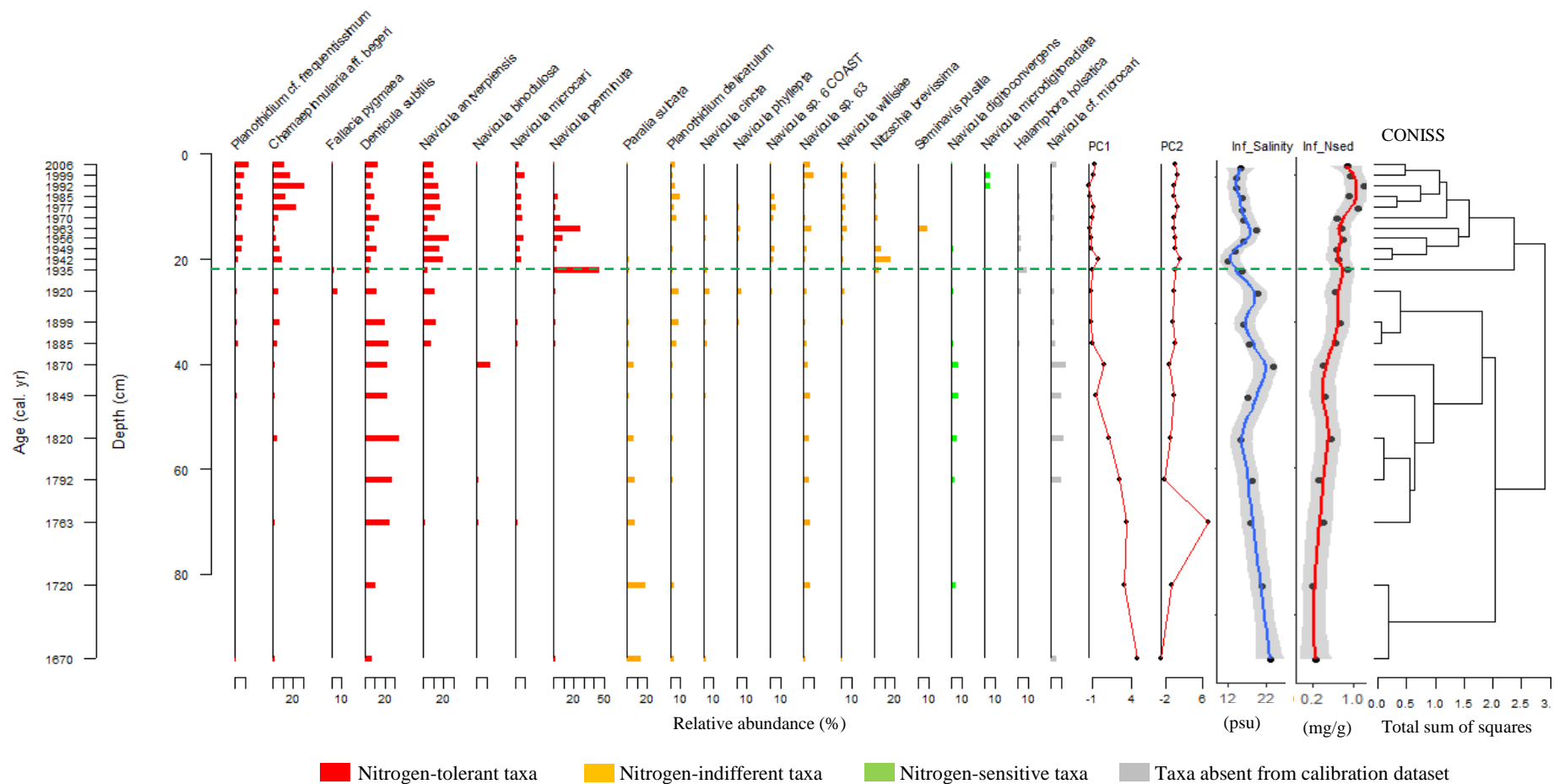


Figure 21. Diatom stratigraphy plot for Barnegat Bay core 4 showing relative abundances of taxa that reached at least 5% in at least one sample, Principal Component (PC1 and PC2) sample scores, diatom-based reconstruction of salinity (Inf\_Salinity) and nitrogen content in the sediment (Inf\_Nsed) with a loess smoother fitted to reconstructed values and calculated 95% confidence intervals (grey area), and a dendrogram illustrating depth-constrained cluster analysis of diatom data (CONISS). Green dotted lines separate two diatom zones identified by CONISS.

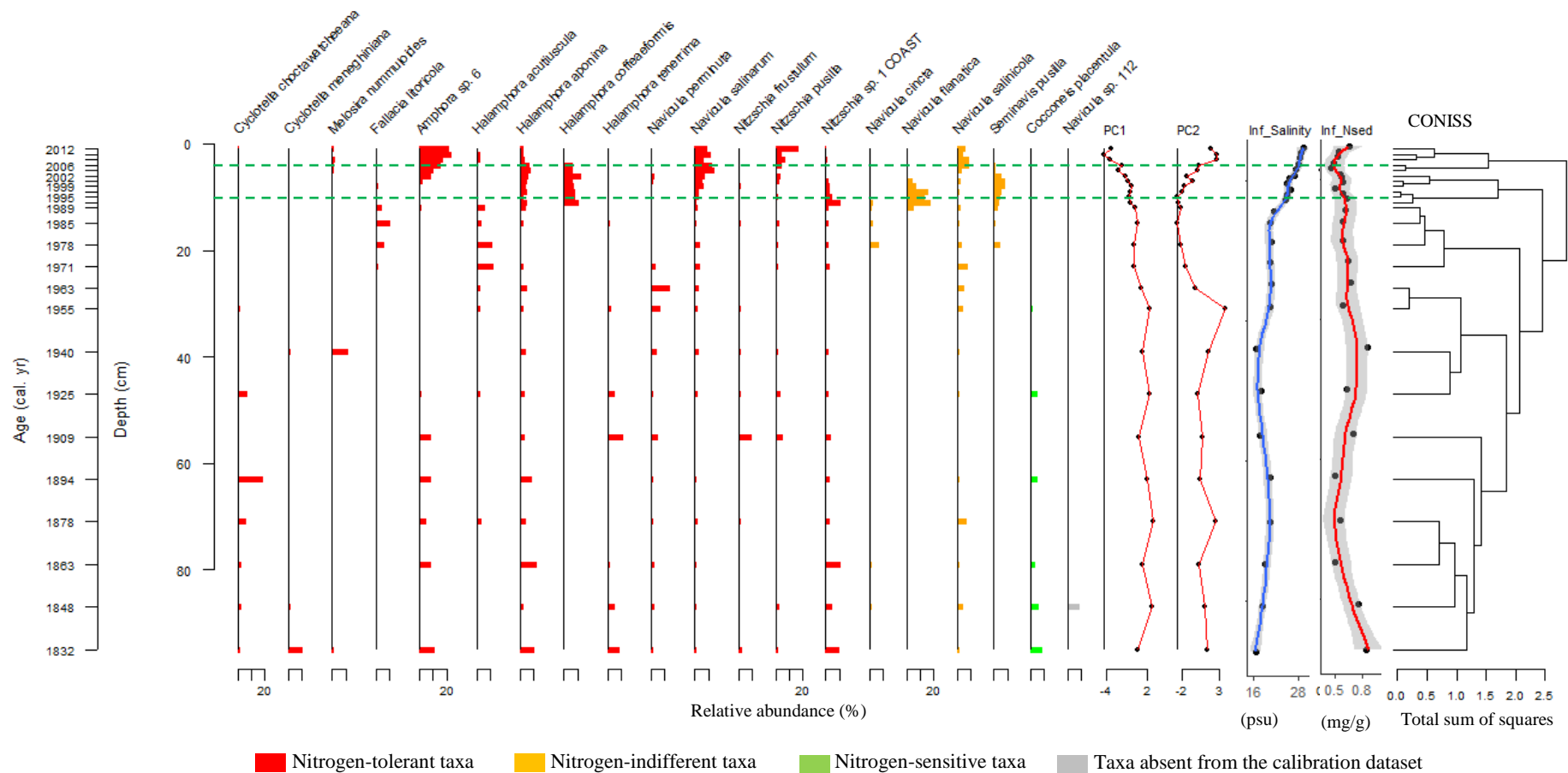


Figure 22. Diatom stratigraphy plot for Great Bay core showing relative abundances of taxa that reached at least 5% in at least one sample, Principal Component (PC1 and PC2) sample scores, diatom-based reconstruction of salinity (Inf\_Salinity) and nitrogen content in the sediment (Inf\_Nsed) with a loess smoother fitted to reconstructed values and calculated 95% confidence intervals (grey area), and a dendrogram illustrating depth-constrained cluster analysis of diatom data (CONISS). Green dotted lines separate three diatom zones identified by CONISS.

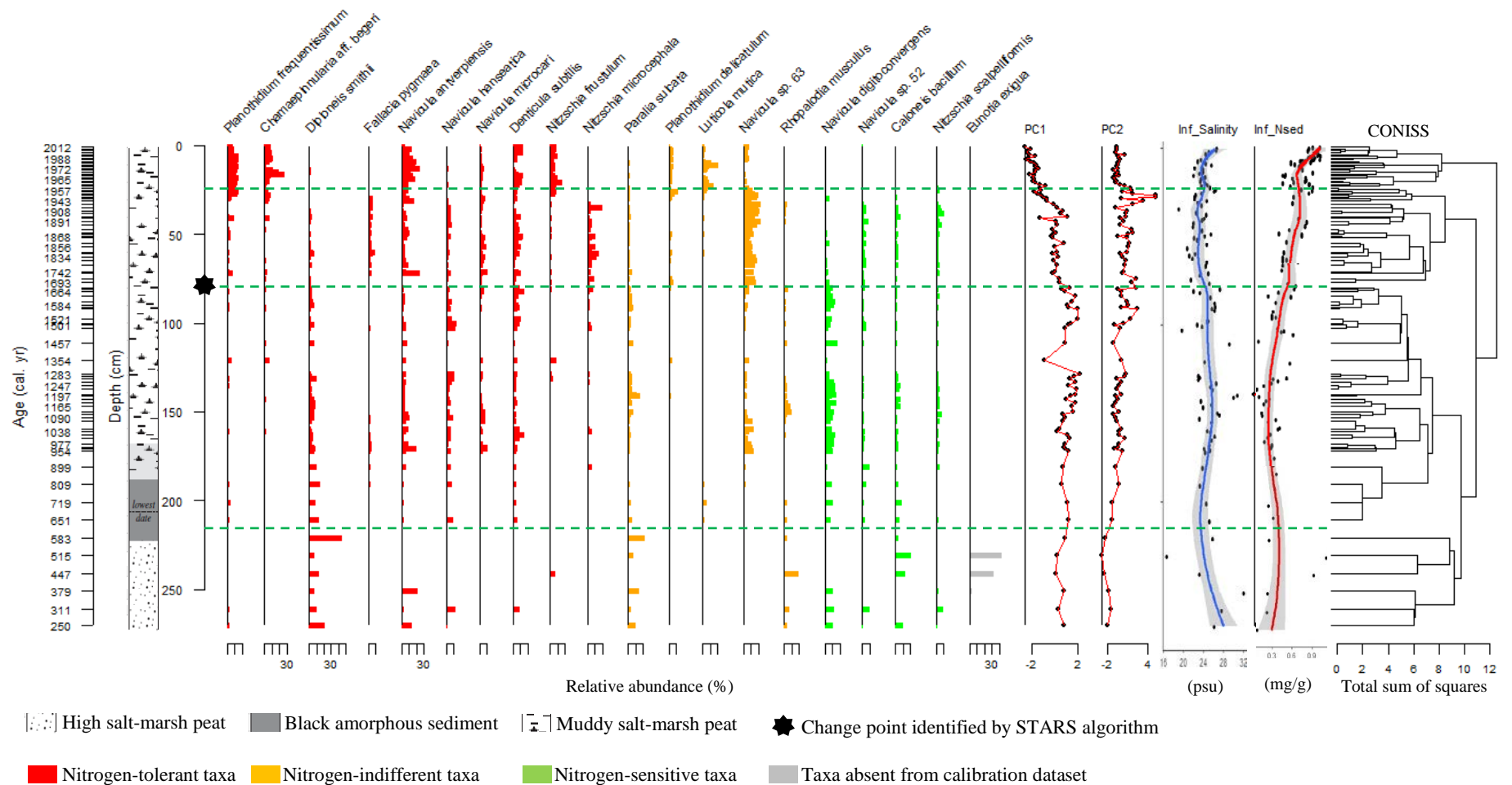


Figure 23. Diatom stratigraphy plot for Cape May Courthouse core showing relative abundances of taxa that reached at least 10% in at least one sample, Principal Component (PC1 and PC2) sample scores, diatom-based reconstruction of salinity (Inf\_Salinity) and nitrogen content in the sediment (Inf\_Nsed) with a loess smoother fitted to reconstructed values and calculated 95% confidence intervals (grey area), and a dendrogram illustrating depth-constrained cluster analysis of diatom data (CONISS). Green dotted lines separate four diatom zones identified by CONISS. Star symbol shows the major transition in the diatom assemblage composition identified by the STARS algorithm. Both STARS algorithm and CONISS identified a major transition at ca. 1675.

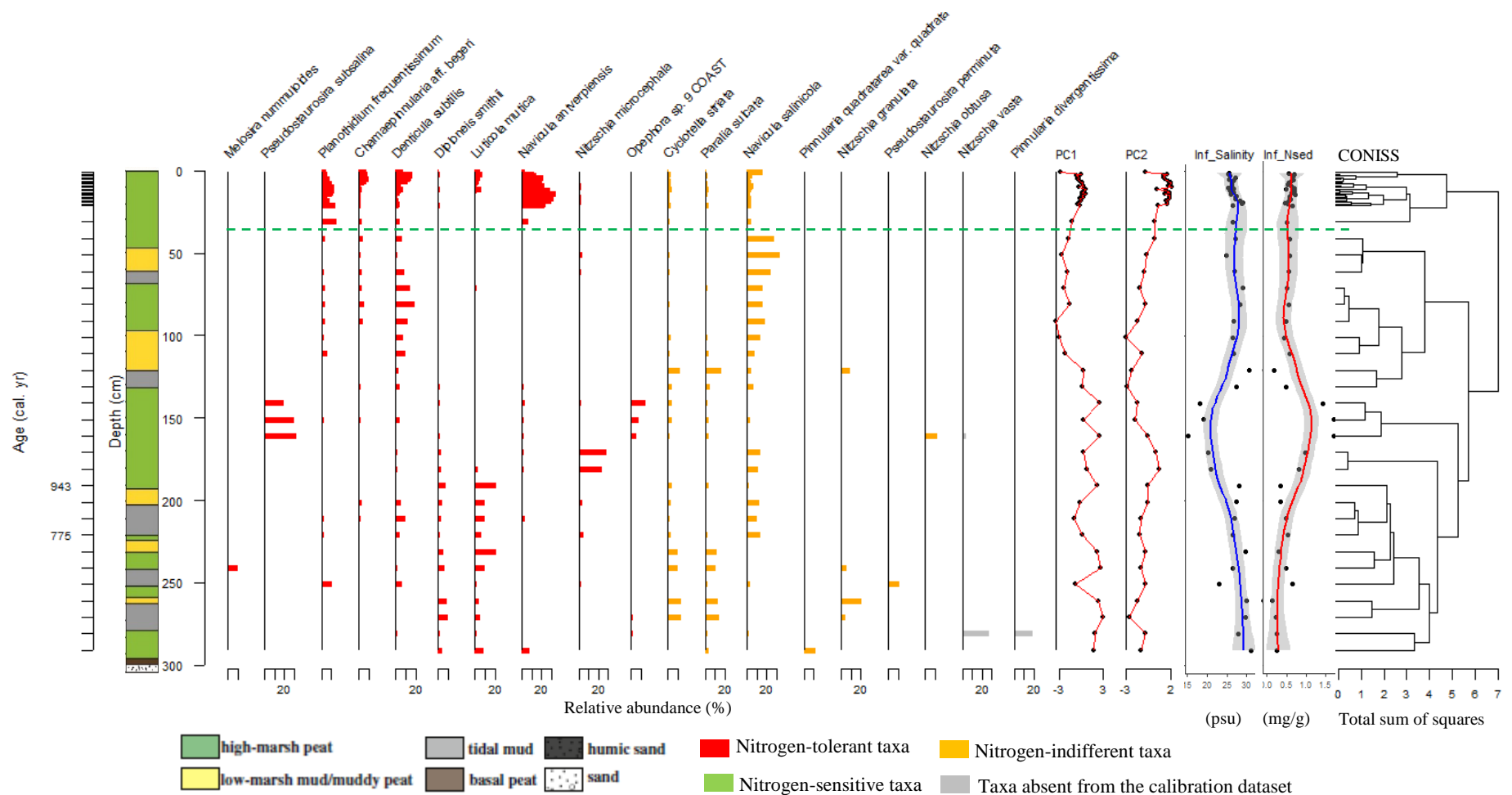


Figure 24. Diatom stratigraphy plot for Fortescue core 9E showing relative abundances of taxa that reached at least 10% in at least one sample, Principal Component (PC1 and PC2) sample scores, diatom-based reconstruction of salinity (Inf\_Salinity) and nitrogen content in the sediment (Inf\_Nsed) with a loess smoother fitted to reconstructed values and calculated 95% confidence intervals (grey area), and a dendrogram illustrating depth-constrained cluster analysis of diatom data (CONISS). Green dotted line separates two diatom zones identified by CONISS.

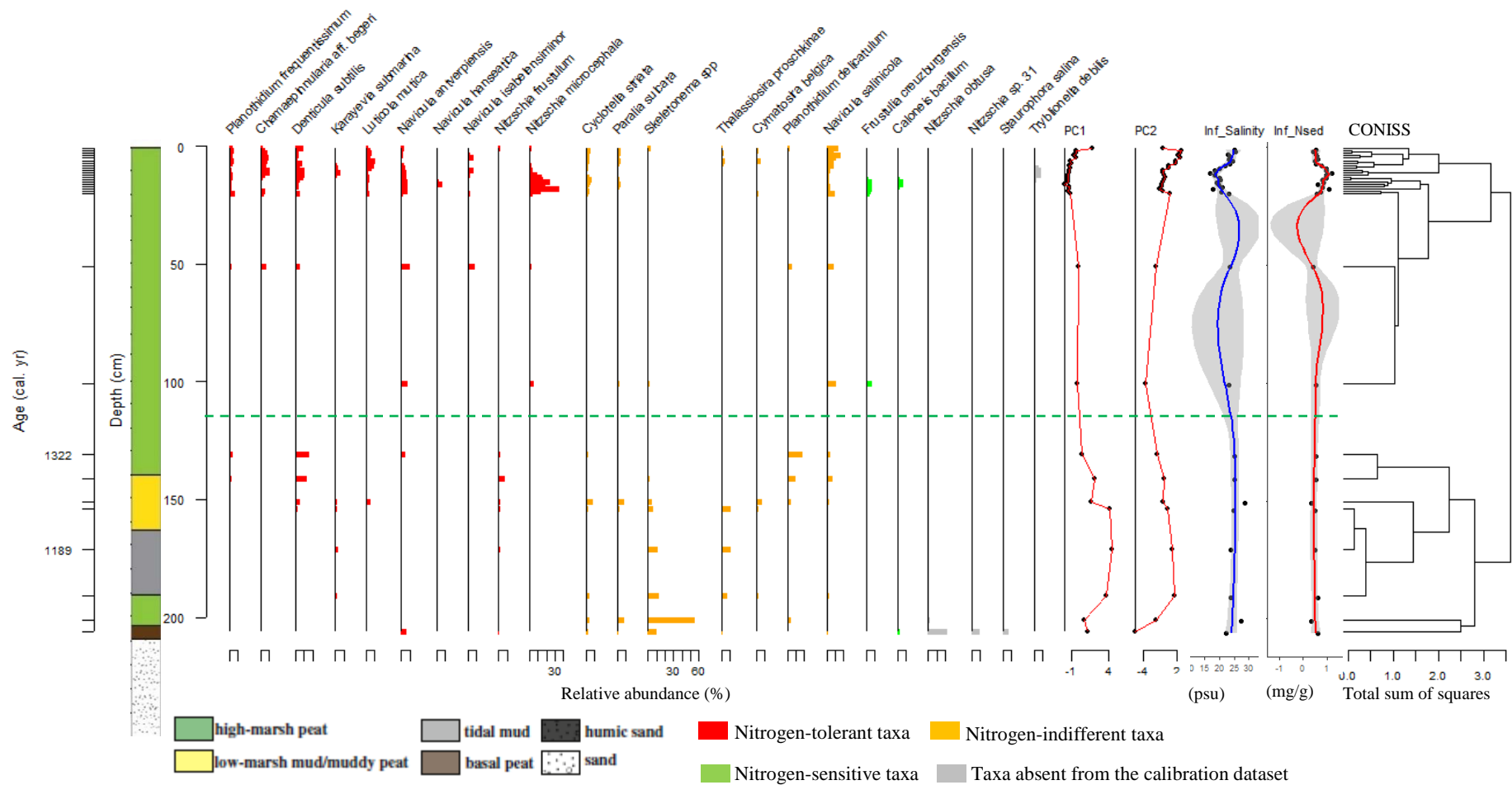


Figure 25. Diatom stratigraphy plot for Fortescue core 11A showing relative abundances of taxa that reached at least 5% in at least one sample, Principal Component (PC1 and PC2) sample scores, diatom-based reconstruction of salinity (Inf\_Salinity) and nitrogen content in the sediment (Inf\_Nsed) with a loess smoother fitted to reconstructed values and calculated 95% confidence intervals (grey area), and a dendrogram illustrating depth-constrained cluster analysis of diatom data (CONISS). Green dotted line separates two main diatom zones identified by CONISS.

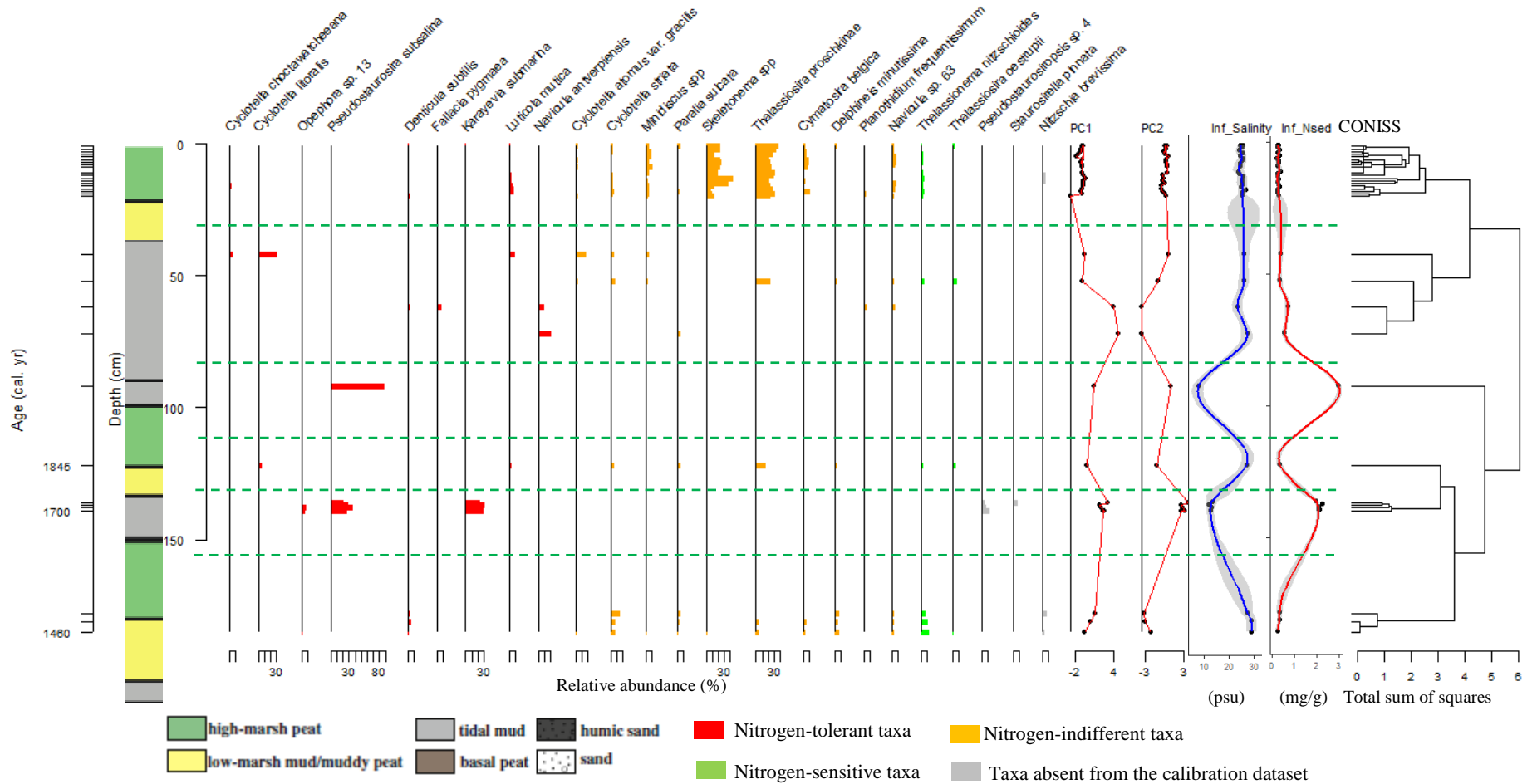
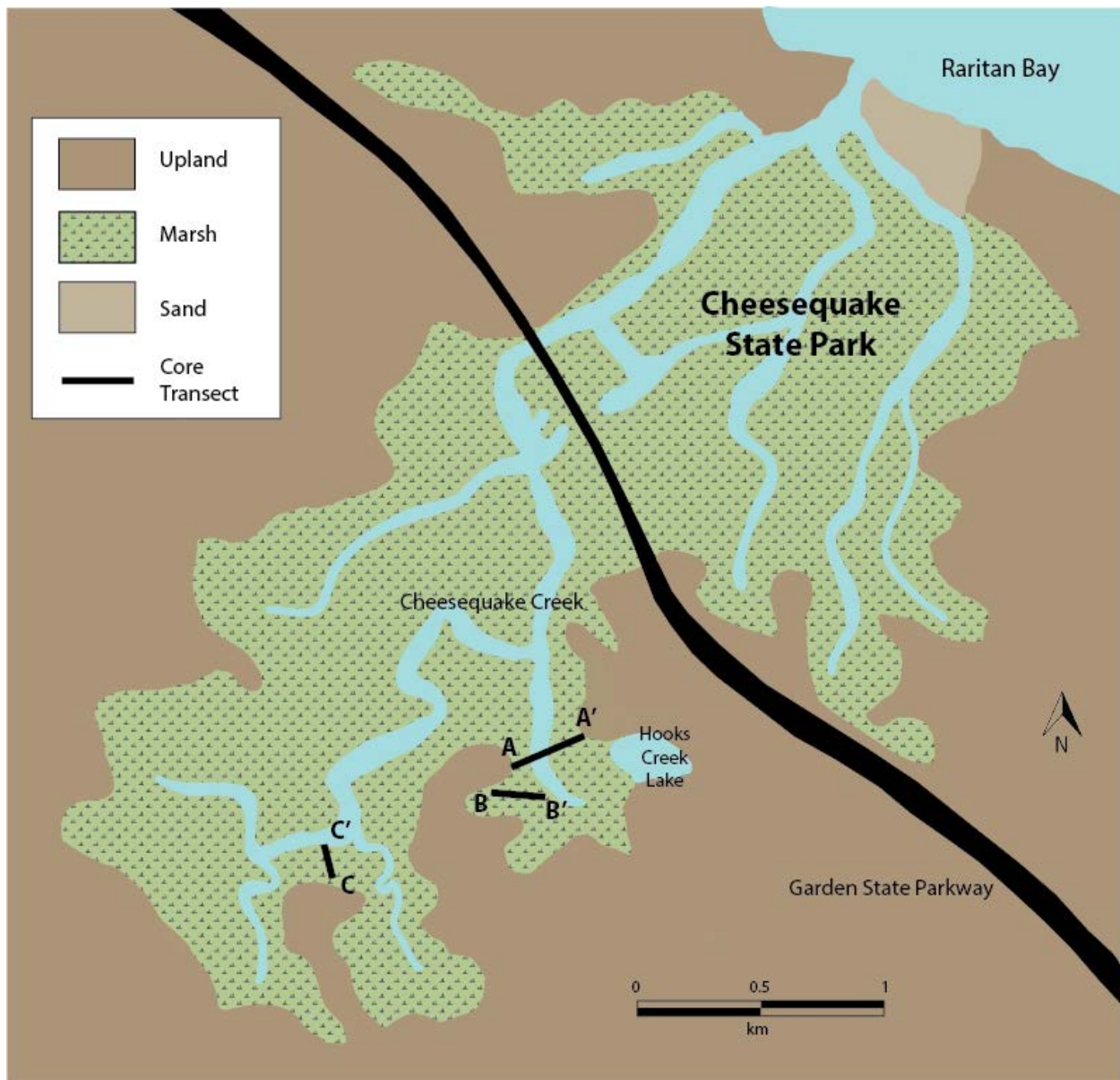
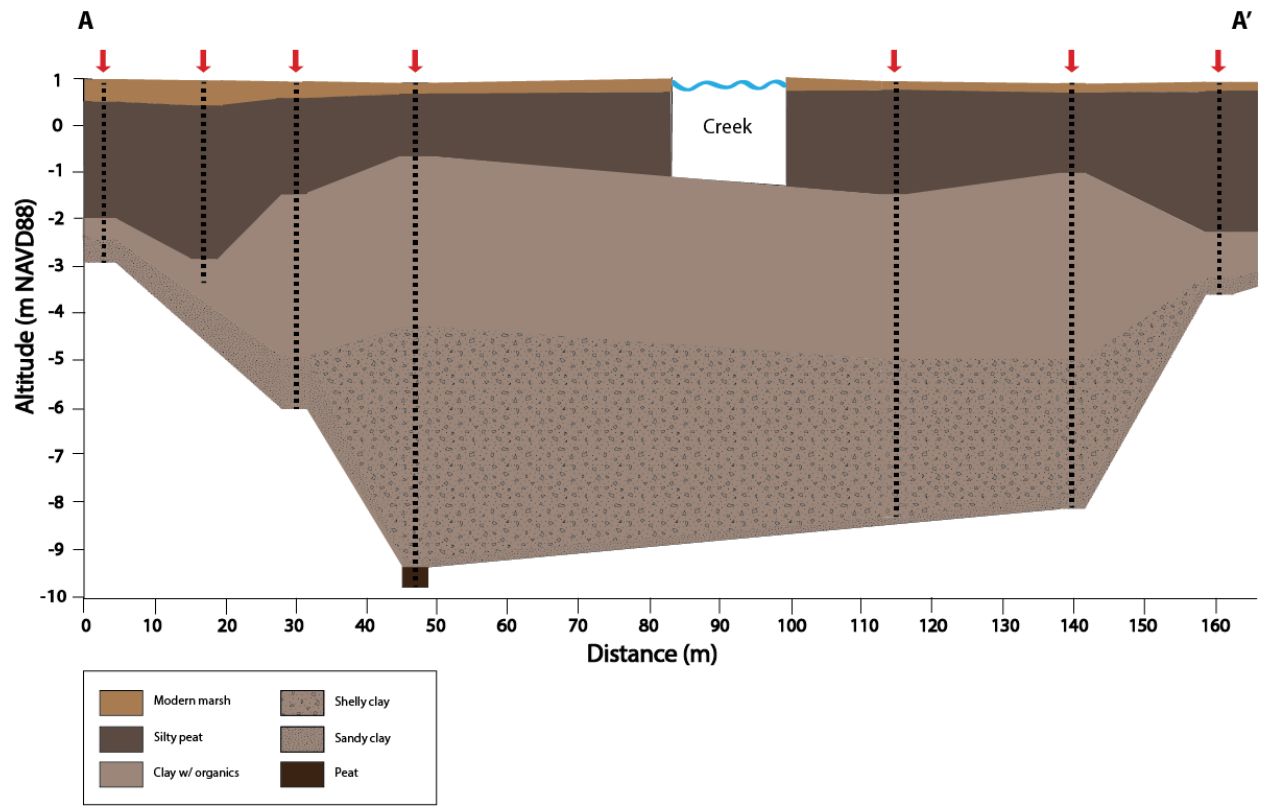
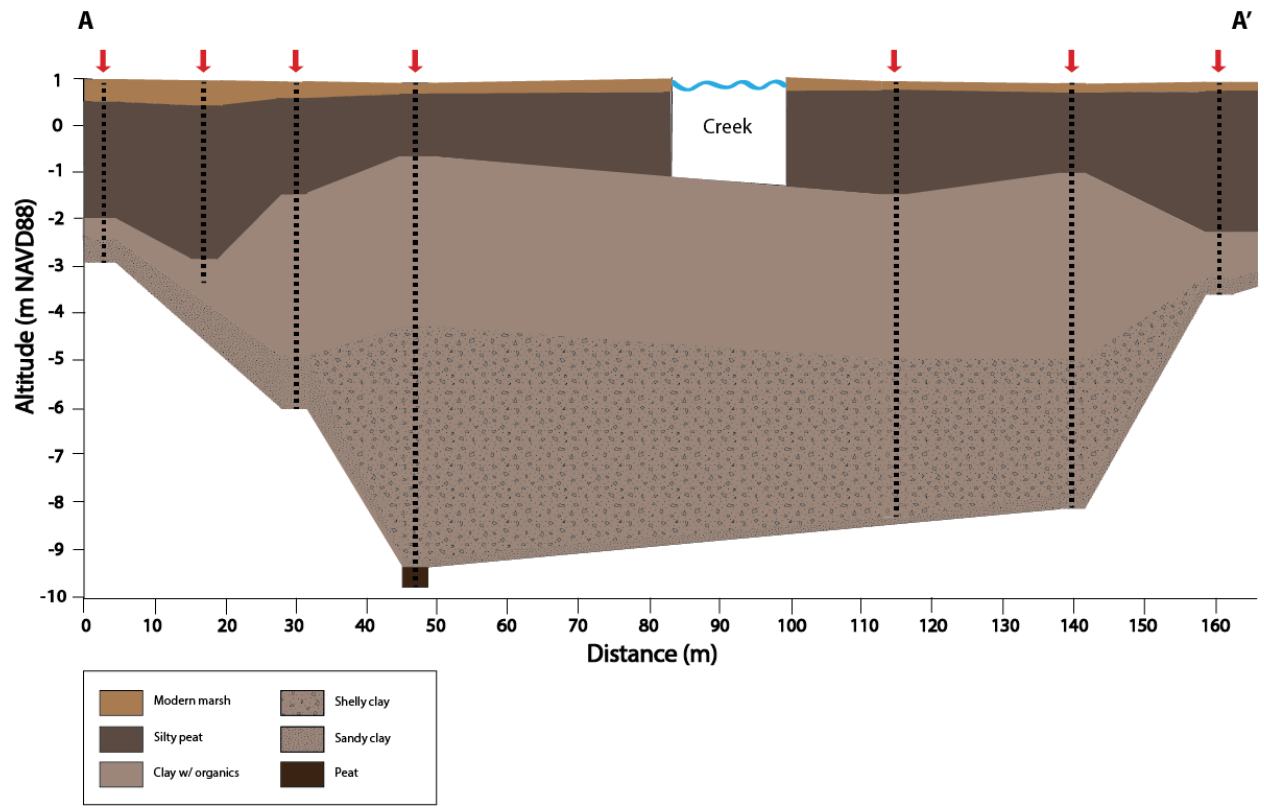


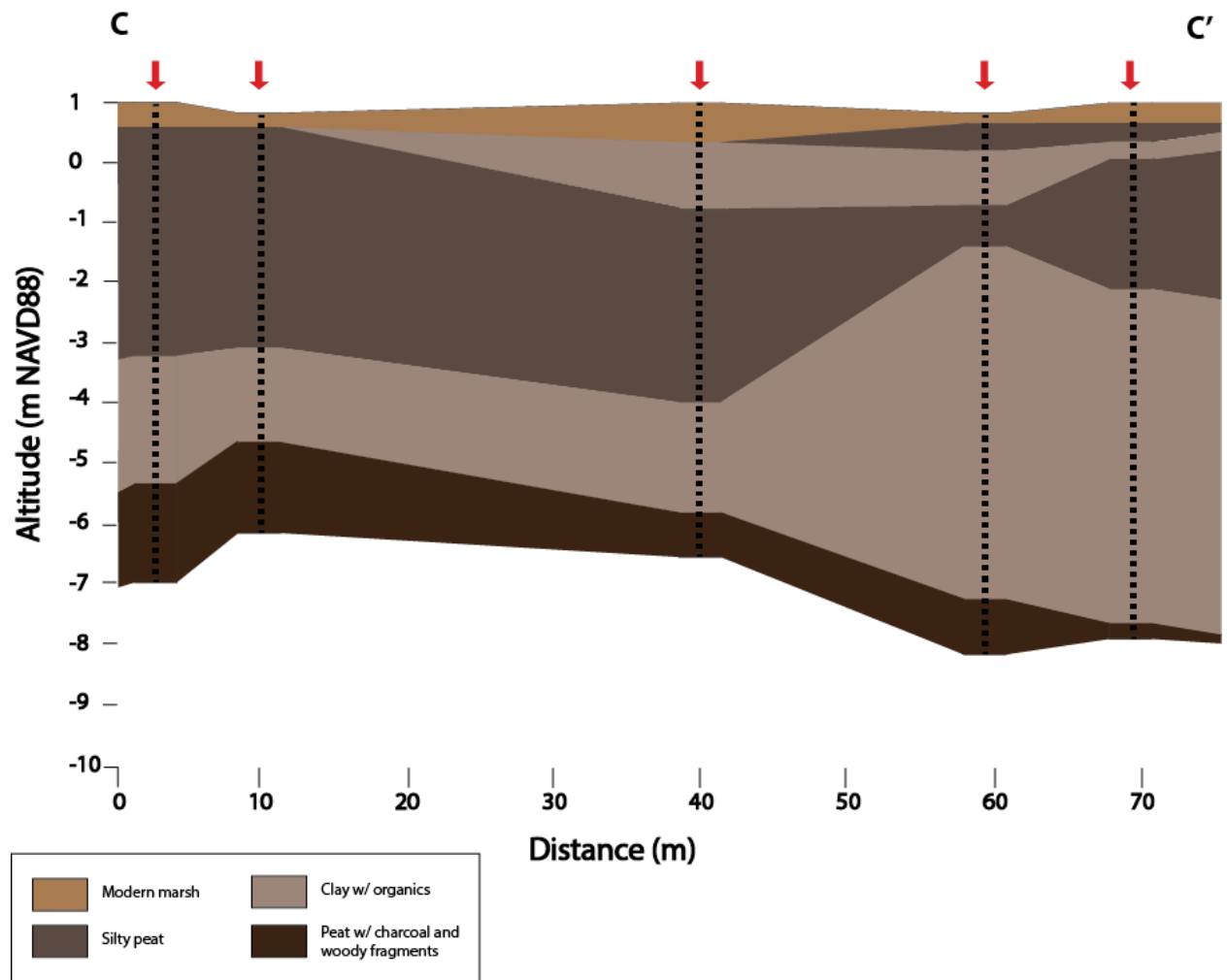
Figure 26. Diatom stratigraphy plot for Sea Breeze core showing relative abundances of taxa that reached at least 5% in at least one sample, Principal Component (PC1 and PC2) sample scores, diatom-based reconstruction of salinity (Inf\_Salinity) and nitrogen content in the sediment (Inf\_Nsed) with a loess smoother fitted to reconstructed values and calculated 95% confidence intervals (grey area), and a dendrogram illustrating depth-constrained cluster analysis of diatom data (CONISS). Green dotted lines separate two main diatom zones at 90-cm depth with six sub-zones identified by CONISS.

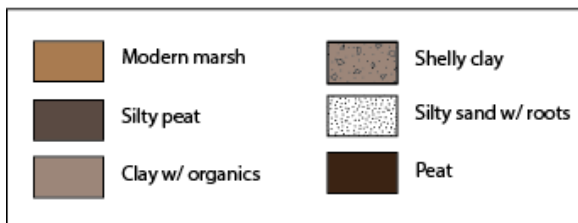
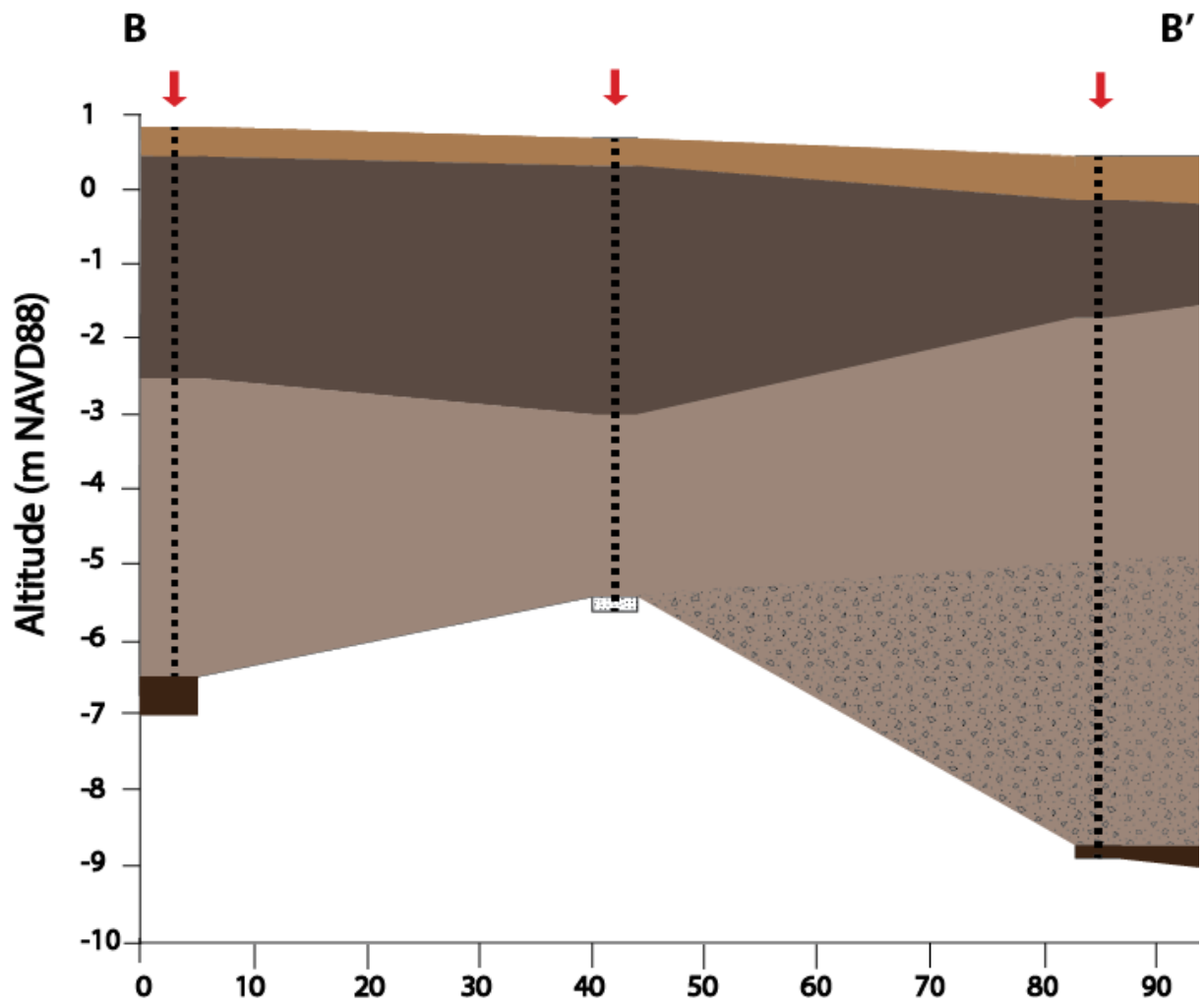
Appendix 1

Stratigraphic profiles developed based on Geoprobe® sediment cores collected in Cheesequake state Park









Distance (m)